P-07-52

Forsmark site investigation

Groundwater flow measurements and SWIW tests in borehole KFM01D

Pernilla Thur, Rune Nordqvist, Erik Gustafsson
Geosigma AB

October 2007

Svensk Kärnbränslehantering AB
Swedish Nuclear Fuel
and Waste Management Co
Box 250, SE-101 24 Stockholm
Tel +46 8 459 84 00

ISSN 1651-4416
SKB P-07-52

Forsmark site investigation

Groundwater flow measurements and SWIW tests in borehole KFM01D

Pernilla Thur, Rune Nordqvist, Erik Gustafsson
Geosigma AB

October 2007

Keywords: AP PF 400-06-105, Forsmark, Hydrogeology, Borehole, Groundwater, Flow, Tracer tests, Dilution probe, SWIW test.

Abstract

This report describes the performance, evaluation and interpretation of in situ groundwater flow measurements and two single well injection withdrawal tracer tests (SWIW tests) at the Forsmark site. The objectives of the activity were to determine the natural groundwater flow in selected fractures intersecting the core drilled borehole KFM01D, as well as to determine transport properties of fractures by means of SWIW tests in the borehole.

Groundwater flow measurements were carried out in five single fractures at borehole lengths ranging from c 147 to c 571 m (120 to 448 m vertical depth). The hydraulic transmissivity ranged within $T = 1.3 \cdot 10^{-8}$–$1.6 \cdot 10^{-5}$ m^2/s. The results of the dilution measurements in borehole KFM01D show that the groundwater flow varies in fractures during natural, i.e. undisturbed, conditions. The lowest flow rate is measured in the deepest section at c 571 m borehole length (c 448 m vertical depth), which also has the lowest hydraulic transmissivity. The flow rate ranged from 0.015 to 0.173 ml/min and the Darcy velocity from $1.7 \cdot 10^{-9}$ to $1.9 \cdot 10^{-8}$ m/s ($1.5 \cdot 10^{-4}$–$1.6 \cdot 10^{-3}$ m/d), results which are in accordance with results from previously performed dilution measurements under natural gradient conditions at the Forsmark site. Measured flow rate and Darcy velocity are highest in the section at c 431 m borehole length (c 344 m vertical depth). Hydraulic gradients, calculated according to the Darcy concept, are within or close to the expected range (0.001–0.05) in three of five measured sections. The hydraulic gradient is lowest in the upper sections at c 147 and c 316 m borehole length (c 120 and c 255 m vertical depth), then increasing with depth. No clear correlation between flow rate and transmissivity is indicated.

The SWIW tests were carried out in two single fractures at borehole lengths of c 377 and 431 m (302 and 344 m vertical depth) with hydraulic transmissivities of $T = 3.1 \cdot 10^{-7}$ and $9.9 \cdot 10^{-7}$ m^2/s, respectively. The model evaluation was made using a radial flow model with advection, dispersion and linear equilibrium sorption as transport processes.

A result from the SWIW tests is that there is a clear retardation/sorption effect of both cesium and rubidium. In the section at 377.4–378.4 m the value of the retardation factor R is for cesium about 530 and for rubidium about 920. Estimated tracer recovery in this section at the last sampling time yields approximately 104%, 92% and 68% for Uranine, cesium and rubidium, respectively. The retardation factor R, in the section at 431.0–432.0 m, is for cesium 910 and for rubidium about 240. Tracer recovery in this section yields approximately 102%, 87% and 90% for Uranine, cesium and rubidium, respectively. Recovery larger than 100% for Uranine most probably emanates from Uranine labelled drilling flushing water and the uncertainty in the tracer analysis. The model simulations were carried out for five different values of porosity for each SWIW section; 0.002, 0.005, 0.01, 0.02, 0.05 (assuming a 0.1 m thick transport zone), resulting in estimates of longitudinal dispersivity within the range of 0.06–0.39 m.

Sammanfattning

Denna rapport beskriver genomförandet, utvärderingen samt tolkningen av in situ grundvattenflödesmätningar och två enhålsspårförsök (SWIW tester) i Forsmark. Syftet med aktiviteten var dels att bestämma det naturliga grundvattenflödet i enskilda sprickor som skär borrhålet KFM01D, dels att karaktärisera transportegenskaperna i potentiella flödesvägar genom att utföra och utvärdera två SWIW tester i borrhålet.

Grundvattenflödesmätningar genomfördes i fem enskilda sprickor på nivåer från ca 147 till ca 571 m borrhålslängd (120 till 448 m vertikalt djup). Den hydrauliska transmissiviteten varierade inom intervallet $T = 1{,}3 \cdot 10^{-8}$–$1{,}6 \cdot 10^{-5}$ m^2/s. Resultaten från utspädningsmätningarna i borrhålet KFM01D visar att grundvattenflödet varierar under naturliga, dvs ostörda, hydrauliska förhållanden. Lägst flöde uppmättes i den djupaste sektionen, som också har den lägsta hydrauliska transmissiviteten, vid ca 571 m borrhålslängd. Beräknade grundvattenflöden låg inom intervallet 0,015–0,173 ml/min och Darcy hastigheterna varierade mellan $1{,}7 \cdot 10^{-9}$ och $1{,}9 \cdot 10^{-8}$ m/s ($1{,}5 \cdot 10^{-4}$–$1{,}6 \cdot 10^{-3}$ m/d). Resultaten överensstämmer med tidigare genomförda mätningar i Forsmark. Flödet och Darcy hastigheten är högst i sektionen på ca 431 m borrhålslängd (ca 344 m vertikalt djup). Hydrauliska gradienter, beräknade enligt Darcy konceptet, ligger inom eller nära det förväntade området (0,001–0,05) i tre av fem testade sprickor/zoner. Den hydrauliska gradienten är lägst i de grunda sektionerna på ca 147 m och ca 316 m borrhålslängd (ca 120 och ca 255 m vertikalt djup), sedan ökande med djupet. Ingen klar korrelation mellan flöde och transmissivitet syns.

SWIW testerna genomfördes vid ca 377 och 431 m borrhålslängd (302 m resp. 344 m vertikalt djup) med $T = 3{,}1 \cdot 10^{-7}$ resp. $9{,}9 \cdot 10^{-7}$ m^2/s. Modellutvärderingen genomfördes med en radiell flödesmodell med advektion, dispersion och linjär jämviktssorption som transportprocesser.

Ett resultat från SWIW testerna är att det finns en klar effekt av fördröjning/sorption av både cesium och rubidium. I sektionen vid ca 377,4–378,4 m är retardationsfaktorn R för cesium 530 och för rubidium 920. Beräknad återhämtning av spårämnena i återpumpningsfasen var ca 104 %, 92 % och 68 % för Uranin, cesium och rubidium. Retardationsfaktorn R i sektionen vid ca 431,0–432,0 m är för cesium ca 910 och för rubidium 240. Massåterhämtningen var här ca 102 %, 87 % och 90 % för Uranin, cesium och rubidium. Återhämtning större än 100 % av Uranin beror sannolikt på viss inblandning av Uraninmärkt spolvatten från borrningen samt osäkerhet i analysen. Modellpassningar till mätdata gjordes för fem olika värden på porositet; 0,002, 0,005, 0,01, 0,02 och 0,05 (antagande en 0,1 m bred transportzon), vilket resulterade i beräknad longitudinell dispersivitet från 0,06 till 0,39 m.

Contents

1 Introduction

SKB is currently conducting a site investigation for a deep repository in Forsmark, according to general and site specific programmes /SKB 2001ab/. Two, among several, methods for site characterisation are in situ groundwater flow measurements and single well injection withdrawal tests (SWIW tests).

This document reports the results gained by SWIW tests and groundwater flow measurements with the borehole dilution probe in borehole KFM01D. The work was conducted by Geosigma AB and carried out between December 2006 and March 2007 in borehole KFM01D according to Activity Plan AP PF 400-06-105. In Table 1-1 controlling documents for performing this activity are listed. Both Activity Plans and Method Descriptions/instructions are SKB's internal controlling documents. Data and results were delivered to the SKB site characterization database Sicada.

Borehole KFM01D is located in the north-western part of the investigation area, Figure 1-1. KFM01D is a telescopic borehole where the part below 90 m borehole length is core drilled. KFM01D is inclined –54.90° from the horizontal plane at collaring. The borehole is in total 800 m long and cased down to 91 m. From 91 m down to 800 m the diameter is 76 mm.

Detailed information about borehole KFM01D is listed in Appendix A (excerpt from the SKB database Sicada).

Table 1-1. Controlling documents for performance of the activity.

Activity Plan	**Number**	**Version**
Grundvattenflödesmätningar och SWIW-tester KFM01D	AP PF 400-06-105	1.0
Method Documents	**Number**	**Version**
Metodbeskrivning för grundvattenflödesmätning	SKB MD 350.001	1.0
Kalibrering av tryckgivare, temperaturgivare och flödesmätare	SKB MD 353.014	2.0
Kalibrering av fluorescensmätning	SKB MD 353.015	2.0
Kalibrering Elektrisk konduktivitet	SKB MD 353.017	2.0
Utspädningsmätning	SKB MD 353.025	2.0
Löpande och avhjälpande underhåll av Utspädningssond	SKB MD 353.065	1.0
Systemöversikt – SWIW-test utrustning	SKB MD 353.069	1.0
Löpande och avhjälpande underhåll av SWIW-test utrustning	SKB MD 353.070	1.0
Kalibrering av flödesmätare i SWIW-test utrustning	SKB MD 353.090	1.0
Instruktion för rengöring av borrhålsutrustning och viss markbaserad utrustning	SKB MD 600.004	1.0
Instruktion för längdkalibrering vid undersökningar i kärnborrhål	SKB MD 620.010	1.0

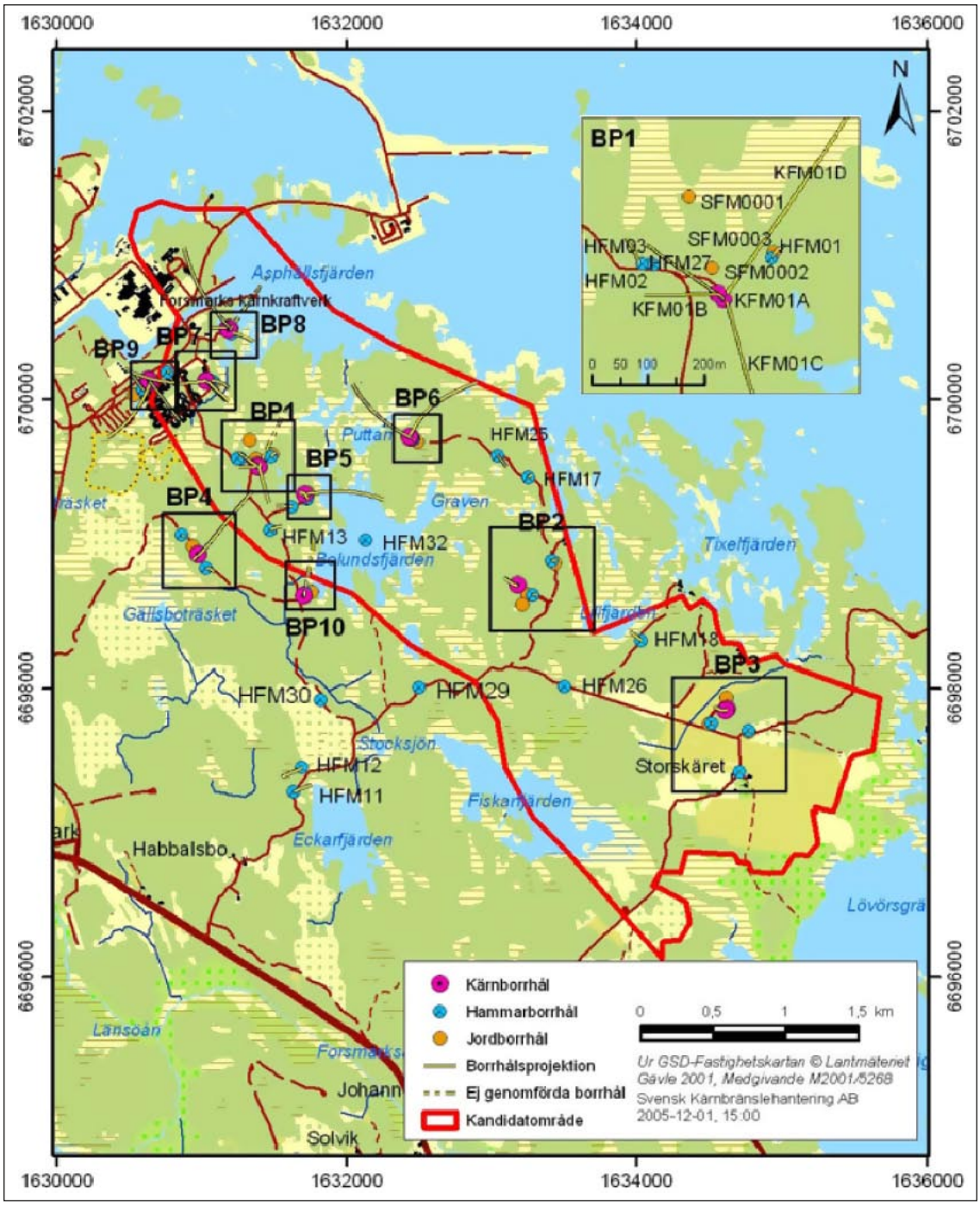

Figure 1-1. *Overview of the Forsmark site investigation area, showing core boreholes (purple) and percussion boreholes (blue). A close-up of Drill Site 1 with KFM01D is shown in the upper right corner.*

2 Objectives and scope

One objective of the activity was to determine groundwater flow under natural gradient as well as hydraulic gradients in the Forsmark area.

The objective of the SWIW tests was to determine transport properties of groundwater flow paths in fractures/fracture zones in a depth range of 300–700 m and a hydraulic transmissivity of $1 \cdot 10^{-8}$–$1 \cdot 10^{-6}$ m^2/s in the test section.

The groundwater flow measurements were performed in fractures at a borehole length range of 147–571 m (120–449 m vertical depth) using the SKB borehole dilution probe. The hydraulic transmissivity in the test sections ranged between $1.3 \cdot 10^{-8}$–$1.6 \cdot 10^{-5}$ m^2/s. Groundwater flow measurements were carried out in totally five test sections. In two of these sections a SWIW test was also conducted using both sorbing and non-sorbing tracers, simultaneously.

3 Equipment

3.1 Borehole dilution probe

The borehole dilution probe is a mobile system for groundwater flow measurements, Figure 3-1. Measurements can be made in boreholes with 56 mm or 76–77 mm diameter and the test section length can be arranged for 1, 2, 3, 4 or 5 m with an optimised special packer/dummy system and section lengths between 1 and 10 m with standard packers. The maximum measurement depth is at 1,030 m borehole length. The vital part of the equipment is the probe which measures the tracer concentration in the test section down hole and in situ. The probe is equipped with two different measurement devices. One is the Optic device, which is a combined fluorometer and light-transmission meter. Several fluorescent and light absorbing tracers can be used with this device. The other device is the Electrical Conductivity device, which measures the electrical conductivity of the water and is used for detection/analysis of saline tracers. The probe and the packers that straddle the test section are lowered down the borehole with an umbilical hose. The hose contains a tube for hydraulic inflation/deflation of the packers and electrical wires for power supply and communication/data transfer. Besides tracer dilution detection, the absolute pressure and temperature are measured. The absolute pressure is measured during the process of dilution because a change in pressure indicates that the hydraulic gradient, and thus the groundwater flow, may have changed. The pressure gauge and the temperature gauge are both positioned in the dilution probe, about seven metres from top of test section. This bias is not corrected for as only changes and trends relative to the start value are of great importance for the dilution measurement. Since the dilution method requires homogenous distribution of the tracer in the test section, a circulation pump is also installed and circulation flow rate measured.

A caliper log, attached to the dilution probe, is used to position the probe and test section at the pre-selected borehole length. The caliper detects reference marks previously made by a drill bit at exact lengths along the borehole, approximately every 50 m. This method makes it possible to position the test section with an accuracy of c ± 0.10 m.

3.1.1 Measurement range and accuracy

The lower limit of groundwater flow measurement is set by the dilution caused by molecular diffusion of the tracer into the fractured/porous aquifer, relative to the dilution of the tracer due to advective groundwater flow through the test section. In a normally fractured granite, the lower limit of a groundwater flow measurement is approximately at a hydraulic conductivity, K, between $6 \cdot 10^{-9}$ and $4 \cdot 10^{-8}$ m/s, if the hydraulic gradient, I, is 0.01. This corresponds to a groundwater flux (Darcy velocity), v, in the range of $6 \cdot 10^{-11}$ to $4 \cdot 10^{-10}$ m/s, which in turn may be transformed into groundwater flow rates, Q_w, corresponding to 0.03–0.2 ml/hour through a one m test section in a 76 mm diameter borehole. In a fracture zone with high porosity, and thus a higher rate of molecular diffusion from the test section into the fractures, the lower limit is about $K = 4 \cdot 10^{-7}$ m/s if I = 0.01. The corresponding flux value is in this case $v = 4 \cdot 10^{-9}$ m/s and flow rate $Q_w = 2.2$ ml/hour. The lower limit of flow measurements is, however, in most cases constrained by the time available for the dilution test. The required time frame for an accurate flow determination from a dilution test is within 7–60 hours at hydraulic conductivity values greater than about $1 \cdot 10^{-7}$ m/s. At conductivity values below $1 \cdot 10^{-8}$ m/s, measurement times should be at least 70 hours for natural (undisturbed) hydraulic gradient conditions.

The upper limit of groundwater flow measurements is determined by the capability of maintaining a homogeneous mix of tracer in the borehole test section. This limit is determined by several factors, such as length of the test section, volume, distribution of the water conducting fractures and how the circulation pump inlet and outlet are designed. The practical upper measurement limit is about 2,000 ml/hour for the equipment developed by SKB.

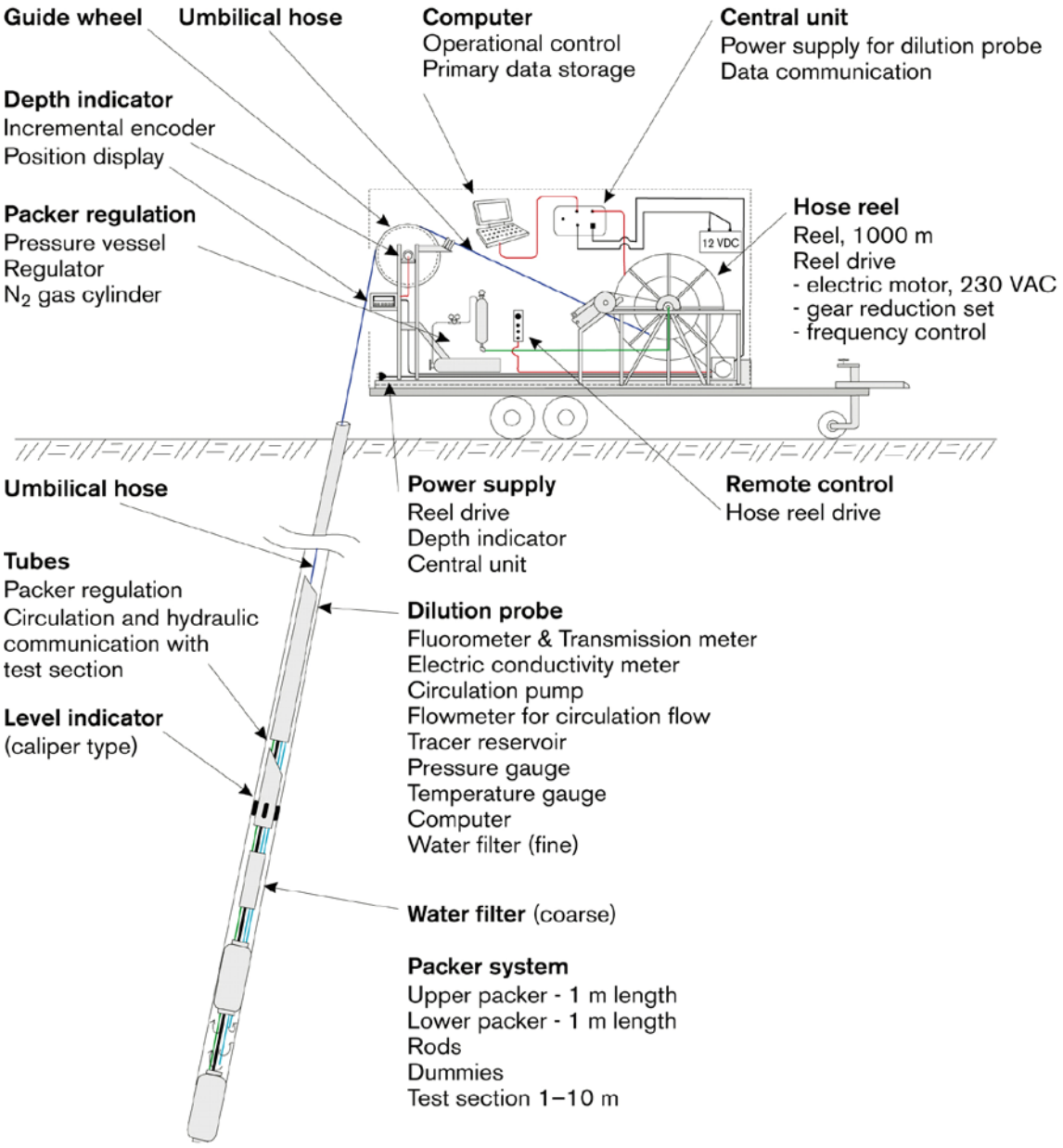

Figure 3-1. *The SKB borehole dilution probe.*

The accuracy of determined flow rates through the borehole test section is affected by various measurement errors related to, for example, the accuracy of the calculated test section volume and determination of tracer concentration. The overall accuracy when determining flow rates through the borehole test section is better than ± 30%, based on laboratory measurements in artificial borehole test sections.

The groundwater flow rates in the rock formation are determined from the calculated groundwater flow rates through the borehole test section and by using some assumption about the flow field around the borehole test section. This flow field depends on the hydraulic properties close to the borehole and is given by the correction factor α, as discussed below in section 4.4.1. The value of α will, at least, vary within $\alpha = 2 \pm 1.5$ in fractured rock /Gustafsson 2002/. Hence, the groundwater flow in the rock formation is calculated with an accuracy of about ± 75%, depending on the flow-field distortion.

3.2 SWIW test equipment

The SWIW (Single Well Injection Withdrawal) test equipment constitutes a complement to the borehole dilution probe making it possible to carry out a SWIW test in the same test section as the dilution measurement, Figure 3-2. Measurements can be made in boreholes with 56 mm or 76–77 mm diameter and the test section length can be arranged for 1, 2, 3, 4 or 5 m with an optimised special packer/dummy system for 76–77 mm boreholes. The equipment is primarily designed for measurements in the depth interval 300–700 m borehole length. However, measurements can be carried out at shallower depths as well at depths larger than 700 m. The possibility to carry out a SWIW test much depends on the hydraulic transmissivity in the investigated test section and frictional loss in the tubing at tracer withdrawal pumping. Besides the dilution probe, the main parts of the SWIW test equipment are:

- Polyamide tubing constituting the hydraulic connection between SWIW test equipment at ground surface and the dilution probe in the borehole.
- Air tight vessel for storage of groundwater under anoxic conditions, i.e. N_2-athmosphere.
- Control system for injection of tracer solution and groundwater (chaser fluid).
- Injection pumps for tracer solution and groundwater.

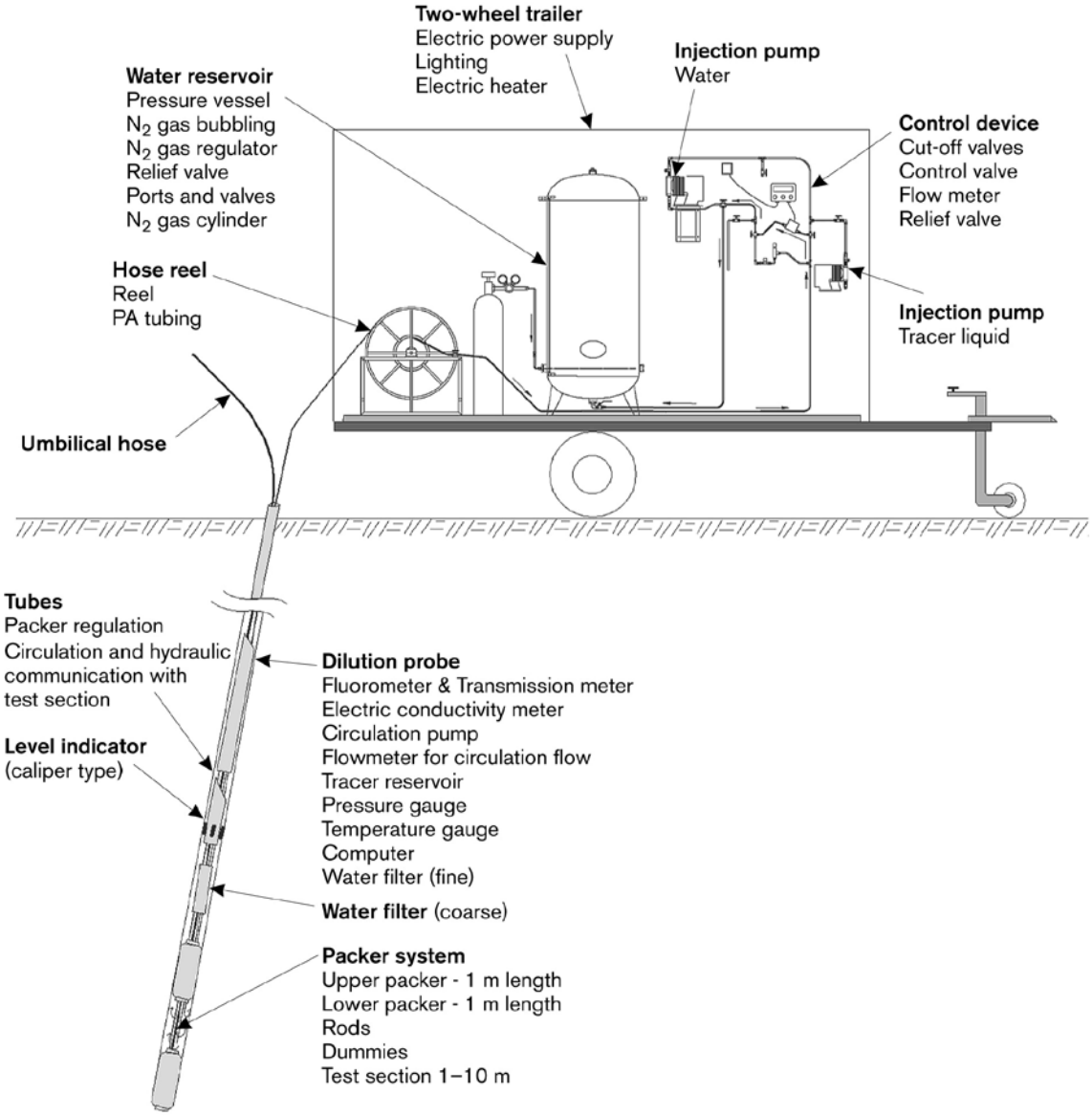

Figure 3-2. *SWIW test equipment, connected to the borehole dilution probe.*

3.2.1 Measurement range and accuracy

The result of a SWIW test depends on the accuracy in the determination of the tracer concentration in injection solutions and withdrawn water. The result also depends on the accuracy in the volume of injection solution and volumes of injected and withdrawn water. For non-sorbing dye tracers (e.g. Uranine) the tracer concentration in collected water samples can be analysed with a resolution of 10 µg/l in the range 0.0–4.0 mg/l. The accuracy is within ± 5%. The volume injected tracer solution can be determined within ± 0.1% and the volume of injected and withdrawn water determined within 5%.

The evaluation of a SWIW test and determination of transport parameters is done with model simulations, fitting the model to the measured data (concentration as a function of time). The accuracy in determined transport parameters depends on selection of model concept and how well the model fit the measured data.

4 Execution

The measurements were performed according to AP PF 400-06-105 (SKB internal controlling document) in compliance with the methodology descriptions for the borehole dilution probe equipment – SKB MD 350.001, Metodbeskrivning för grundvattenflödesmätning – and the measurement system description for SWIW test – SKB MD 353.069, MSB; Systemöversikt – SWIW-test utrustning – (SKB Internal controlling documents), Table 1-1.

4.1 Preparations

The preparations included calibration of the fluorometer and the electric conductivity meter before arriving at the site. Briefly, this was performed by adding certain amounts of the tracer to a known test volume while registering the measured A/D-levels. From this, calibration constants were calculated and saved for future use by using the measurement application. The other sensors had been calibrated previously and were hence only control calibrated.

Extensive functionality checks were accomplished prior to transport to the site and limited function checks were performed at the site. The equipment was cleaned to comply with SKB cleaning level 1 (see SKB MD 600.004) before lowering it into the borehole. All preparations were performed according to SKB Internal controlling documents, cf Table 1-1.

4.2 Procedure

4.2.1 Groundwater flow measurement

In total five groundwater flow measurements were carried out, Table 4-1.

Each measurement was performed according to the following procedure. The equipment was lowered to the correct borehole length where background values of tracer concentration and supporting parameters, pressure and temperature, were measured and logged. Then, after inflating the packers and the pressure had stabilized, tracer was injected in the test section. The tracer concentration and supporting parameters were measured and logged continuously until the tracer had been diluted to such a degree that the groundwater flow rate could be calculated.

Table 4-1. Performed dilution (flow) measurements.

Borehole	Test section (m)+	Number of flowing fractures*	T (m^2/s)*	Tracer	Test period (yymmdd–yymmdd)
KFM01D	147.5–148.5 (120–121)	1	5.32E–06	Uranine	070131–070205
KFM01D	316.4–317.4 (255–256)	1	1.65E–05	Uranine	070215–070219
KFM01D	377.4–378.4 (302–303)	1	3.15E–07	Uranine	070209–070214
KFM01D	431.0–432.0 (344–345)	1	9.95E–07	Uranine	061214–061217
KFM01D	570.7–571.7 (448–449)	1	1.27E–08	Uranine	070103–070117

* /Väisäsvaara et al. 2006/
+ Test section vertical depth is given within brackets.

4.2.2 SWIW tests

Two SWIW tests were performed, Table 4-2. BIPS images of the test sections are shown in Appendix C. To conduct a SWIW test requires that the SWIW equipment is connected to the borehole dilution probe, Figures 3-1 and 3-2.

The SWIW tests were carried out according to the following procedure. The equipment was lowered to the correct borehole length where background values of Uranine and supporting parameters, pressure and temperature, were measured and logged. Then, after inflating the packers and the pressure had stabilized, the circulation pump in the dilution probe was used to pump groundwater from the test section to the air tight vessel at ground surface. Water samples were also taken for analysis of background concentration of Uranine, rubidium and cesium. When pressure had recovered after the pumping in the test section, the injection phases started with pre-injection of the native groundwater to reach steady state flow conditions. Thereafter groundwater spiked with the tracers Uranine, rubidium and cesium was injected. Finally, injection of native groundwater to push the tracers out into the fracture/fracture zone was performed. The withdrawal phase started by pumping water to the ground surface. An automatic sampler at ground surface was used to take water samples for analysis of Uranine, rubidium and cesium in the withdrawn water.

4.3 Data handling

During groundwater flow measurement with the dilution probe, data are automatically transferred from the measurement application to a SQL database. Data relevant for analysis and interpretation are then automatically transferred from SQL to Excel via an MSSQL (ODBC) data link, set up by the operator. After each measurement the Excel data file is copied to a CD.

The water samples from the SWIW test were analysed for Uranine tracer content at the Geosigma Laboratory in Uppsala. Cesium and rubidium contents were analysed at the Analytica laboratory in Luleå.

Table 4-2. Performed SWIW tests.

Borehole	Test section (m)+	Numberof flowing fractures*	T (m^2/s)*	Tracers	Test period (yymmdd–yymmdd)
KFM01D	377.4–378.4 (302–303)	1	3.15E–07	Uranine/ cesium/ rubidium	070208–070302
KFM01D	431.0–432.0 (344–345)	1	9.95E–07	Uranine/ cesium/ rubidium	061214–070102

* /Väisäsvaara et al. 2006/
+ Test section vertical depth is given within brackets.

4.4 Analyses and interpretation

4.4.1 The dilution method – general principles

The dilution method is an excellent tool for in situ determination of flow rates in fractures and fracture zones.

In the dilution method a tracer is introduced and homogeneously distributed into a borehole test section. The tracer is subsequently diluted by the ambient groundwater, flowing through the borehole test section. The dilution of the tracer is proportional to the water flow through the borehole section, Figure 4-1.

The dilution in a well-mixed borehole section, starting at time t = 0, is given by:

$$\ln(C / C_0) = -\frac{Q_w}{V} \cdot t \qquad \text{(Equation 4-1)}$$

where C is the concentration at time t (s), C_0 is the initial concentration, V is the water volume (m^3) in the test section and Q_w is the volumetric flow rate (m^3/s). Since V is known, the flow rate may then be determined from the slope of the line in a plot of ln (C/C_0), or ln C, versus t.

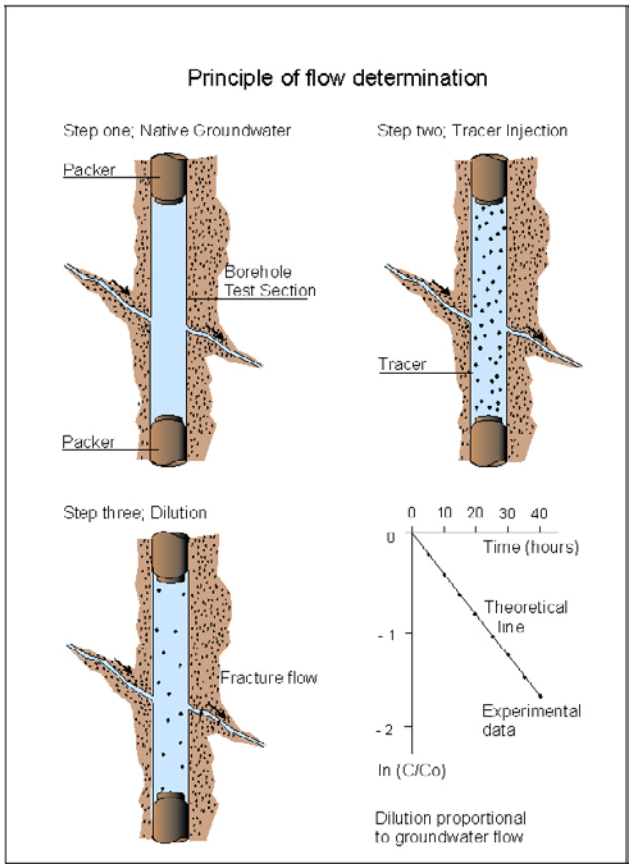

Figure 4-1. *General principles of dilution and flow determination.*

An important interpretation issue is to relate the measured groundwater flow rate through the borehole test section to the rate of groundwater flow in the fracture/fracture zone straddled by the packers. The flow-field distortion must be taken into consideration, i.e. the degree to which the groundwater flow converges and diverges in the vicinity of the borehole test section. With a correction factor, α, which accounts for the distortion of the flow lines due to the presence of the borehole, it is possible to determine the cross-sectional area perpendicular to groundwater flow by:

$$A = 2 \cdot r \cdot L \cdot \alpha \qquad \text{(Equation 4-2)}$$

where A is the cross-sectional area (m^2) perpendicular to groundwater flow, r is the borehole radius (m), L is the length (m) of the borehole test section and α is the correction factor. Figure 4-2 schematically shows the cross-sectional area, A, and how flow lines converge and diverge in the vicinity of the borehole test section.

Assuming laminar flow in a plane parallel fissure or a homogeneous porous medium, the correction factor α is calculated according to Equation. (4-3), which often is called the formula of Ogilvi /Halevy et al. 1967/. Here it is assumed that the disturbed zone, created by the presence of the borehole, has an axis-symmetrical and circular form.

$$\alpha = \frac{4}{1 + (r/r_d) + (K_2/K_1)(1 - (r/r_d)^2)} \qquad \text{(Equation 4-3)}$$

where r_d is the outer radius (m) of the disturbed zone, K_1 is the hydraulic conductivity (m/s) of the disturbed zone, and K_2 is the hydraulic conductivity of the aquifer. If the drilling has not caused any disturbances outside the borehole radius, then $K_1 = K_2$ and $r_d = r$ which will result in $\alpha = 2$. With $\alpha = 2$, the groundwater flow within twice the borehole radius will converge through the borehole test section, as illustrated in Figures 4-2 and 4-3.

If there is a disturbed zone around the borehole the correction factor α is given by the radial extent and hydraulic conductivity of the disturbed zone. If the drilling has caused a zone with a lower hydraulic conductivity in the vicinity of the borehole than in the fracture zone, e.g. positive skin due to drilling debris and clogging, the correction factor α will decrease. A zone of higher hydraulic conductivity around the borehole will increase α. Rock stress redistribution, when new boundary conditions are created by the drilling of the borehole, may also change the hydraulic conductivity around the borehole and thus affect α. In Figure 4-3, the correction factor, α, is given as a function of K_2/K_1 at different normalized radial extents of the disturbed zone (r/r_d). If the fracture/fracture zone and groundwater flow are not perpendicular to the borehole axis, this also has to be accounted for. At a 45 degrees angle to the borehole axis the value of α will be about 41% larger than in the case of perpendicular flow. This is further discussed in /Gustafsson 2002/ and /Rhén et al. 1991/.

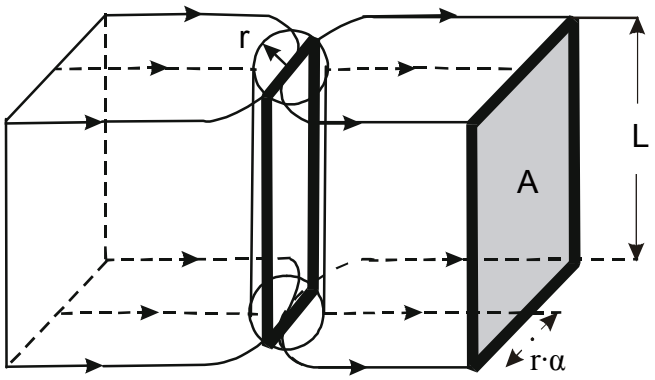

Figure 4-2. *Diversion and conversion of flow lines in the vicinity of a borehole test section.*

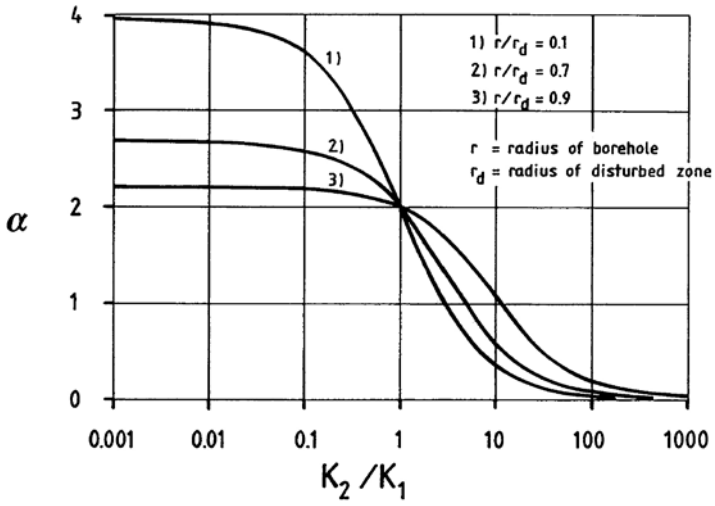

Figure 4-3. *The correction factor, α, as a function of K_2/K_1 at different radial extent (r/r_d) of the disturbed zone (skin zone) around the borehole.*

In order to obtain the Darcy velocity in the undisturbed rock the calculated groundwater flow, Q_w is divided by A, Equation (4-4).

$$v = Q_w/A \qquad \text{(Equation 4-4)}$$

The hydraulic gradient is then calculated as

$$I = v/K \qquad \text{(Equation 4-5)}$$

where K is the hydraulic conductivity.

4.4.2 The dilution method – evaluation and analysis

The first step of evaluation included studying a graph of the measured concentration versus time data. For further evaluation background concentration, i.e. any tracer concentration in the groundwater before tracer injection, was subtracted from the measured concentrations. Thereafter ln (C/C_0) was plotted versus time. In most cases that relationship was linear and the proportionality constant was then calculated by performing a linear regression. In the cases where the relationship between ln (C/C_0) and time was non-linear, a sub-interval was chosen in which the relationship was linear.

The value of ln (C/C_0)/t obtained from the linear regression was then used to calculate Q_w according to Equation (4-1).

The hydraulic gradient, I, was calculated by combining Equations (4-2), (4-4) and (4-5), and choosing $\alpha = 2$. The hydraulic conductivity, K, in Equation (4-5) was obtained from previously performed Posiva Flow Log measurements (PFL) /Väisäsvaara et al. 2006/.

4.4.3 SWIW test – basic outline

A Single Well Injection Withdrawal Test (SWIW) may consist of all or some of the following phases:

1. filling-up pressure vessel with groundwater from the selected fracture,
2. injection of water to establish steady state hydraulic conditions (pre-injection),
3. injection of one or more tracers,
4. injection of groundwater (chaser fluid) after tracer injection is stopped,
5. waiting phase,
6. withdrawal (recovery) phase.

The tracer breakthrough data used for evaluation are obtained from the withdrawal phase. The injection of chaser fluid, i.e. groundwater from the pressure vessel, has the effect of pushing the tracer out as a "ring" in the formation surrounding the tested section. This is generally a benefit, because when the tracer is pumped back, both ascending and descending parts are obtained in the recovery breakthrough curve. During the waiting phase there is no injection or withdrawal of fluid. The purpose of this phase is to increase the time available for time-dependent transport-processes so that these may be more easily evaluated from the resulting breakthrough curve. A schematic example of a resulting breakthrough curve during a SWIW test is shown in Figure 4-4.

The design of a successful SWIW test requires prior determination of injection and withdrawal flow rates, duration of tracer injection, duration of the various injections, waiting and pumping phases, selection of tracers, tracer injection concentrations, etc.

4.4.4 SWIW test – evaluation and analysis

The model evaluation of the experimental results was carried out assuming homogenous conditions. Model simulations were made using the model code SUTRA /Voss 1984/ and the experiments were simulated without a background hydraulic gradient. It was assumed that flow and transport occur within a planar fracture zone of some thickness. The volume available for flow was represented by assigning a porosity value to the assumed zone. Modelled transport processes include advection, dispersion and linear equilibrium sorption.

The sequence of the different injection phases was modelled as accurately as possible based on supporting data for flows and tracer injection concentration. Generally, experimental flows and times may vary from one phase to another, and the flow may also vary within phases. The specific experimental sequences for the borehole sections are listed below.

In the simulation model, tracer injection was simulated as a function accounting for mixing in the borehole section and sorption (for cesium and rubidium) on the borehole walls. The function assumes a completely mixed borehole section and linear equilibrium surface sorption:

$$C = (C_0 - C_{in})e^{-(\frac{Q}{V_{bh}+K_a A_{bh}})t} + C_{in} \qquad \text{(Equation 4-6)}$$

where C is concentration in water leaving the borehole section and entering the formation (kg/m^3), V_{bh} is the borehole volume including circulation tubes (m^3), A_{bh} is area of borehole walls (m^2), Q_{in} is flow rate (m^3/s), C_{in} is concentration in the water entering the borehole section (kg/m^3), C_0 is initial concentration in the borehole section (kg/m^3), K_a is surface sorption coefficient (m) and t is elapsed time (s).

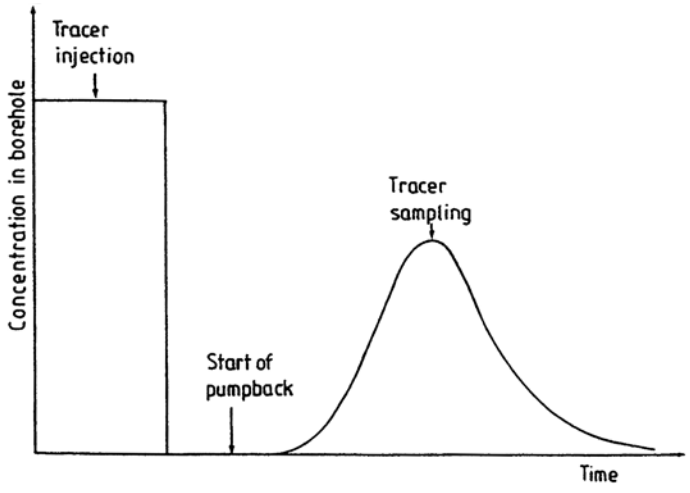

Figure 4-4. *Schematic tracer concentration sequence during a SWIW test /Andersson 1995/.*

Based on in situ experiments /Andersson et al. 2002/ and laboratory measurements on samples of crystalline rock /Byegård and Tullborg 2005/ the sorption coefficient K_a was assigned a value of 10^{-2} m in all simulations. An example of the tracer injection input function is given in Figure 4-5, showing a 50 minutes long tracer injection phase followed by a chaser phase.

Non-linear regression was used to fit the simulation model to experimental data. The estimation strategy was generally to estimate the dispersivity (a_L) and a retardation factor (R), while setting the porosity (i.e. the available volume for flow) to a fixed value. Simultaneous fitting of both tracer breakthrough curves (Uranine and cesium in the example), and calculation of fitting statistics, was carried out using the approach described in /Nordqvist and Gustafsson 2004/. Tracer breakthrough curves for Uranine and rubidium are related and calculated in the same way.

4.5 Nonconformities

Problem occurred when lowering the equipment in the deeper part of the borehole. However, when the packers were shaped with a well-balanced pressure, lowering was possible.

The borehole water was found to have a high particle content and a chemical composition that caused clogging of the optical measurement device. Hoisting of the borehole probe for cleaning took some time and delayed the measurements. At 377.4–378.4 and 570.7–571.7 m borehole length, clean water was pumped down to the section with open packers to rinse the section. Circulation and further rinsing with expanded packers also increased the cleansing of the borehole water in the section. In section 147.5–148.5 m an apparent increase of groundwater flow occurred after c 75 hours of elapsed time due to the clogging of the optical device and only the first part of the dilution was used for final evaluation.

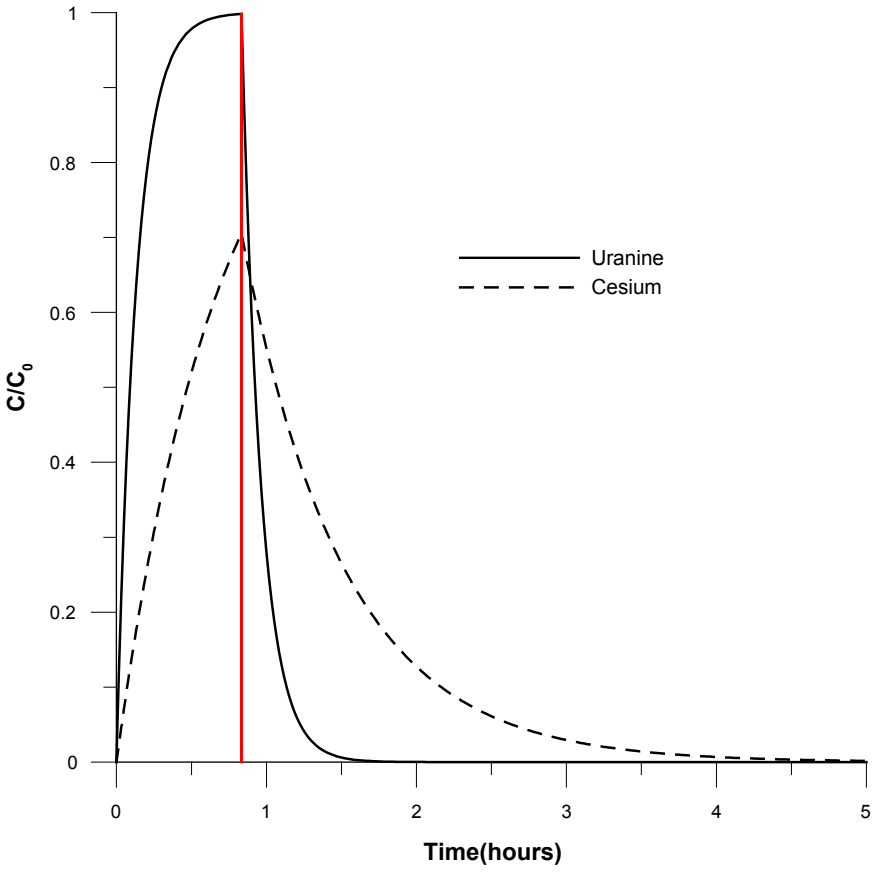

Figure 4-5. *Example of simulated tracer injection functions for a tracer injection phase (ending at 50 minutes shown by the vertical red line) immediately followed by a chaser phase.*

Due to freezing of the equipment the Electrical Conductivity device had to be removed from the dilution probe and replaced by a pipe. The sections at 147.5–148.5, 316.4–317.4 and 377.4–378.4 m borehole length were measured without the Electrical Conductivity device. Since the temperature gauge is placed within the Electrical Conductivity device the temperature could not be measured in these sections.

A planned SWIW test at 570.7–571.7 m borehole length was not feasible to perform due to problems with pumping groundwater from the test section to the SWIW tank. Instead, a SWIW test was executed at 377.4–378.4 m borehole length.

5 Results

5.1 General

Original data from the reported activity are stored in the primary database Sicada. Data are traceable in Sicada by the Activity Plan number (AP PF 400-06-100). Only data in databases are accepted for further interpretation and modelling. The data presented in this report are regarded as copies of the original data. Data in the databases may be revised, if needed. However, such revision of the database will not necessarily result in a revision of this report, although the normal procedure is that major data revisions entail a revision of P-reports. Minor data revisions are normally presented as supplements, available at www.skb.se.

5.2 Dilution measurements

Figure 5-1 exemplifies a typical dilution curve in a fracture zone straddled by the test section at 377.4–378.4 m borehole length (302–303 m vertical depth) in borehole KFM01D. In the first phase the background value is recorded for about 19 hours, see section 5.1.3. In phase two, Uranine tracer is injected, and after mixing a start concentration (C_0) of about 1.7 mg/l is achieved. In phase three the dilution is measured for about 112 hours. Thereafter the packers are deflated and the remaining tracer flows out of the test section. Figure 5-2 shows the measured pressure during the dilution measurement. Since the pressure gauge is positioned about seven metres above top of test section there is a bias from the pressure in the test section which is not corrected for, as only changes and trends relative to the start value are of great importance for the dilution measurement. Figure 5-3 is a plot of the ln (C/C_0) versus time data and linear regression best fit to data showing a good fit with correlation $R^2 = 0.9976$. The standard deviation, STDAV, shows the mean divergence of the values from the best fit line and is calculated from

$$\text{STDAV} = \sqrt{\frac{n\sum x^2 - \left(\sum x\right)^2}{n(n-1)}}$$

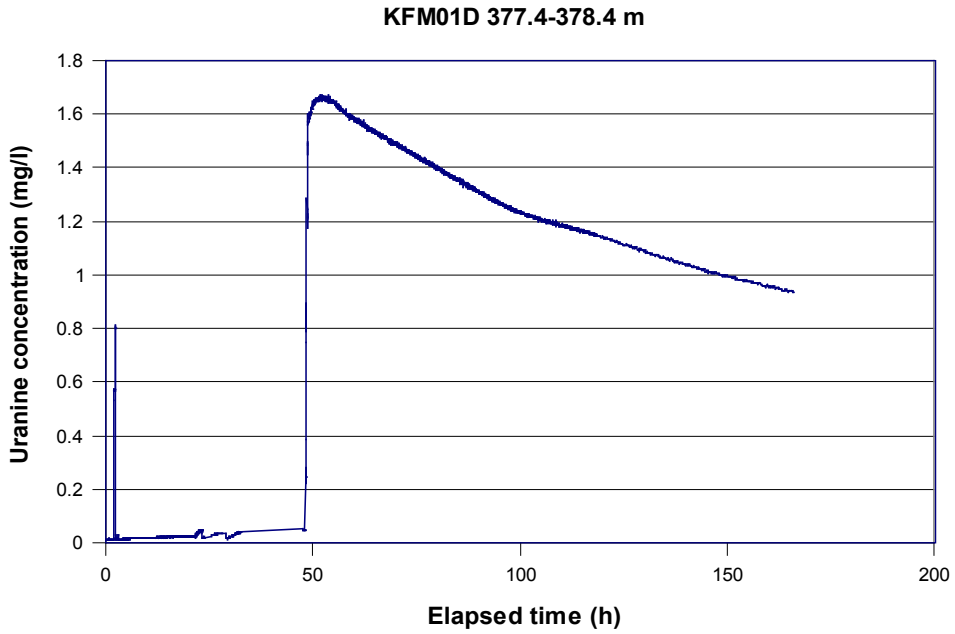

Figure 5-1. *Dilution measurement in borehole KFM01D, section 377.4–378.4 m. Uranine concentration versus time.*

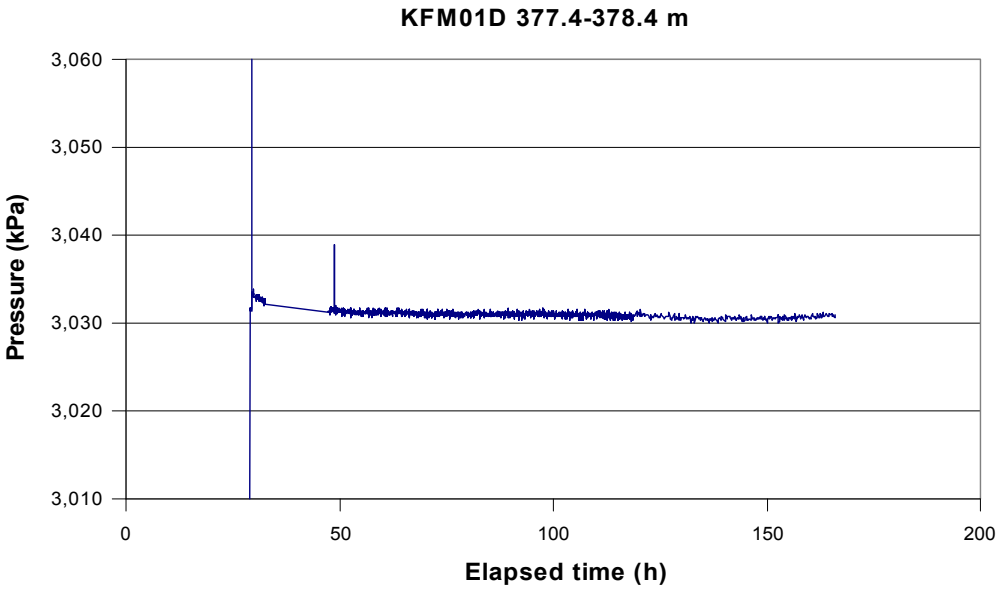

Figure 5-2. *Measured pressure during dilution measurement in borehole KFM01D, section 377.4–378.4 m.*

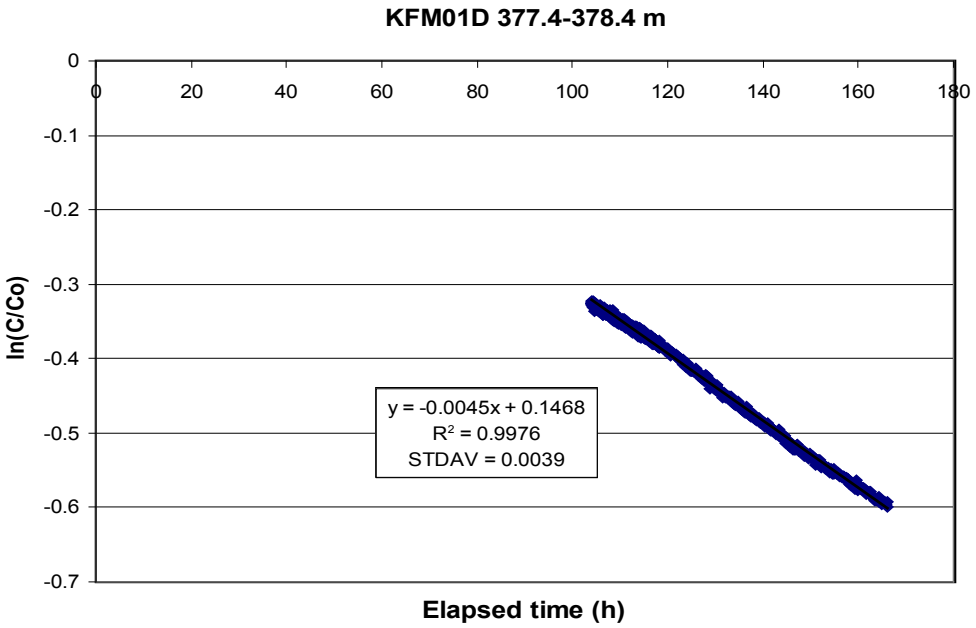

Figure 5-3. *Linear regression best fit to data from dilution measurement in borehole KFM01D, section 377.4–378.4 m.*

Calculated groundwater flow rate, Darcy velocity and hydraulic gradient are presented in Table 5-1 together with the results from all other dilution measurements carried out in borehole KFM01D.

The dilution measurements were carried out with the dye tracer Uranine. Uranine tracer normally has a low background concentration and the tracer can be injected and measured in concentrations far above the background value, which gives a large dynamic range and accurate flow determinations. Changes in the background concentration may have an influence on the measured tracer concentration in the test section, and thus also on the determined groundwater flow rate. For measurements in sections where the fluorescence technique is impossible to apply due to high particle content, the tracer NaCl could be used instead and electric conductivity measured. This was not required in borehole KFM01D.

Details of all dilution measurements, with diagrams of dilution versus time and the supporting parameters pressure, temperature and circulation flow rate are presented in Appendix B1–B5.

5.2.1 KFM01D, section 147.5–148.5 m

This dilution measurement was carried out in a test section with a single flowing fracture. The complete test procedure can be followed in Figure 5-4. On position the background concentration (0.040 mg/l) is measured for about two hours. Thereafter the Uranine tracer is injected in four steps, and after mixing it finally reaches a start concentration of 0.77 mg/l above background. Dilution is measured for about 110 hours, the packers are then deflated and the remaining tracer flows out of the test section. Hydraulic pressure is stable but shows small diurnal pressure variations due to earth tidal effects (Appendix B1). The borehole water was found to have high particle content and a chemical composition which caused a clogging on the optical device. Therefore, the latter part of the dilution curve was excluded and the final evaluation was made on the 30 to 75 hours part of the dilution curve where the clogging not influenced the measurement. The regression line fits well to the slope of the dilution with a correlation coefficient of $R^2 = 0.9487$ for the best fit line (Figure 5-5). The groundwater flow rate, calculated from the best fit line, is 0.021 ml/min. Calculated hydraulic gradient is 0.0004 and Darcy velocity $2.3 \cdot 10^{-9}$ m/s. According to evaluated Pipe String System measurement in section 143.6–148.6 m the flow regime is defined as a PRF (Pseudo-radial flow regime) for the injection phase, which suggest a uniform flow in one plane, and a PRF or a PSS (Pseudo-stationary flow regime) for the recovery phase, indicating high transmissivity /Florberger et al. 2006/. However, in the Pipe String System section there are 2 fractures lying outside the dilution test section with T-values $2 \cdot 10^{-6}$ and $2 \cdot 10^{-7}$ m^2/s /Väisäsvaara et al. 2006/.

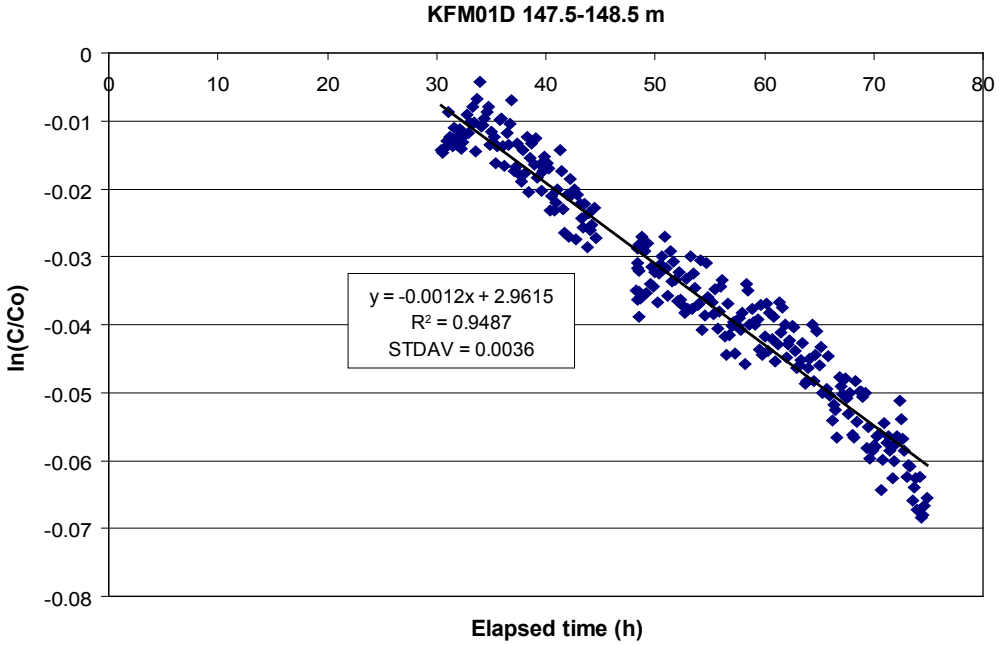

Figure 5-4. *Dilution measurement in borehole KFM01D, section 147.5–148.5 m. Uranine concentration versus time.*

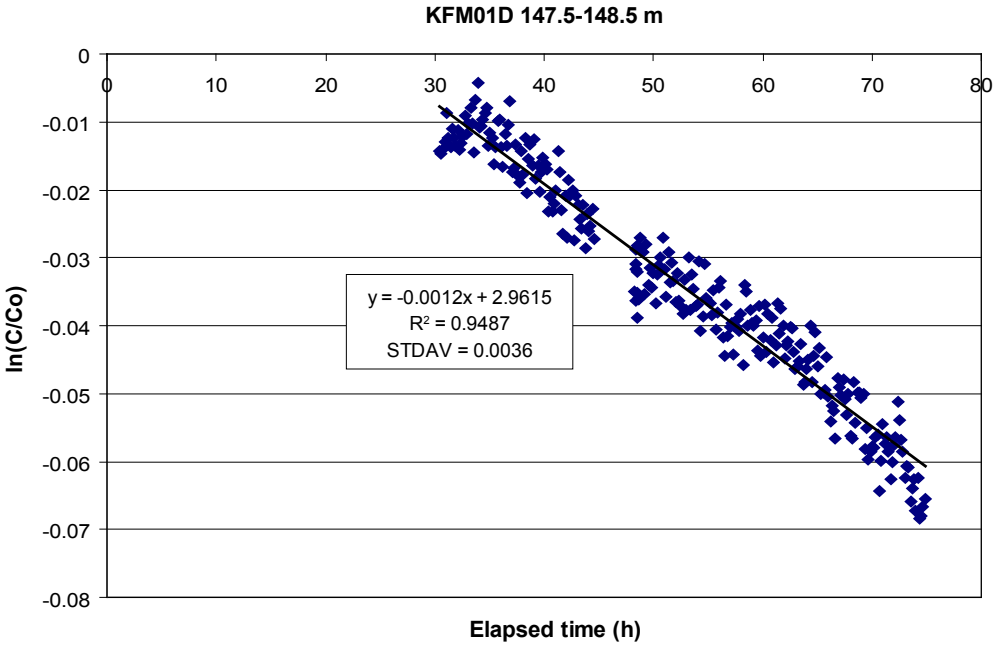

Figure 5-5. *Linear regression best fit to data from dilution measurement in borehole KFM01D , section 147.5–148.5 m.*

5.2.2 KFM01D, section 316.4–317.4 m

This dilution measurement was carried out with the dye tracer Uranine in a test section with a single flowing fracture. The background measurement, tracer injection and dilution can be followed in Figure 5-6. Background concentration is 0.027 mg/l. The Uranine tracer is injected in four steps and after mixing it reaches a start concentration of 0.84 mg/l above background. Dilution is measured for about 87 hours, thereafter the packers are deflated. Hydraulic pressure shows a rapid peak at ca 30 hours of elapsed time, thereafter the pressure decrease. When the pressure stabilizes it still shows a small decreasing trend and small diurnal pressure variations due to earth tide (Appendix B2). Groundwater flow is determined from the 60 to 94 hours part of the dilution measurement when the pressure is stabilized. The regression line fits well to the slope of the dilution with a correlation coefficient of $R^2 = 0.9457$ for the best fit line (Figure 5-7), and the groundwater flow rate, calculated from the best fit line, is 0.021 ml/min. Calculated hydraulic gradient is 0.0001 and Darcy velocity $2.3 \cdot 10^{-9}$ m/s. The Pipe String System measurement for 313.6–318.6 m gives the flow regime no-flow boundary (NFB) for the injection and PRF transferring to NFB for the recovery phase. A fracture plane close to the borehole is probable confined by a denser border 20–30 m from the borehole. The flow is restricted by this less permeable rock. No fractures are included in the Pipe String System measurement outside the dilution test section.

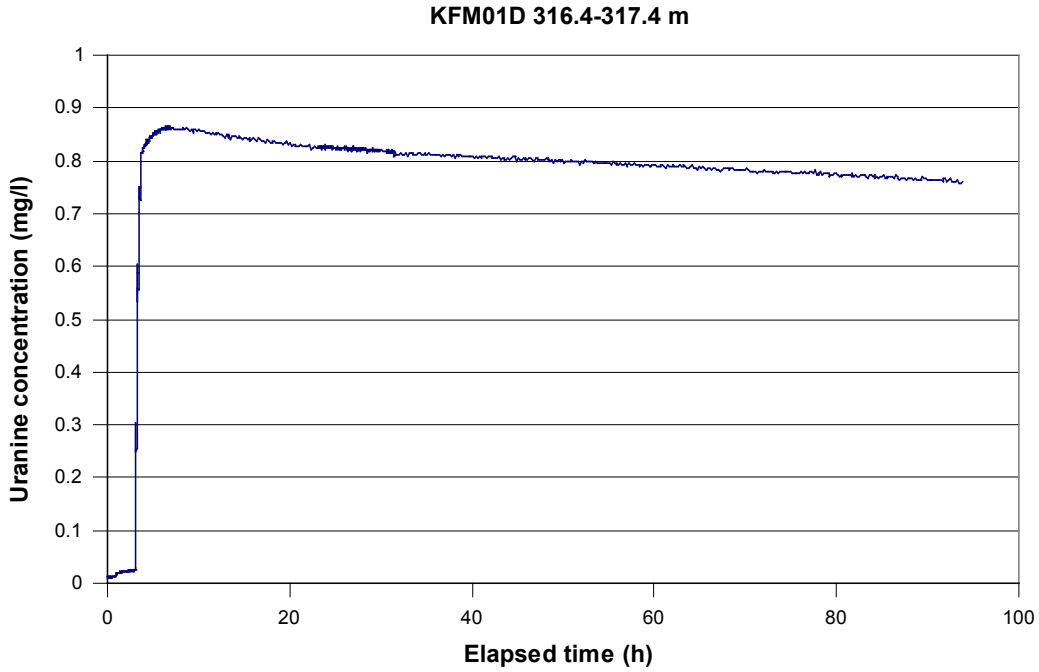

Figure 5-6. *Dilution measurement in borehole KFM01D, section 316.4–317.4 m. Uranine concentration versus time.*

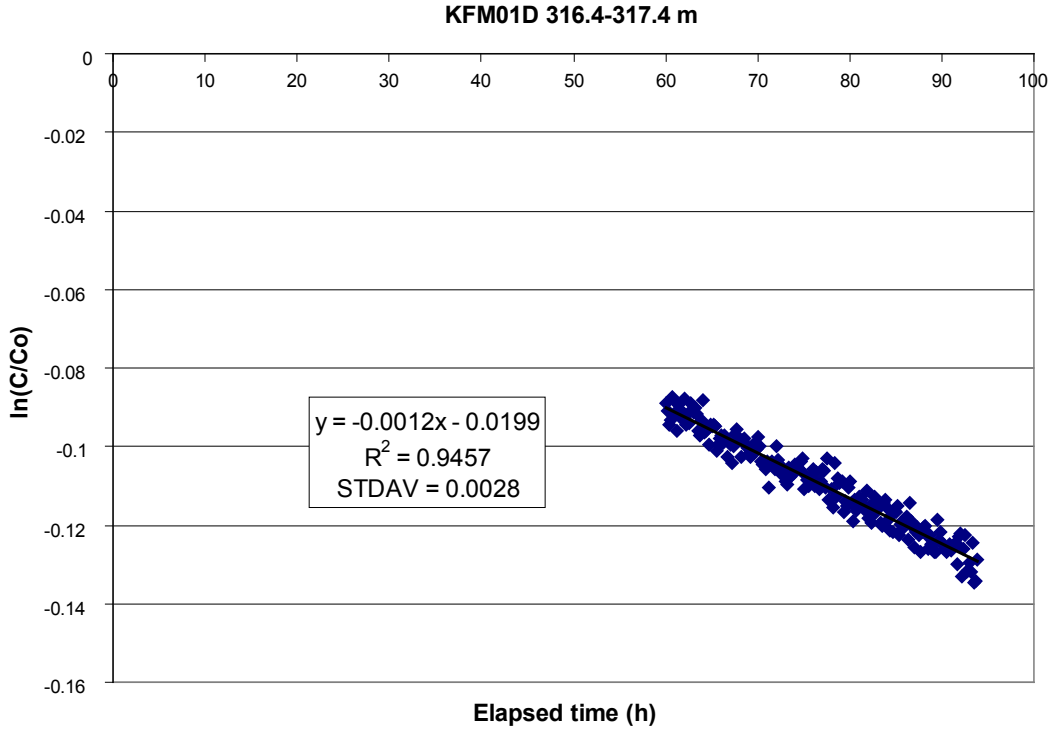

Figure 5-7. *Linear regression best fit to data from dilution measurement in borehole KFM01D, section 316.4–317.4 m.*

5.2.3 KFM01D, section 377.4–378.4 m

This dilution measurement was carried out in a test section with a single flowing fracture. The background measurement, tracer injection and dilution can be followed in Figure 5-1. Background concentration (0.049 mg/l) is measured for about 19 hours with the packers inflated. The Uranine tracer is injected in six steps and after mixing it reaches a start concentration of 1.61 mg/l above background. Dilution is measured for about 112 hours, thereafter the packers are deflated. Hydraulic pressure is stable but shows small diurnal pressure variations due to earth tidal effects (Figure 5-2) The final evaluation was made from 104 to 166 hours of elapsed time where the regression line fits well to the slope of the dilution with a correlation coefficient of $R^2 = 0.9976$ for the best fit line (Figure 5-3). The groundwater flow rate, calculated from the best fit line, is 0.079 ml/min. Calculated hydraulic gradient is 0.03 and Darcy velocity $8.7 \cdot 10^{-9}$ m/s. According to the Pipe String System (section 373.6–378.6 m, no fractures added) the flow regime correlates to a Pseudo-linear flow regime (PLF) transitioning into a PRF in the injection phase. This is interpreted as a single fracture of channel flow transferring to a fracture system in one plane. The recovery phase possibly displays a PRF transferring to a PLF.

5.2.4 KFM01D, section 431.0–432.0 m

This dilution measurement was carried out with the dye tracer Uranine in a test section with a single flowing fracture. The background measurement, tracer injection and dilution can be followed in Figure 5-8. Background concentration (0.056 mg/l) is measured for about 20 minutes. Thereafter the Uranine tracer is injected in two steps and after mixing it finally reaches a start concentration of 1.41 mg/l above background. Dilution is measured for about 64 hours. Thereafter the packers are deflated and the remaining tracer flows out of the test section. Hydraulic pressure shows a decreasing trend at the beginning (Appendix B4). Therefore, the first part of the dilution curve was excluded and the final evaluation was made on the 65 to 96 hours part of the dilution curve where the pressure is stable. The regression line fits well to the ln (C/C_0) versus time data with a correlation coefficient of $R^2 = 0.9866$ for the best fit line (Figure 5-9). The groundwater flow rate, calculated from the best fit line, is 0.173 ml/min. Calculated hydraulic gradient is 0.019 and Darcy velocity $1.9 \cdot 10^{-8}$ m/s. The Pipe String System measurement for the section 428.6–433.6 m (no fractures outside the dilution test section) shows the flow regime PRF for the injection phase. The recovery starts with a short initial wellbore storage (WBS) transitioning into a PRF and a Pseudo-spherical flow regime (PSF) at the end. The interpretation of the flow regimes gives a fracture system in one plane transferring to a net of fractures and flow paths.

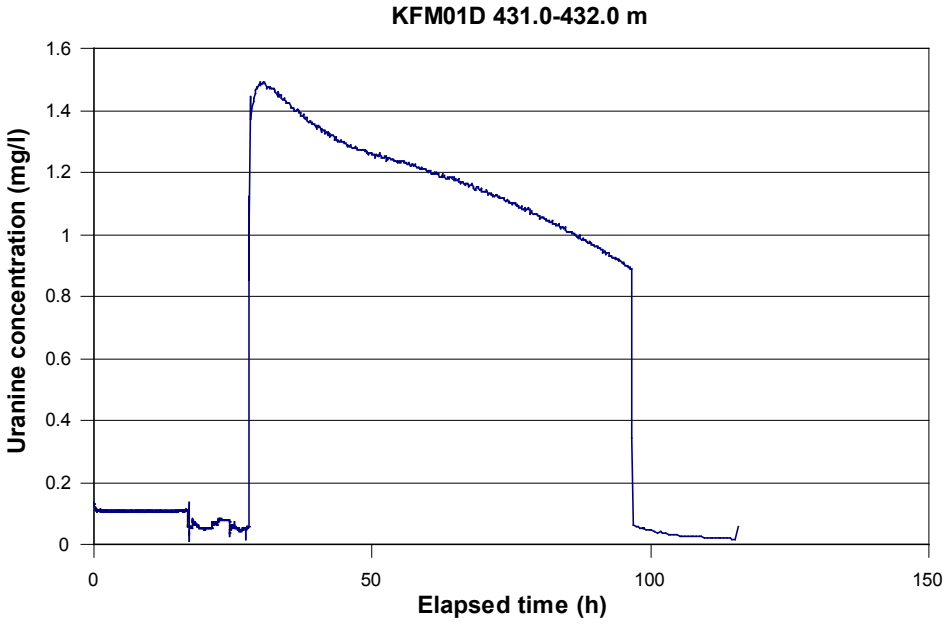

Figure 5-8. *Dilution measurement in borehole KFM01D, section 431.0–432.0 m. Uranine concentration versus time.*

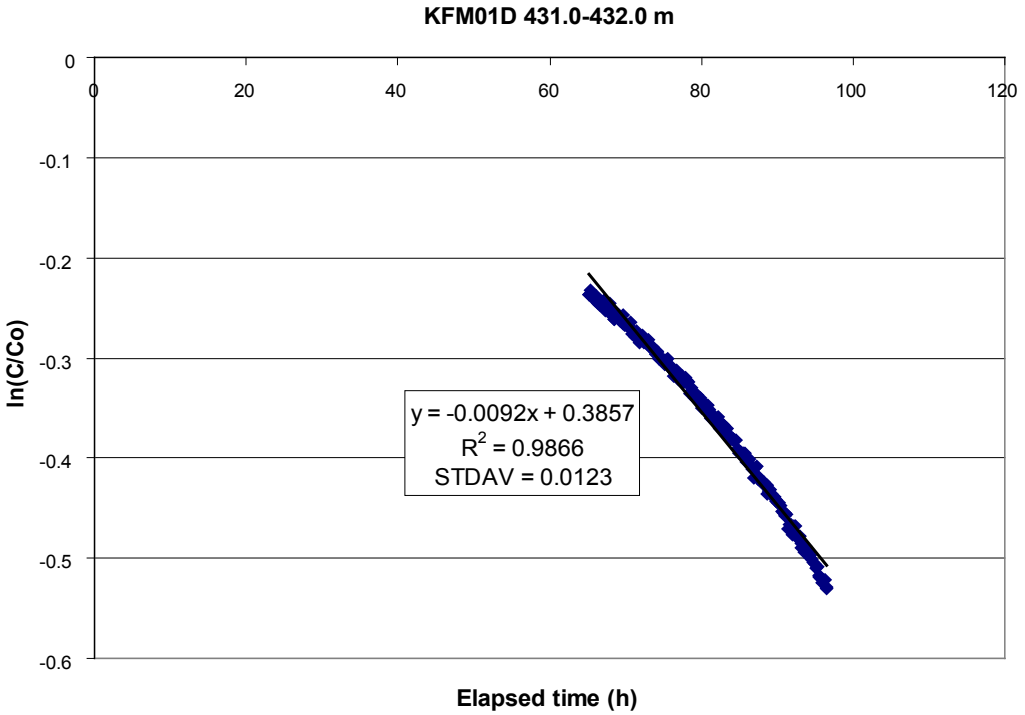

Figure 5-9. *Linear regression best fit to data from dilution measurement in borehole KFM01D, section 431.0–432.0 m.*

5.2.5 KFM01D, section 570.7–571.7 m

This dilution measurement was carried out with the dye tracer Uranine in a test section with a single flowing fracture. The background measurement, tracer injection and dilution can be followed in Figure 5-10. Due to high particle content in the section, circulation of the section water is required for about 18 hours to improve the visibility before tracer injection. Background concentration (0.012 mg/l) is measured during the circulation. Thereafter the Uranine tracer is injected in nine steps and after mixing it finally reaches a start concentration of 0.52 mg/l above background. Dilution is measured for about 290 hours. Thereafter the packers are deflated and the remaining tracer flows out of the test section. Hydraulic pressure is stable but shows small diurnal pressure variations due to earth tidal effects (Appendix B5). The regression line fits well to the ln (C/C_0) versus time data with a correlation coefficient of $R^2 = 0.9932$ for the best fit line (Figure 5-11). The groundwater flow rate, calculated from the best fit line, is 0.015 ml/min. Calculated hydraulic gradient is 0.130 and Darcy velocity $1.6 \cdot 10^{-9}$ m/s. The hydraulic gradient is large and may be caused by local effects, where the measured fracture constitutes a hydraulic conductor between other fractures with different hydraulic heads, or may only be apparently high due to wrong estimates of the correction factor, α, and/or the hydraulic conductivity of the fracture. The hydraulic transmissivity of the section is near the lower limit of measurement range for the dilution probe which may decrease accuracy in determined groundwater flow rate.

According to the Pipe String System (section 568.6–573.6 m, no fractures added) the flow regime correlates to a PSF in the injection phase. The recovery phase starts with a WBS transferring to a possible PSF. As in this section, a common result in a rock unit of low transmissivity is a spherical flow regime. The flow seeks all possible flow paths in a dense medium.

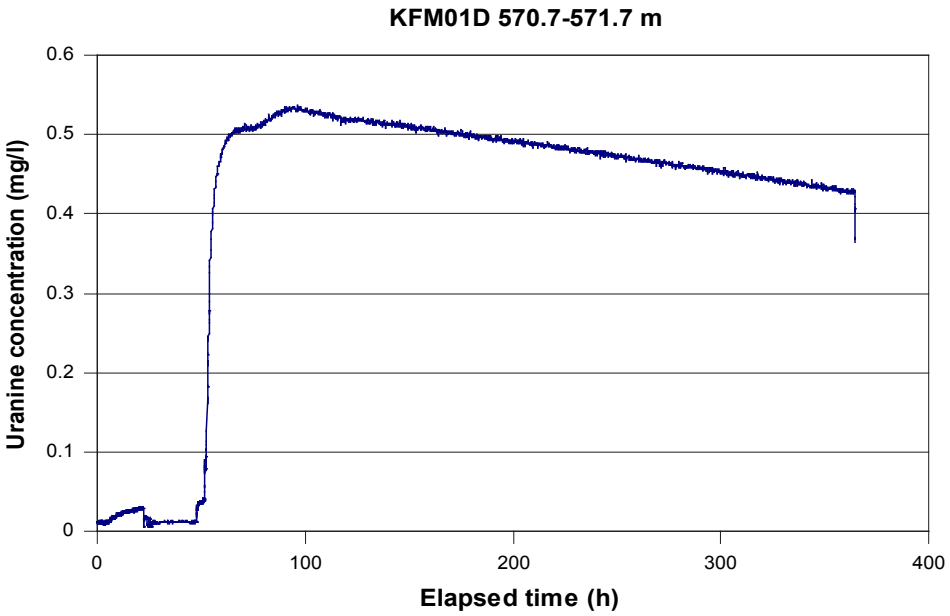

Figure 5-10. *Dilution measurement in borehole KFM01D, section 570.7–571.7 m. Uranine concentration versus time.*

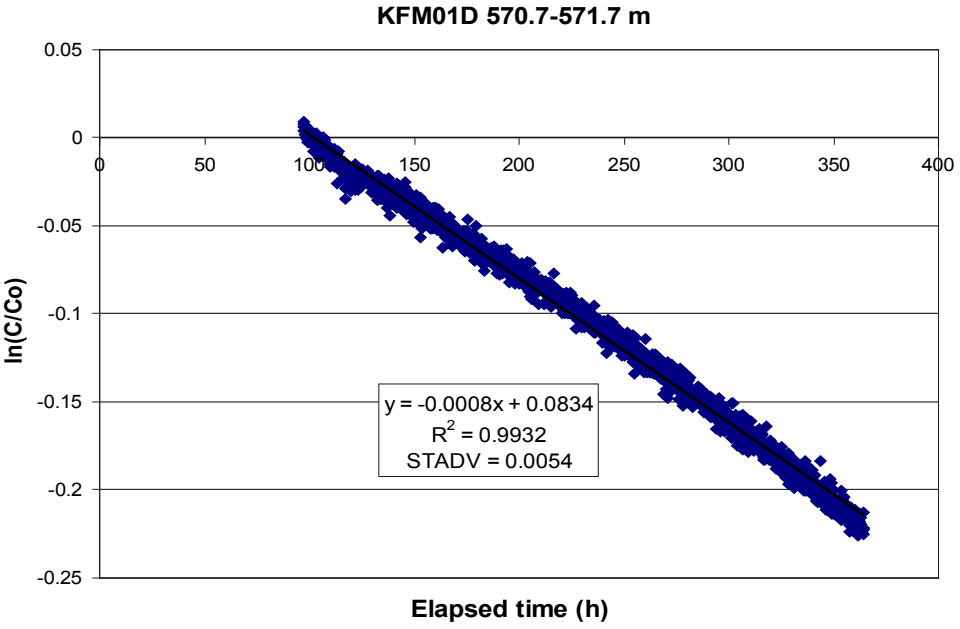

Figure 5-11. *Linear regression best fit to data from dilution measurement in borehole KFM01D, section 570.7–571.7 m.*

5.2.6 Summary of dilution results

Calculated groundwater flow rates, Darcy velocities and hydraulic gradients from all dilution measurements carried out in borehole KFM01D are presented in Table 5-1.

The results show that the groundwater flow varies during natural, i.e. undisturbed, conditions, with flow rates from 0.015 to 0.173 ml/min and Darcy velocities from $1.7 \cdot 10^{-9}$ to $1.9 \cdot 10^{-8}$ m/s. The lowest flow rate is measured in the deepest section at c 571 m borehole length (c 448 m vertical depth), which also has the lowest hydraulic transmissivity. Measured flow rate and Darcy velocity are highest in the section at c 431 m borehole length (c 344 m vertical depth), Figure 5-12 and 5-13. The hydraulic gradient is lowest in the upper sections at c 147 and c 316 m borehole length (c 120 and c 255 m vertical depth), then increasing with depth, Figure 5-14. No clear correlation between flow rate and transmissivity is indicated, Figure 5-15. In the shallow sections at c 147 and 316 m borehole length the flow rates are low in spite of high transmissivity.

Hydraulic gradient, calculated according to the Darcy concept, is large in the section at c 571 m (448 m vertical depth), Figure 5-14. It is not clear if the large gradient is caused by local effects where the measured fracture constitutes a hydraulic conductor between other fractures with different hydraulic heads or is just illusorily high due to wrong estimates of the correction factor, α, and/or the hydraulic conductivity of the fracture. The hydraulic transmissivity of the section is at the lower limit of measurement range for the dilution probe which may decrease accuracy in determined groundwater flow rate. The section at c 316 m (255 m vertical depth) shows low hydraulic gradient. The Pipe String System indicates high transmissivity in the region close to the borehole confined by a denser border around. This gives low hydraulic gradient in proportion to the T-value. In the other measured sections the hydraulic gradient is within the expected range.

Table 5-1. Groundwater flow rates, Darcy velocities and hydraulic gradients for all measured sections in borehole KFM01D.

Borehole	Test section (m)+	T (m^2/s)*	Q (ml/min)	Q (m^3/s)	Darcy velocity (m/s)	Hydraulic gradient	Flow regime++ according to the Pipe String System**
KFM01D	147.5–148.5 (120–121)	5.32E–06	0.021	3.51E–10	2.32E–09	0.0004	PRF PRF/PSS?
KFM01D	316.4–317.4 (255–256)	1.65E–05	0.021	3.51E–10	2.32E–09	0.0001	NFB PRF → NFB
KFM01D	377.4–378.4 (302–303)	3.15E–07	0.079	1.32E–09	8.69E–09	0.030	PLF → PRF PRF? → PLF
KFM01D	431.0–432.0 (344–345)	9.95E–07	0.173	2.88E–09	1.90E–08	0.019	PRF (WBS) → PRF → PSF
KFM01D	570.7–571.7 (448–449)	1.27E–08	0.015	2.50E–10	1.65E–09	0.130	PSF WBS → PSF?

* /Väisäsvaara et al. 2006/
** /Florberger et al. 2006/
\+ Test section vertical depth is given within brackets.
++ Injection phase and recovery phase.

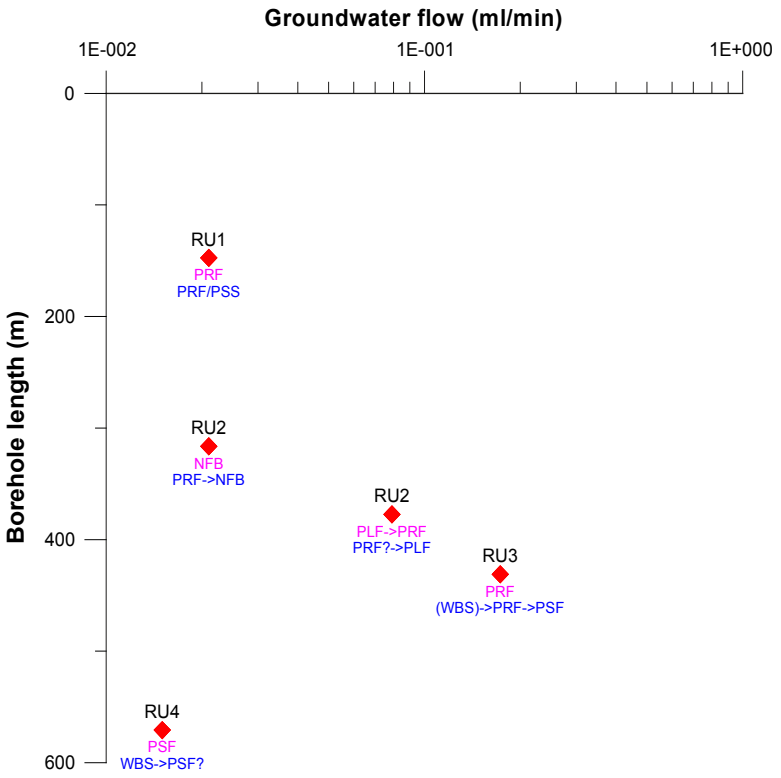

Figure 5-12. *Groundwater flow rate versus borehole length during natural hydraulic gradient conditions. Results from dilution measurements in single fractures in borehole KFM01D. Labels RU1-RU4 refer to rock unit notation /Carlsten et al. 2006/. Labels WBS, PRF, PLF, PSF, PSS and NFB refer to defined flow regimes (injection phase pink, recovery phase blue) /Florberger et al. 2006/.*

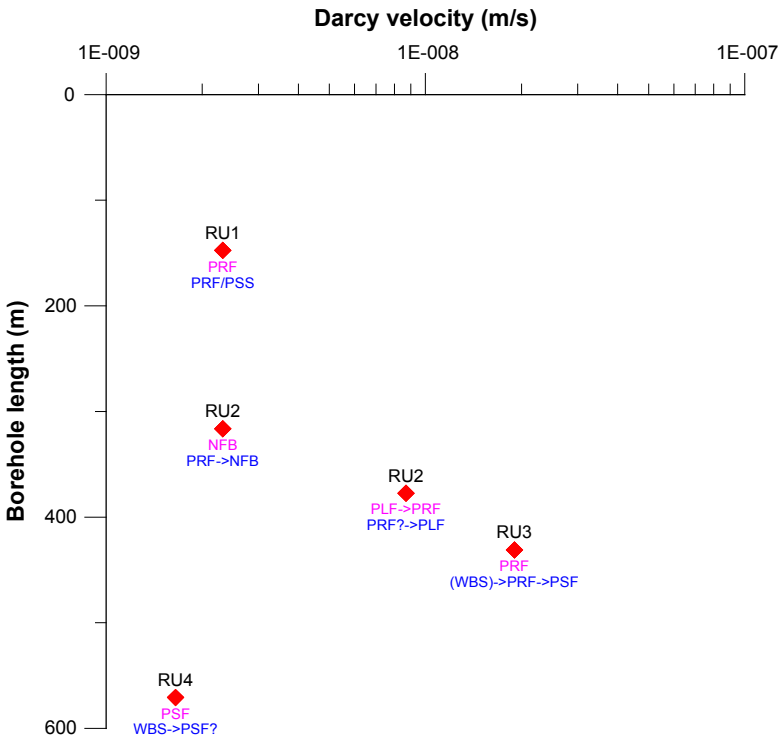

Figure 5-13. *Darcy velocity versus borehole length during natural hydraulic gradient conditions. Results from dilution measurements in single fractures in borehole KFM01D. Labels RU1-RU4 refer to rock unit notation /Carlsten et al. 2006/. Labels WBS, PRF, PLF, PSF, PSS and NFB refer to defined flow regimes (injection phase pink, recovery phase blue) /Florberger et al. 2006/.*

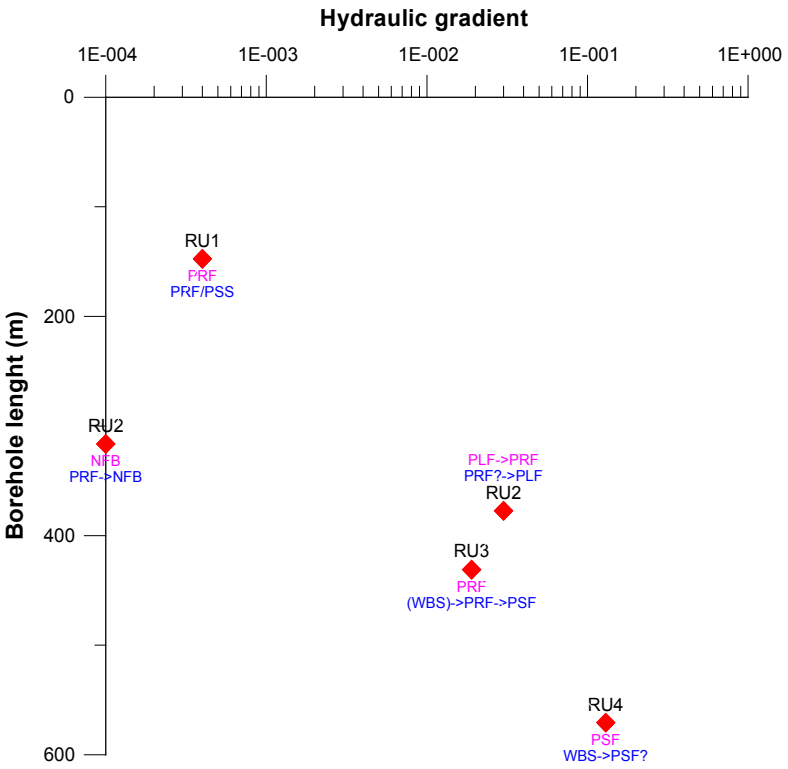

Figure 5-14. *Hydraulic gradient versus borehole length during natural hydraulic gradient conditions. Results from dilution measurements in single fractures in borehole KFM01D. Labels RU1-RU4 refer to rock unit notation /Carlsten et al. 2006/. Labels WBS, PRF, PLF, PSF, PSS and NFB refer to defined flow regimes (injection phase pink, recovery phase blue) /Florberger et al. 2006/.*

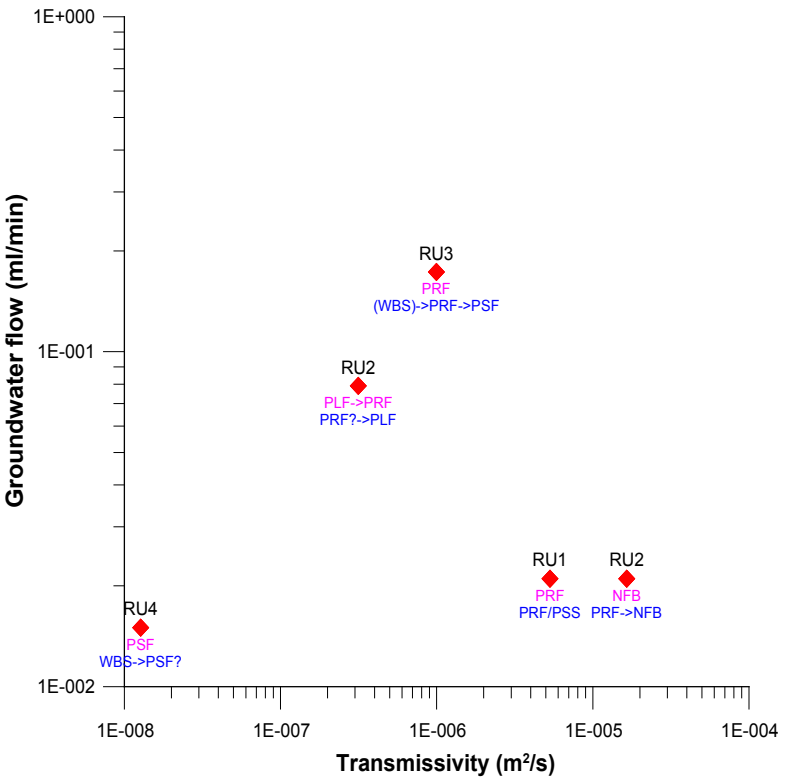

Figure 5-15. *Groundwater flow rate versus transmissivity during undisturbed, i.e. natural hydraulic gradient conditions. Results from dilution measurements in single fractures in borehole KFM01D. Labels RU1-RU4 refer to rock unit notation /Carlsten et al. 2006/. Labels WBS, PRF, PLF, PSF, PSS and NFB refer to defined flow regimes (injection phase pink, recovery phase blue) /Florberger et al. 2006/.*

5.3 SWIW tests

5.3.1 Treatment of experimental data

The experimental data presented in this section have been corrected for background concentrations. Sampling times have been adjusted to account for residence times in injection and sampling tubing. Thus, time zero does in all plots refer to when the fluid containing the tracer mixture begins to enter the tested borehole section.

5.3.2 Tracer recovery breakthrough in KFM01D, 377.4–378.4 m

Durations and flows for the various experimental phases are summarised in Table 5-2. Injected mass and start concentration in the section for the three tracers are given in Table 5-3.

The experimental breakthrough curves from the recovery phase for Uranine, rubidium, and cesium, respectively, are shown in Figures 5-16a to 5-16c. The time coordinates are corrected for residence time in the tubing, as described above, and concentrations are normalised through division by the total injected tracer mass.

Table 5-2. Durations (h) and fluid flows (L/h) during various experimental phases for section 377.4–378.4 m in borehole KFM01D. All times have been corrected for tubing residence time so that time zero refers to the time when the tracer mixture begins to enter the borehole section.

Phase	Start (h)	Stop (h)	Volume (L)	Average flow (L/h)	Cumulative injected volume (L)
Pre-injection	–1.26	0.00	17.4	13.8	17.4
Tracer injection	0.00	0.89	11.9	13.4	29.3
Chaser injection	0.98	7.33	88.9	13.8	118.2
Recovery	7.33	255.39	3,394	13.8	

Table 5-3. Injected mass (mg) and start concentration (mg/l) for section 377.4–378.4 m in borehole KFM01D.

Tracer	Injected mass (mg)	Start concentration (mg/l)
Uranine	1,040	84.90
Cesium	665	54.29
Rubidium	1,570	128.16

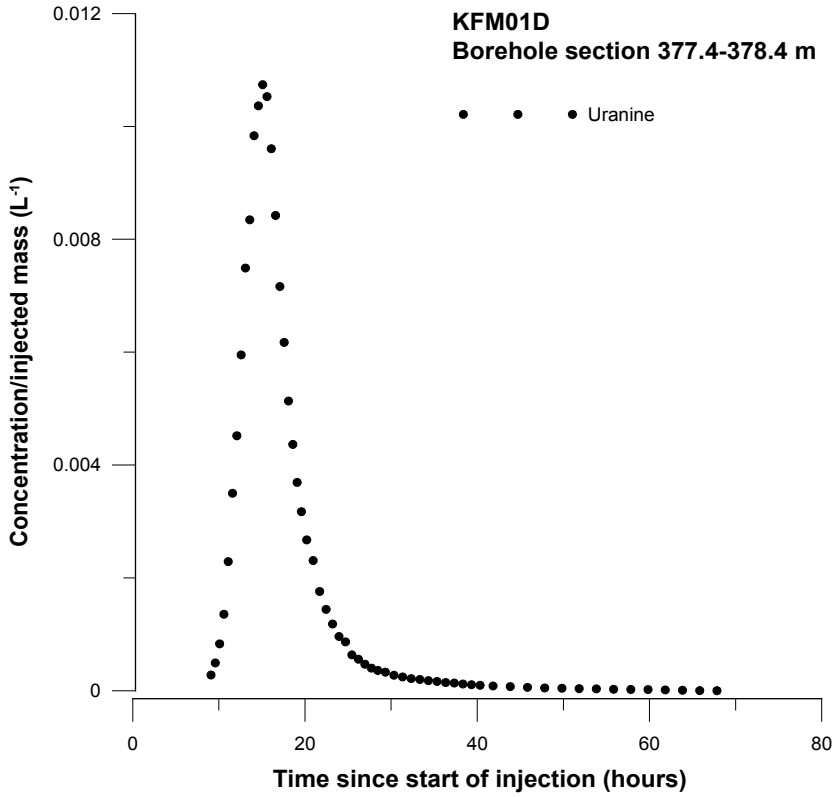

Figure 5-16a. *Normalised withdrawal (recovery) phase breakthrough curve for Uranine in section 377.4–378.4 m in borehole KFM01D.*

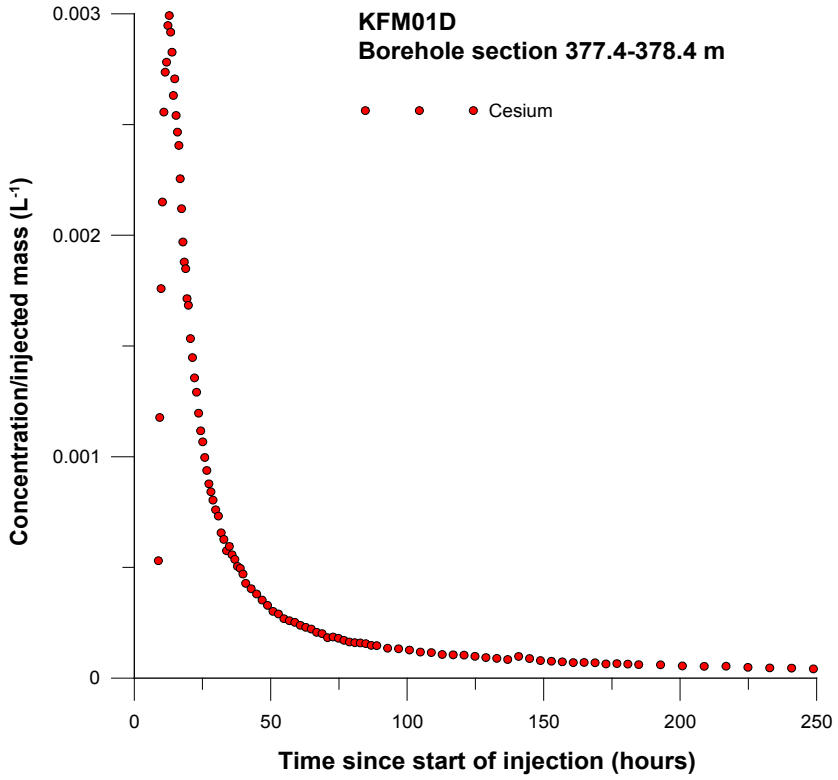

Figure 5-16b. *Normalised withdrawal (recovery) phase breakthrough curve for cesium in section 377.4–378.4 m in borehole KFM01D.*

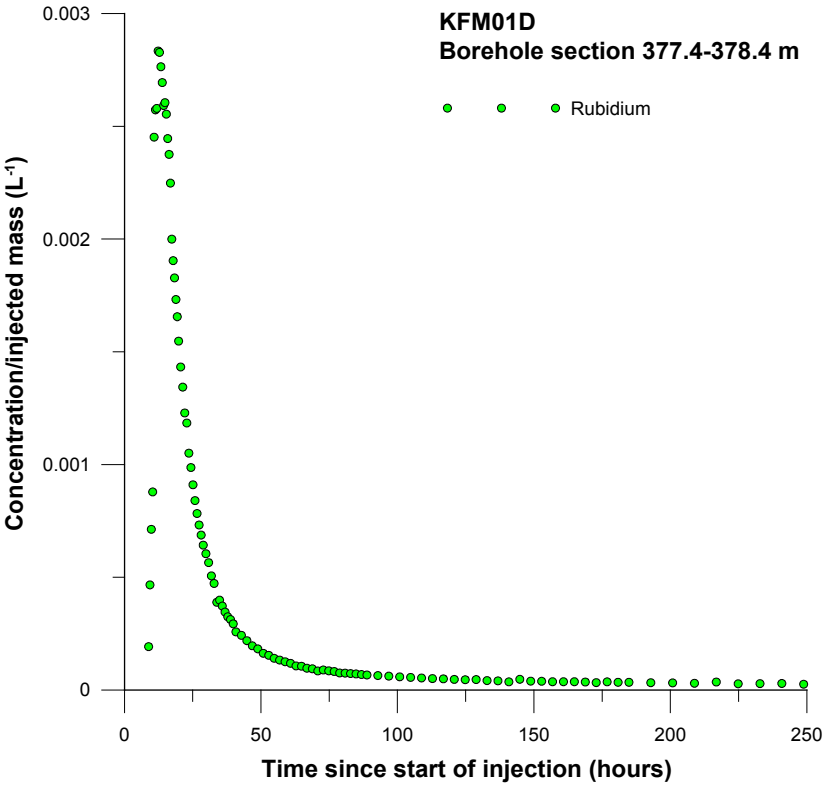

Figure 5-16c. *Normalised withdrawal (recovery) phase breakthrough curve for rubidium in section 377.4–378.4 in borehole KFM01D.*

Normalised breakthrough curves (concentration divided by total injected tracer mass) for all three tracers are plotted in Figure 5-17a and 5-17b. The considerable difference between Uranine and the two other curves may be seen as an indication of a relatively strong retardation effect for cesium and rubidium. The breakthrough curves conform to what would be expected from a SWIW test using tracers of different sorption properties. The figures indicate similar tracer behaviour as in previously performed SWIW tests within the site investigation programmes /Gustafsson and Nordqvist 2005, Gustafsson et al. 2005, 2006ab, Thur et al. 2007/, where the appearance of breakthrough curves for sorbing tracers have been relatively consistent with standard models of flow and transport during a SWIW test.

Tracer recovery based on available experimental data results in values of 104% for Uranine, 92% for cesium and 68% for rubidium. These estimates are based on the average pumping flow rate during the recovery phase. From all SWIW tests in the SKB site specific programmes in Forsmark and Oskarshamn, these are the most complete recoveries. Recovery larger than 100% for Uranine most probably emanates from Uranine labelled drilling flushing water and the uncertainty in the tracer analysis.

Plausible visual extrapolations of the curves do not clearly indicate incomplete recovery and that the tracer recovery would be different among the three tracers. Thus, for the subsequent model evaluation, it is assumed that tracer recovery is the same for all of the tracers.

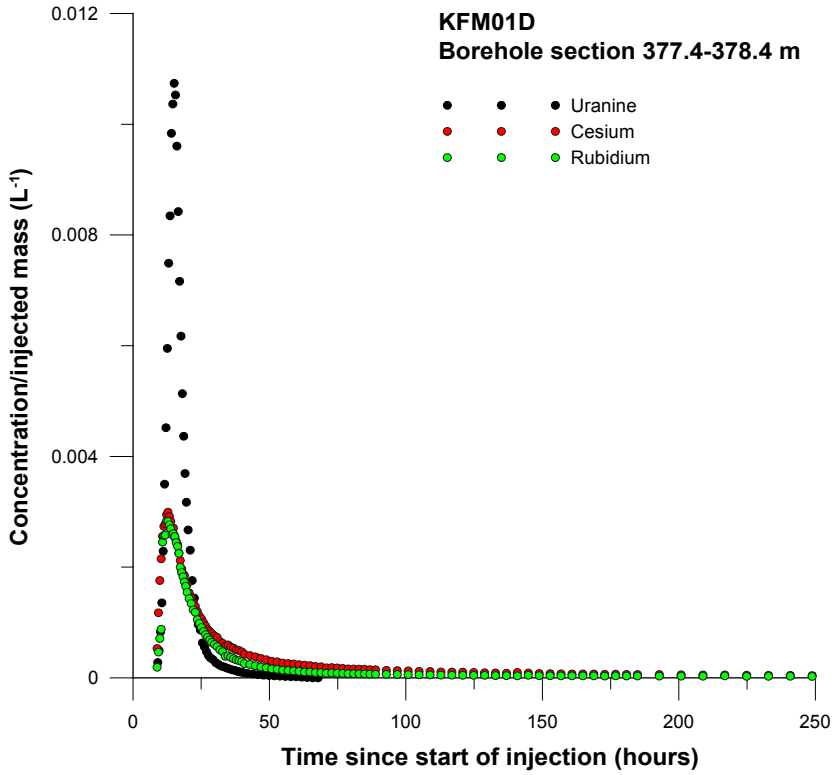

Figure 5-17a. *Normalised withdrawal (recovery) phase breakthrough curves for Uranine, cesium and rubidium in section 377.4–378.4 m, linear scale.*

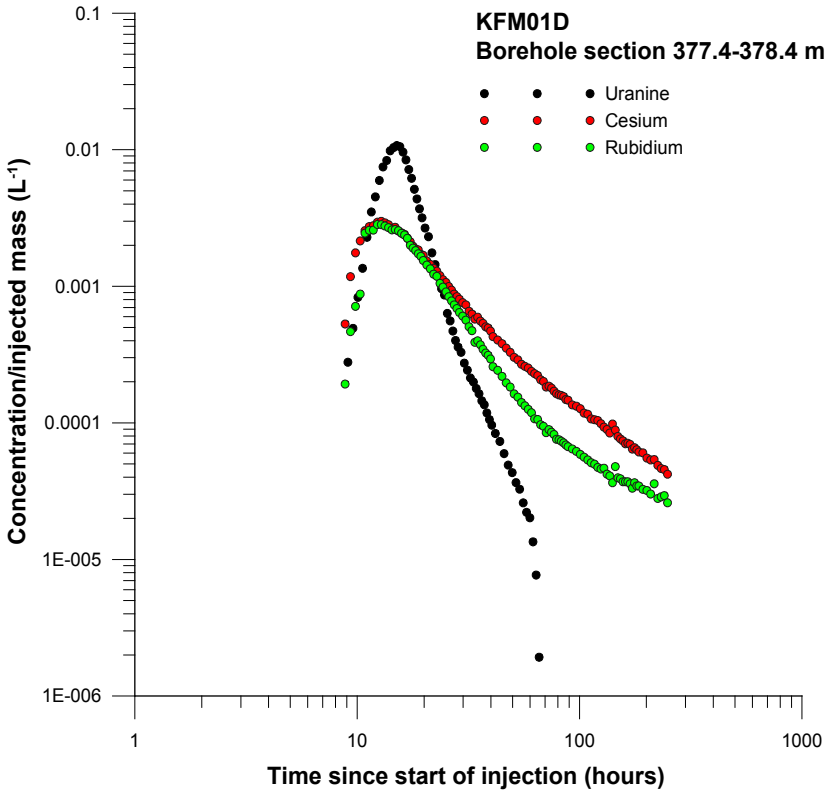

Figure 5-17b. *Normalised withdrawal (recovery) phase breakthrough curves for Uranine, cesium and rubidium in section 377.4–378.4 m, logarithmic scale.*

5.3.3 Model evaluation KFM01D, 377.4–378.4 m

The model simulations were carried out assuming negligible hydraulic background gradient, i.e. radial flow. The simulated times and flows for the various experimental phases are given in Table 5-2. In the simulation model, the flow zone is approximated by a 0.1 m thick fracture zone.

The experimental evaluation was carried out by simultaneous model fitting of Uranine and a sorbing tracer as outlined in Section 4.4. Thus, separate regression analyses were carried out for simultaneous fitting of Uranine/cesium and Uranine/rubidium, respectively.

For a given regression run, estimation parameters were longitudinal dispersivity (a_L) and a linear retardation factor (R), while the porosity is given a fixed value. Regression was carried out for five different values of porosity: 0.002, 0.005, 0.01, 0.02 and 0.05. For all cases, the fits between model and experimental data are similar. Example of model fits are shown in Figure 5-18a, 5-18b, 5-18c and 5-18d.

The model fits to the experimental breakthrough curves are generally fairly good, although some discrepancies can be noted. In the tailing part of the Uranine curve, the simulated curve levels out to background values faster than the experimental curve, while the tailing parts for cesium and rubidium are slower than the simulated. Further, the simulated peaks for cesium and rubidium, respectively, occur somewhat earlier than the observed peaks.

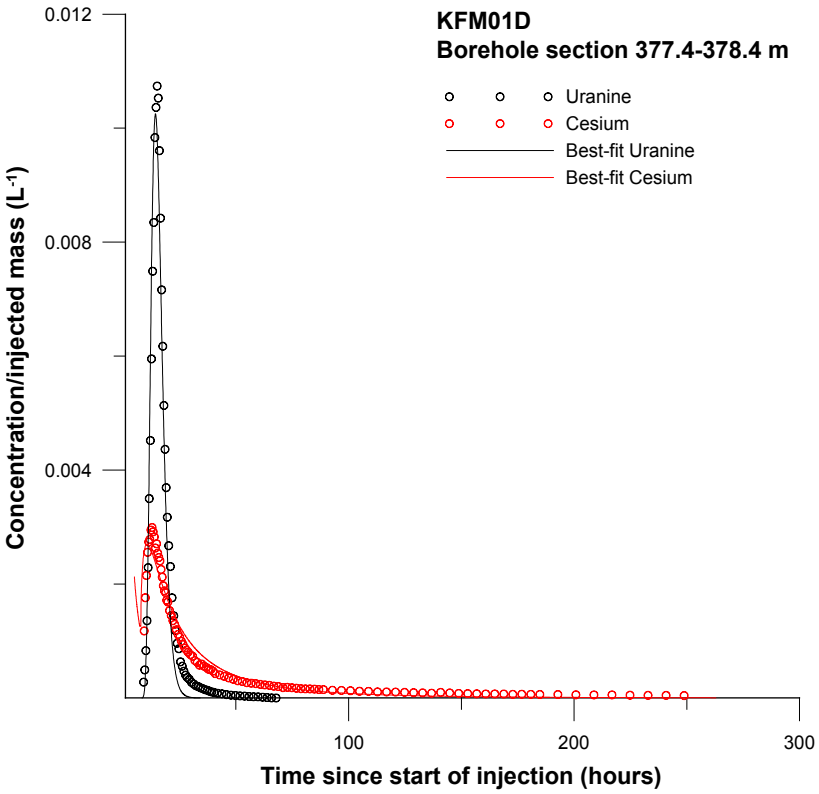

Figure 5-18a. *Example of simultaneous fitting of Uranine and cesium for section 377.4–378.4 m in borehole KFM01D, linear scale.*

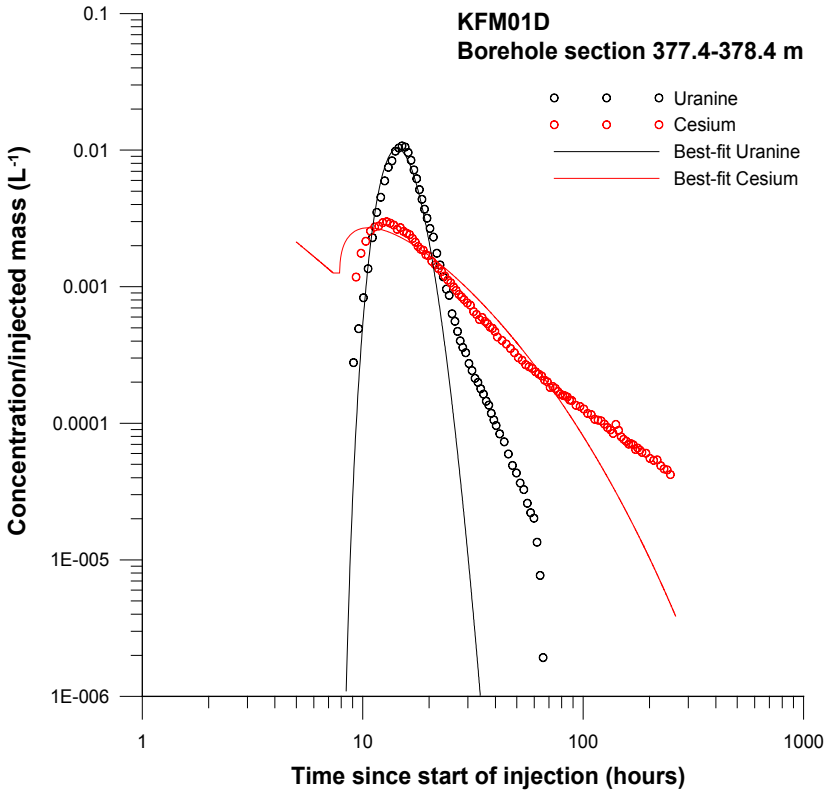

Figure 5-18b. *Example of simultaneous fitting of Uranine and cesium for section 377.4–378.4 m in borehole KFM01D, logarithmic scale.*

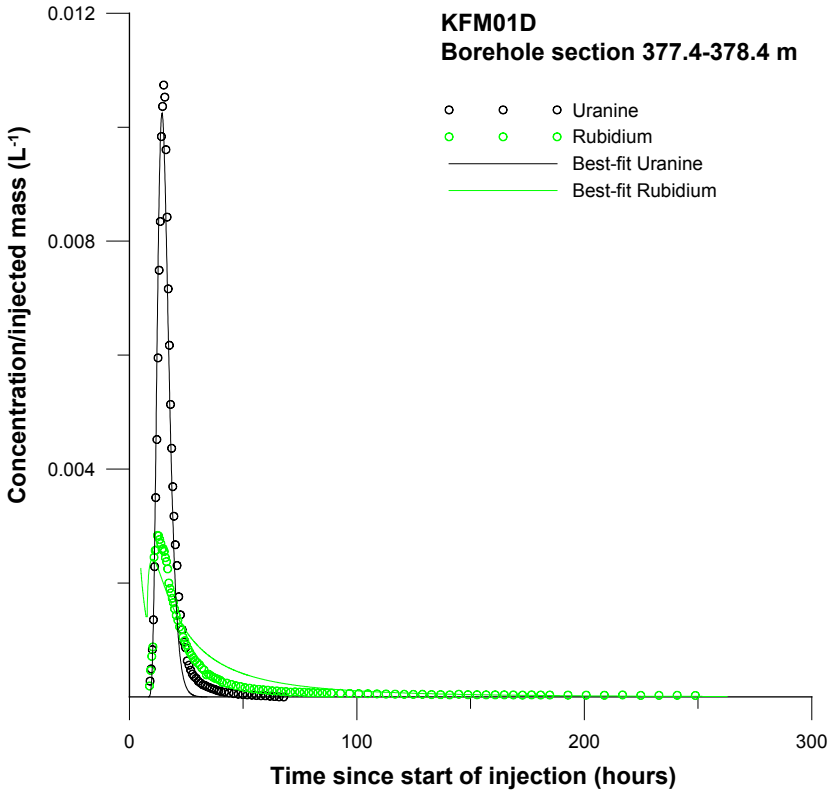

Figure 5-18c. *Example of simultaneous fitting of Uranine and rubidium for section 377.4–378.4 m in borehole KFM01D, linear scale.*

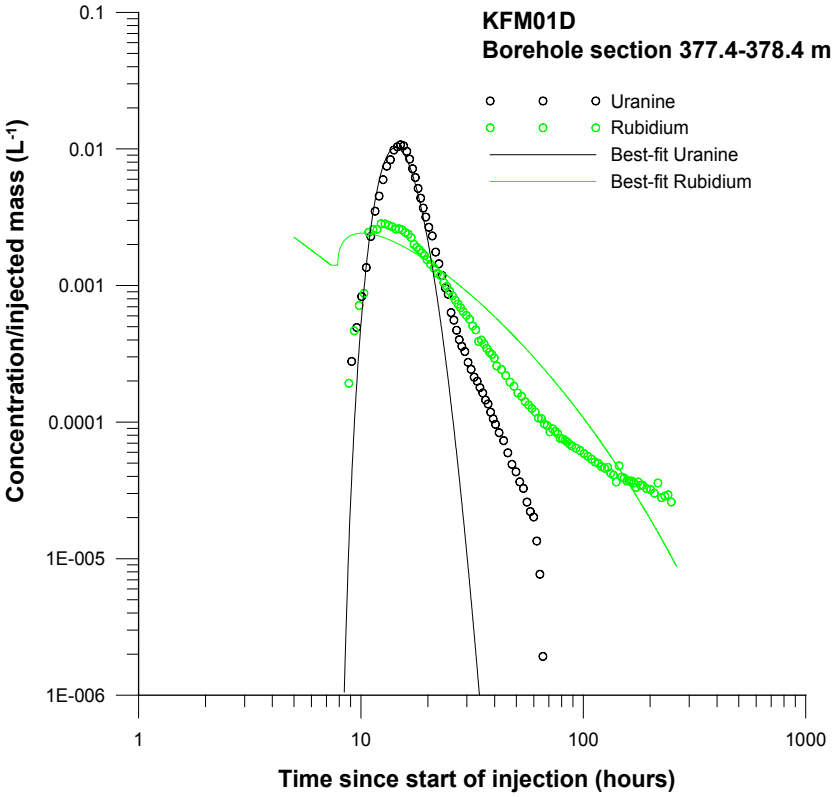

Figure 5-18d. *Example of simultaneous fitting of Uranine and rubidium for section 377.4–378.4 m in borehole KFM01D, linear scale.*

All of the regression runs (Tables 5-4a and 5-4b) resulted in similar values of the retardation coefficient for each sorbing tracer, while the estimated values of the longitudinal dispersivity are strongly dependent on the assumed porosity value. Both of these observations are consistent with prior expectations of the relationships between parameters in a SWIW test /Nordqvist and Gustafsson 2004, Gustafsson and Nordqvist 2005, Gustafsson et al. 2005, 2006ab, Thur et al. 2007/.

The estimated values of R for cesium (496–548) and rubidium (848–960) indicate very strong sorption effects, and agree approximately with values from cross-hole tests, obtained using similar transport models (advection-dispersion and linear sorption) /Nordqvist and Gustafsson 2004, Gustafsson and Nordqvist 2005, Gustafsson et al. 2005, 2006ab, Thur et al. 2007/. As a comparison, in previous SWIW tests, the mean values of R in KLX03 are 235 for cesium and 391 for rubidium, /Gustafsson et al. 2006a/, in KFM08A 35 for cesium and 21 for rubidium, /Gustafsson et al. 2006b/ and in KLX18A 529 for cesium and 2,661 for rubidium /Thur et al. 2007/. In this test, estimated values of R for cesium are lower than for rubidium, although one may consider the values being of similar magnitudes. This is somewhat contrary to literature data from the TRUE Block Scale Project /Anderson et al. 2002/, which indicate about one order of magnitude lower values of R for rubidium than for cesium. On the other hand, the previously performed SWIW tests within the Forsmark and Oskarshamn site investigations where these three tracers have been used, resulted in more or less the same retardation factor for cesium and rubidium, respectively, with lower R for cesium than for rubidium /Gustafsson et al. 2006ab, Thur et al. 2007/.

Table 5-4a. Results of simultaneous fitting of Uranine and cesium for section 377.4–378.4 m in borehole KFM01D. Approximate values of the coefficient of variation (estimation standard error divided by the estimated value) are given within parenthesis.

Porosity (fixed)	a_L (estimated)	R (estimated)
0.002	0.31 (0.05)	548 (0.19)
0.005	0.20 (0.05)	542 (0.19)
0.01	0.14 (0.05)	535 (0.19)
0.02	0.10 (0.05)	523 (0.19)
0.05	0.06 (0.05)	496 (0.18)

Table 5-4b. Results of simultaneous fitting of Uranine and rubidium for section 377.4–378.4 m in borehole KFM01D. Approximate values of the coefficient of variation (estimation standard error divided by the estimated value) are given within parenthesis.

Porosity (fixed)	a_L (estimated)	R (estimated)
0.002	0.31 (0.05)	960 (0.23)
0.005	0.20 (0.05)	948 (0.23)
0.01	0.14 (0.05)	930 (0.23)
0.02	0.10 (0.05)	903 (0.22)
0.05	0.06 (0.05)	848 (0.22)

5.3.4 Tracer recovery breakthrough in KFM01D, 431.0–432.0 m

Durations and flows for the various experimental phases are summarised in Table 5-5. Injected mass and start concentration in the section for the three tracers are given in Table 5-6.

The experimental breakthrough curves from the recovery phase for Uranine, rubidium, and cesium, respectively, are shown in Figures 5-19a to 5-19c. The time coordinates are corrected for residence time in the tubing, as described above, and concentrations are normalised through division by the total injected tracer mass.

Table 5-5. Durations (h) and fluid flows (L/h) during various experimental phases for section 431.0–432.0 m in borehole KFM01D. All times have been corrected for tubing residence time so that time zero refers to the time when the tracer mixture begins to enter the borehole section.

Phase	Start (h)	Stop (h)	Volume (L)	Average flow (L/h)	Cumulative injected volume (L)
Pre-injection	–1.27	0.00	17.2	13.83	17.2
Tracer injection	0.00	0.92	13.8	4.17	31.0
Chaser injection	0.92	7.37	87.6	3.77	118.6
Recovery	7.51	329.33	4,427	3.84	

Table 5-6. Injected mass (mg) and start concentration (mg/l) for section 431.0–432.0 m in borehole KFM01D.

Tracer	Injected mass (mg)	Start concentration (mg/l)
Uranine	955	76.36
Cesium	673	53.84
Rubidium	1,510	120.80

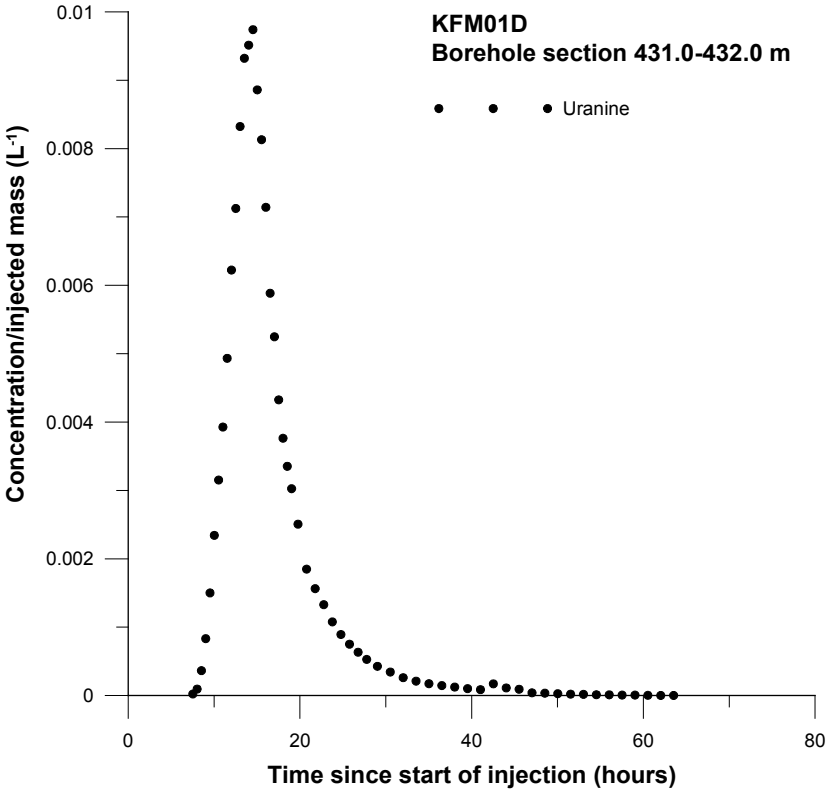

Figure 5-19a. *Normalised withdrawal (recovery) phase breakthrough curve for Uranine in section 431.0–432.0 m in borehole KFM01D.*

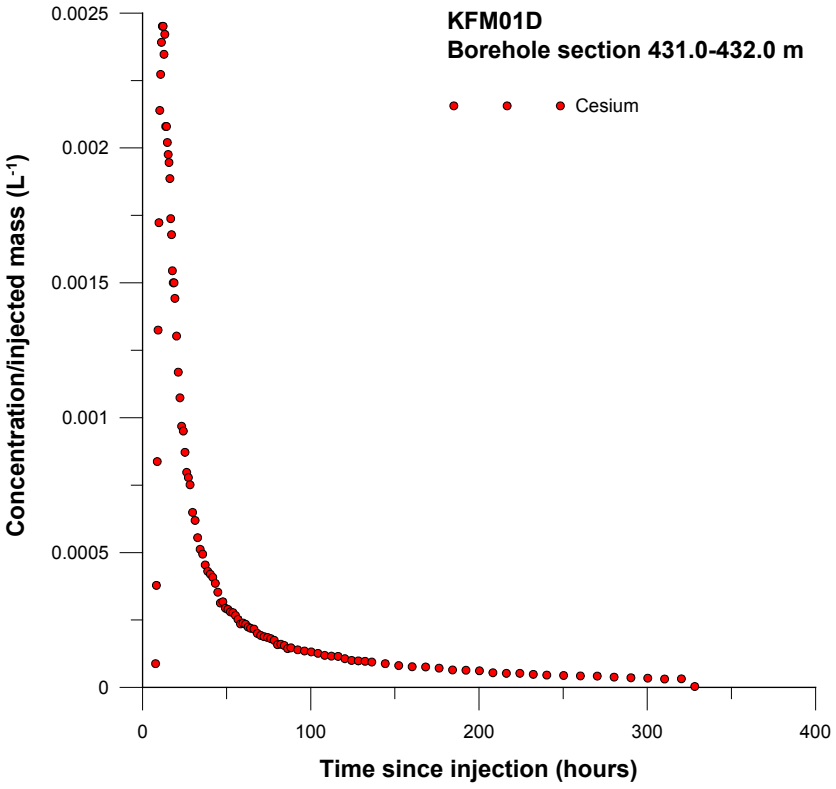

Figure 5-19b. *Normalised withdrawal (recovery) phase breakthrough curve for cesium in section 431.0–432.0 m in borehole KFM01D.*

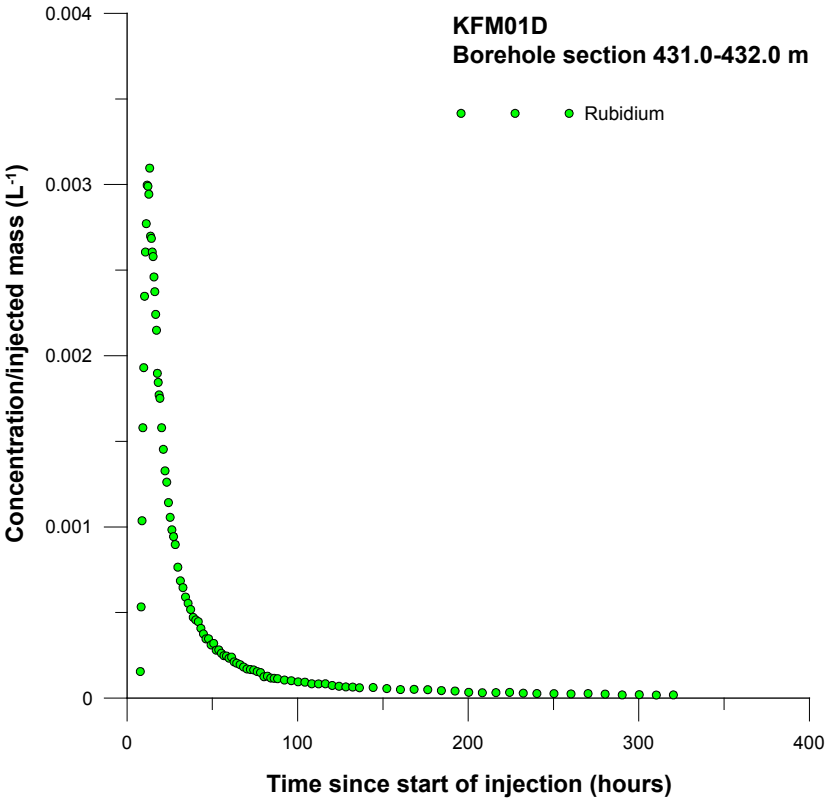

Figure 5-19c. *Normalised withdrawal (recovery) phase breakthrough curve for rubidium in section 431.0–432.0 in borehole KFM01D.*

Normalised breakthrough curves (concentration divided by total injected tracer mass) for all three tracers are plotted in Figure 5-20a and 5-20b. The considerable differences between Uranine and the two other curves may be seen as an indication of a relatively strong sorption effect for cesium and rubidium. The breakthrough curves conform to what would be expected from a SWIW test using tracers of different sorption properties. The figures indicate similar tracer behaviour as in previously performed SWIW tests within the site investigation programmes, for references see 5.2.2, where the appearance of breakthrough curves for sorbing tracers have been relatively consistent with standard models of flow and transport of SWIW tests.

The peak of the rubidium curve is higher than for cesium, which would indicate weaker sorption capacity.

The tracer recoveries for the different tracers are nearly completed and the background values are regaining. Tracer recovery based on available experimental data result in values of 102% for Uranine, 87% for cesium and 90% for rubidium. These estimates are based on the average pumping flow rate during the recovery phase. Recovery larger than 100% for Uranine most probably emanates from Uranine labelled drilling flushing water and the uncertainty in the tracer analysis.

Plausible visual extrapolations of the curves do not clearly indicate incomplete recovery and that the tracer recovery would be different among the three tracers. Thus, for the subsequent model evaluation, it is assumed that tracer recovery is the same for all of the tracers.

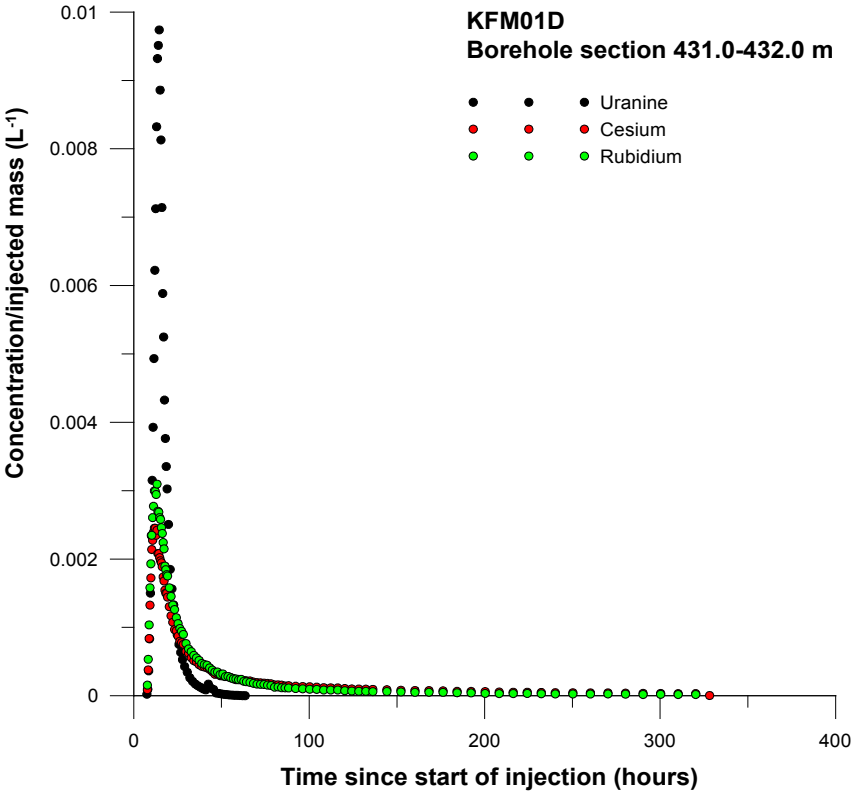

Figure 5-20a. *Normalised withdrawal (recovery) phase breakthrough curves for Uranine, cesium and rubidium in section 431.0–432.0 m, linear scale.*

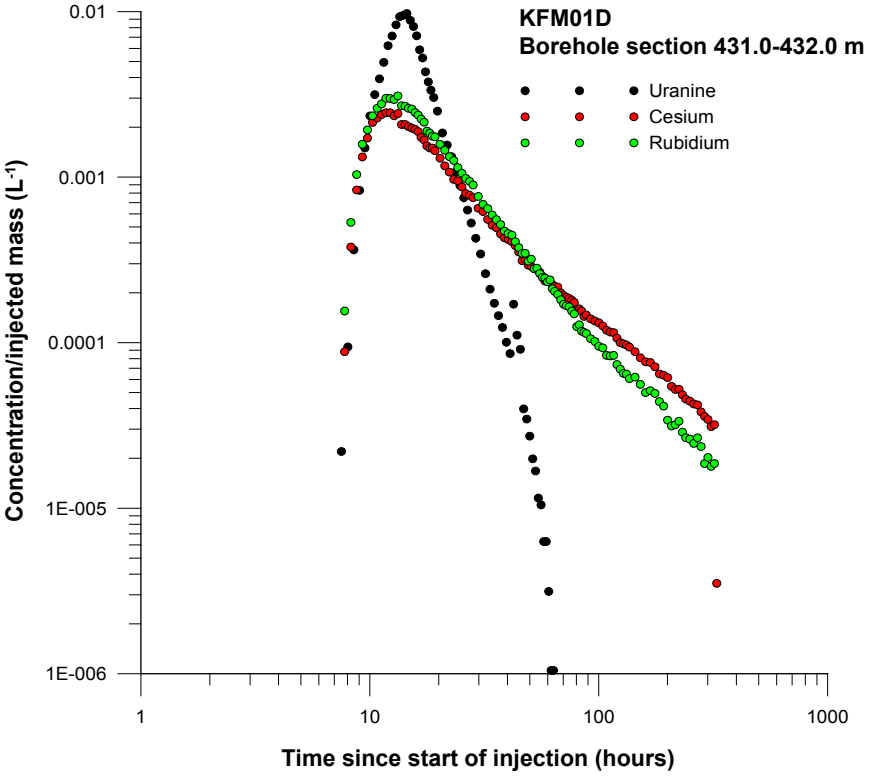

Figure 5-20b. *Normalised withdrawal (recovery) phase breakthrough curves for Uranine, cesium and rubidium in section 431.0–432.0 m, logarithmic scale.*

5.3.5 Model evaluation KFM01D, 431.0–432.0 m

The model simulations were carried out assuming negligible hydraulic background gradient, i.e. radial flow. The simulated times and flows for the various experimental phases are given in Table 5-5. In the simulation model, the flow zone is approximated by a 0.1 m thick fracture zone.

The experimental evaluation was carried out by simultaneous model fitting of Uranine and a sorbing tracer as outlined in section 4.4. Thus, separate regression analyses were carried out for simultaneous fitting of Uranine/cesium and Uranine/rubidium, respectively.

For a given regression run, estimation parameters were longitudinal dispersivity (a_L) and a linear retardation factor (R), while the porosity is given a fixed value. Regression was carried out for five different values of porosity: 0.002, 0.005, 0.01, 0.02 and 0.05. For all cases, the fits between model and experimental data are similar. Example of model fits are shown in Figure 5-21a to 5-21d.

The model fits to the experimental breakthrough curves are fairly good. The most notable discrepancy is in the tailing part of the Uranine curve where the simulated curve levels out to background values faster than the experimental curve.

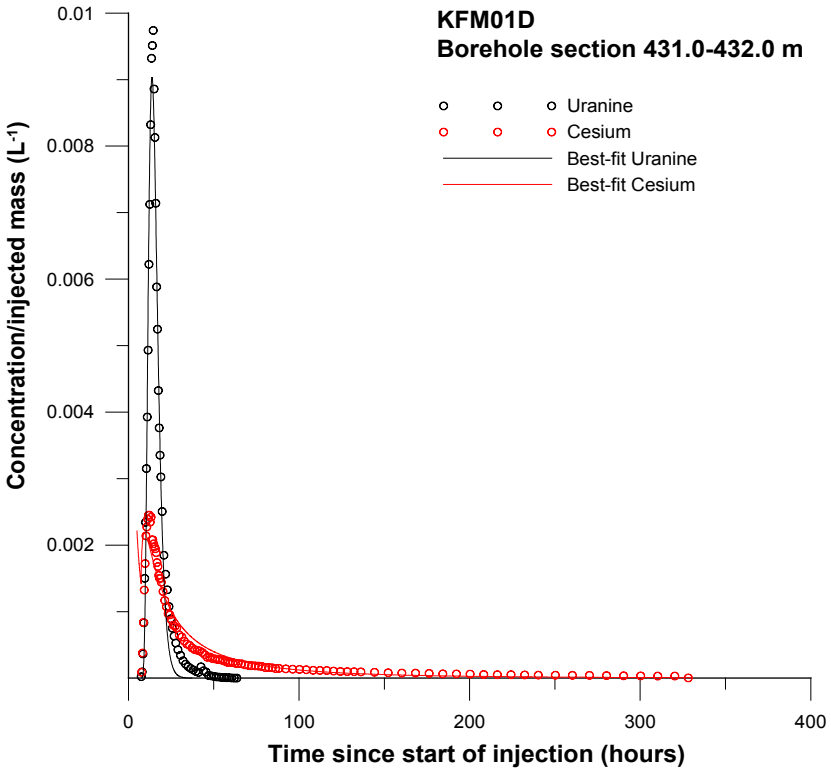

Figure 5-21a. *Example of simultaneous fitting of Uranine and cesium for section 431.0–432.0 m in borehole KFM01D, linear scale.*

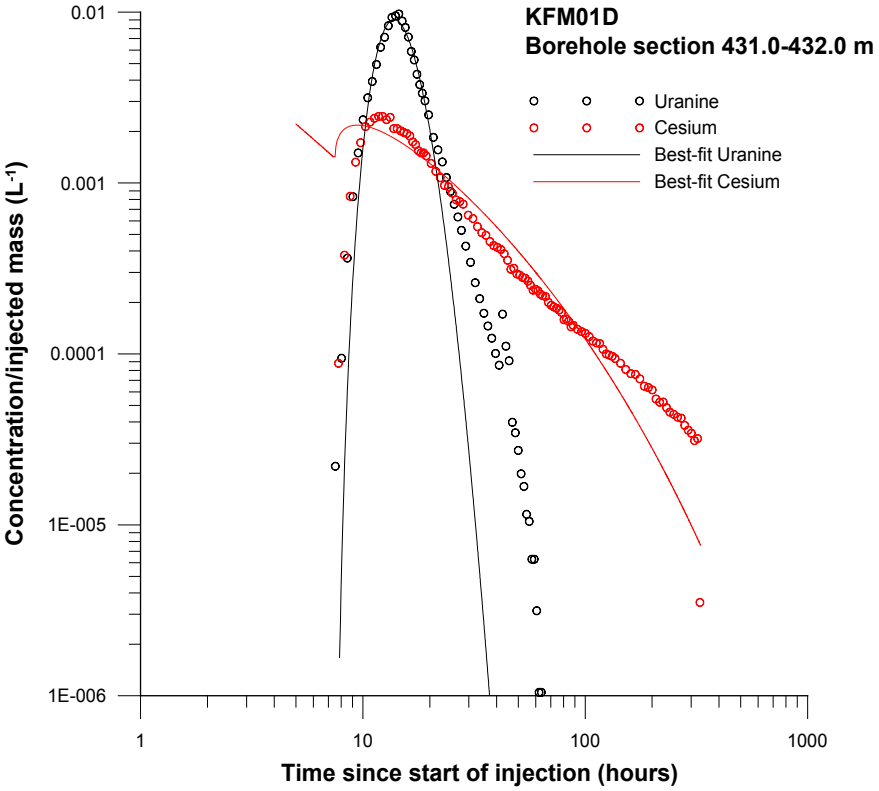

Figure 5-21b. *Example of simultaneous fitting of Uranine and cesium for section 431.0–432.0 m in borehole KFM01D, logarithmic scale.*

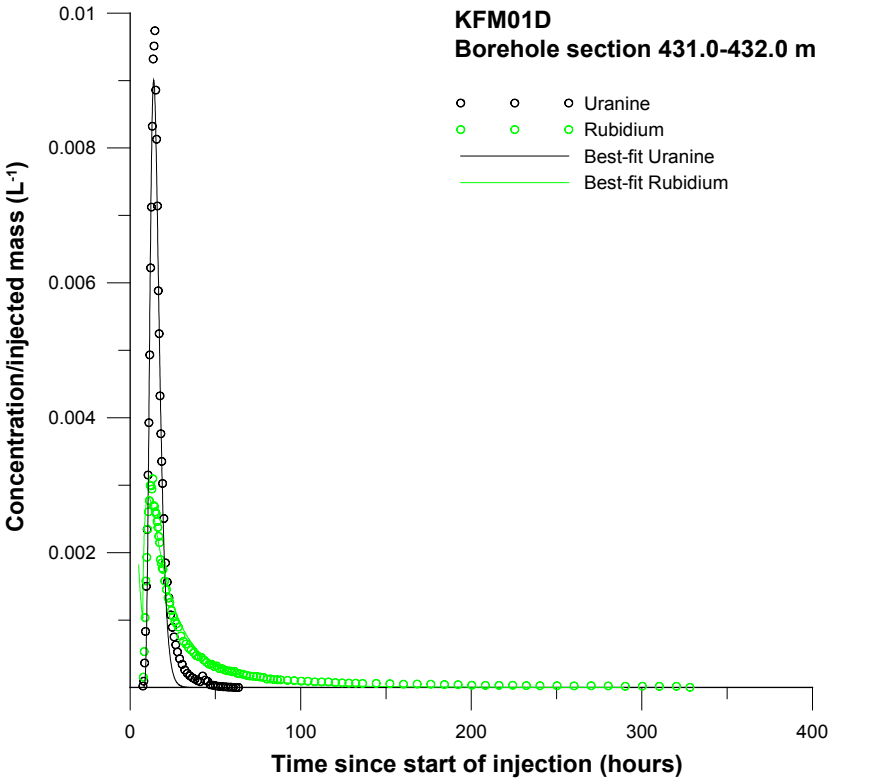

Figure 5-21c. *Example of simultaneous fitting of Uranine and rubidium for section 431.0–432.0 m in borehole KFM01D, linear scale.*

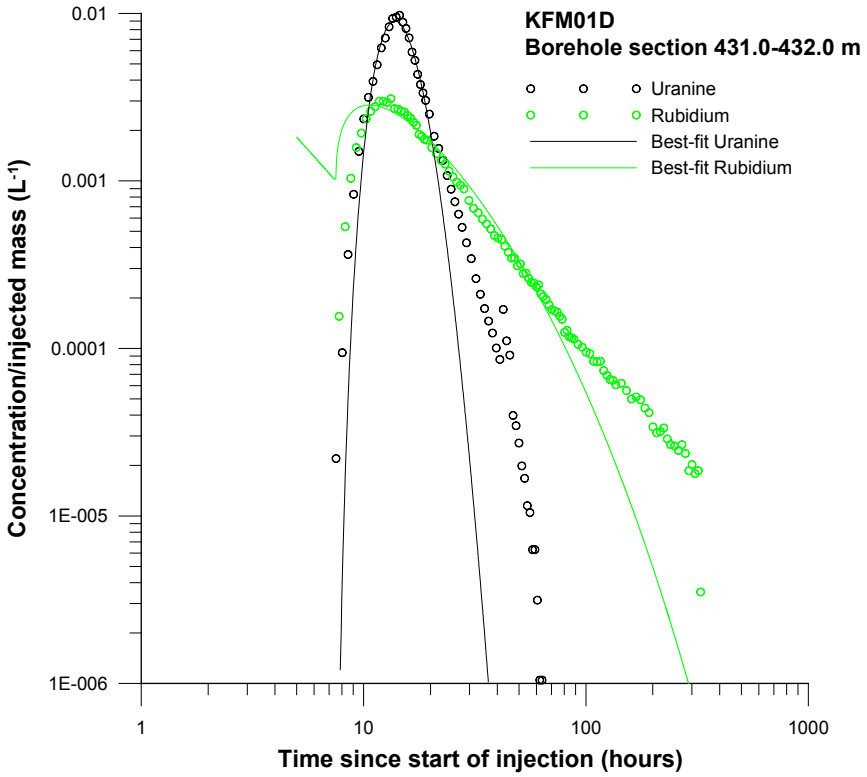

Figure 5-21d. *Example of simultaneous fitting of Uranine and rubidium for section 431.0–432.0 m in borehole KFM01D, logarithmic scale.*

All of the regression runs (Tables 5-7a and 5-7b) resulted in similar values of the retardation coefficient for each sorbing tracer, while the estimated values of the longitudinal dispersivity are strongly dependent on the assumed porosity value. Both of these observations are consistent with prior expectations of the relationships between parameters in a SWIW test (for references see section 5.2.3).

The estimated values of R for cesium (857–940) and rubidium (223–243) indicate very strong sorption effects, and agree approximately with values from cross-hole tests, obtained using similar transport models (advection-dispersion and linear sorption /Anderson et al. 2002/), for references see section 5.2.3. Estimated values of R for rubidium are lower than for cesium. This is somewhat different compared with previously performed SWIW tests where these three tracers have been used (for references see section 5.2.3).

Table 5-7a. Results of simultaneous fitting of Uranine and cesium for section 431.0–432.0 m in borehole KFM01D. Approximate values of the coefficient of variation (estimation standard error divided by the estimated value) are given within parenthesis.

Porosity (fixed)	a_L (estimated)	R (estimated)
0.002	0.39 (0.04)	940 (0.18)
0.005	0.25 (0.04)	931 (0.17)
0.01	0.18 (0.04)	918 (0.17)
0.02	0.12 (0.04)	899 (0.17)
0.05	0.08 (0.04)	857 (0.16)

Table 5-7b. Results of simultaneous fitting of Uranine and rubidium for section 431.0–432.0 m in borehole KFM01D. Approximate values of the coefficient of variation (estimation standard error divided by the estimated value) are given within parenthesis.

Porosity (fixed)	a_L (estimated)	R (estimated)
0.002	0.38 (0.04)	243 (0.16)
0.005	0.24 (0.04)	241 (0.16)
0.01	0.17 (0.04)	238 (0.16)
0.02	0.12 (0.04)	233 (0.16)
0.05	0.08 (0.04)	223 (0.16)

6 Discussion and conclusions

The dilution measurements were carried out in selected fractures in borehole KFM01D at levels from 147 to 571 m borehole length (120 to 448 m vertical depth), where hydraulic transmissivity ranged within $T = 1.3 \cdot 10^{-8}$–$1.6 \cdot 10^{-5}$ m^2/s. The borehole intersects some minor deformation zones that are defined in the area /Carlsten et al. 2006/. However, none of the measured sections is located within these zones.

The results of the dilution measurements in borehole KFM01D show that the groundwater flow varies during natural conditions with flow rates from 0.015 to 0.173 ml/min and Darcy velocities from $1.7 \cdot 10^{-9}$ to $1.9 \cdot 10^{-8}$ m/s ($1.5 \cdot 10^{-4}$–$1.6 \cdot 10^{-3}$ m/d). These results are in accordance with dilution measurements carried out in boreholes KFM01A, KFM02A, KFM03A, KFM03B, KFM04A and KFM08A. In these boreholes hydraulic transmissivity in the test sections was within $T = 2.7 \cdot 10^{-10}$–$9.2 \cdot 10^{-5}$ m^2/s and flow rate ranged from 0.004 to 23.3 ml/min and Darcy velocity from $3.5 \cdot 10^{-10}$ to $8.4 \cdot 10^{-7}$ m/s ($3.0 \cdot 10^{-5}$–$7.3 \cdot 10^{-2}$ m/d) /Gustafsson et al. 2005, 2006b, Thur et al. 2007/.

Groundwater flow rates and Darcy velocities calculated from dilution measurements in borehole KFM01D are also within the range that can be expected based on experience from previously performed dilution measurements under natural gradient conditions at other sites in Swedish crystalline rock /Gustafsson and Andersson 1991, Gustafsson and Morosini 2002, Gustafsson and Nordqvist 2005, Gustafsson et al. 2005, 2006ab, Thur et al. 2007.

In KFM01D the highest flow rate and Darcy velocity are measured at 431.0–432.0 m borehole length (344–345 m vertical depth). During hydraulic tests with the Pipe String System in a section containing this 431–432 m dilution section a pressure increase was observed in the section below during the injection phase /Florberger et al. 2006/. This might indicate a shortcut between the studied fracture and the borehole which might explain the high flow rate and Darcy velocity.

The lowest flow rate is measured in the low transmissive single fracture at c 571 m borehole length (c 448 m vertical depth).

Hydraulic gradients in KFM01D, calculated according to section 4.4.2, are within or close to the expected range (0.001–0.05) in three out of five measured test sections. In the section at c 571 m (448 m vertical depth) the hydraulic gradient is considered to be large. Local effects where the measured fractures constitute a hydraulic conductor between other fractures with different hydraulic heads or wrong estimations of the correction factor, α, and/or the hydraulic conductivity of the fracture could explain the large hydraulic gradient values. The hydraulic transmissivity of the section is at the lower limit of the measurement range for the dilution probe which may decrease accuracy in determined groundwater flow rate. The section at c 316 m (255 m vertical depth) shows low hydraulic gradient. The Pipe String System measurement for this section gives the flow regime NFB for the injection and PRF transferring to NFB for the recovery phase. This indicates high transmissivity in the region close to the borehole confined by a denser border around. This gives low flow rate, low Darcy velocity and low hydraulic gradient in proportion to the T-value.

Table 6-1. Rock units, groundwater flow rates, Darcy velocities and hydraulic gradients for all measured sections in boreholes KFM01D.

Borehole	Test section (m)+	Rock units**	Number of flowing fractures*	T (m^2/s)*	Q (ml/min)	Q (m^3/s)	Darcy velocity (m/s)	Hydraulic gradient
KFM01D	147.5–148.5 (120–121)	RU1 Medium-grained metagranite-granodiorite	1	5.32E–06	0.021	3.51E–10	2.32E–09	0.0004
KFM01D	316.4–317.4 (255–256)	RU2 Fine- to finely medium-grained metagranite-granodiorite	1	1.65E–05	0.021	3.51E–10	2.32E–09	0.0001
KFM01D	377.4–378.4 (302–303)	RU2 Fine- to finely medium-grained metagranite-granodiorite	1	3.15E–07	0.079	1.32E–09	8.69E–09	0.03
KFM01D	431.0–432.0 (344–345)	RU3 Fine- to finely medium-grained metagranite-granodiorite	1	9.95E–07	0.173	2.88E–09	1.90E–08	0.019
KFM01D	570.7–571.7 (448–449)	RU4 Medium-grained metagranite-granodiorite	1	1.27E–08	0.015	2.50E–10	1.65E–09	0.130

* /Väisäsvaara et al. 2006/
** /Carlsten et al. 2006/
+ Test section vertical depth is given within brackets.

The SWIW tests in section 377.4–378.4 m and 431.0–432.0 m borehole length resulted in high-quality tracer breakthrough data. Experimental conditions (flows, times, events, etc) are well known and documented, as well as borehole geological conditions with BIPS logging (Appendix C). Together they provide a good basis for possible further evaluation.

The results show smooth breakthrough curves without apparent irregularities or excessive experimental noise with a clearly visible effect of retardation/sorption of cesium and rubidium.

The model evaluation was made using a radial flow model with advection, dispersion and linear equilibrium sorption as transport processes. It is important that experimental conditions (times, flows, injection concentration, etc) are incorporated accurately in the simulations. Otherwise artefacts of erroneous input may occur in the simulated results. The evaluation carried out may be regarded as a typical preliminary approach for evaluation of a SWIW test where sorbing tracers are used. Background flows were in most cases assumed to be insignificant. However, in sections such as the one between 431.0–432.0 m, the dilution measurements indicate relatively high natural flow and it may not be excluded that the natural flow can influence the recovery breakthrough curves. Test simulations of Uranine breakthrough (not shown) indicated that incorporation of natural gradient in the simulation model might to some extent, but not fully, improve the overall model fit of the Uranine curve.

The estimated values of the retardation factor, R, indicates strong sorption, in section 377.4–378.4 m c 529 for cesium and c 918 for rubidium and in section 431.0–432.0 m c 909 for cesium and c 236 for rubidium. Rubidium shows stronger sorption than cesium in section 377.4–378.4 m, whereas in section 431.0–432.0 m it is just the other way around. In earlier performed SWIW tests where these three tracers have been used, the retardation factor is lower for cesium than for rubidium /Gustafsson et al. 2006ab, Thur et al. 2007/, contrary to literature data from the TRUE Block Scale

Project /Anderson et al. 2002/. In section 377.4–378.4 m where R is lower for cesium than for rubidium, recovery is higher for cesium than for rubidium, whereas section 431.0–432.0 m recovery is higher for rubidium than for cesium.

It should also be pointed out that the lack of model fit in the tailing parts of the curves (most visible for Uranine) appears to be a consistent feature in the SWIW tests performed so far /Gustafsson and Nordqvist 2005, Gustafsson et al. 2005, 2006ab, Thur et al. 2007/. Thus, there seems to be some generally occurring process that has not yet been identified, but is currently believed to be an effect of the tested medium and not an experimental artefact. Studies to identify possible causes for the observed discrepancy are ongoing.

7 References

Andersson P, 1995. Compilation of tracer tests in fractured rock. SKB PR 25-95-05, Svensk Kärnbränslehantering AB.

Andersson P, Byegård J, Winberg A, 2002. Final report of the TRUE Block Scale project. 2. Tracer tests in the block scale. SKB TR-02-14, Svensk Kärnbränslehantering AB.

Byegård J, Tullborg E-L, 2005. Sorption experiments and leaching studies using fault gouge material and rim zone material from the Äspö Hard Rock Laboratory. SKB Technical Report (in prep.).

Carlsten S, Döse C, Gustafsson J, Mattsson H, Petersson J, Stephens M, 2006. Forsmark site investigation Geological single-hole interpretation of KFM01D, HFM24, HFM25, HFM27 and HFM29. SKB P-06-210, Svensk Kärnbränslehantering AB.

Florberger J, Hjerne C, Ludvigson J-E, Walger E, 2006. Forsmark site investigation, Single-hole injection tests in borehole KFM01D. SKB P-06-195, Svensk Kärnbränslehantering AB.

Gustafsson E, Andersson P, 1991. Groundwater flow conditions in a low-angle fracture zone at Finnsjön, Sweden. Journal of Hydrology, Vol 126, pp 79–111. Elsvier, Amsterdam.

Gustafsson E, 2002. Bestämning av grundvattenflödet med utspädningsteknik – Modifiering av utrustning och kompletterande mätningar. SKB R-02-31 (in Swedish), Svensk Kärnbränslehantering AB.

Gustafsson E, Morosini M, 2002. In situ groundwater flow measurements as a tool for hardrock site characterisation within the SKB programme. Norges geologiske undersøkelse. Bulletin 439, 33–44.

Gustafsson E, Nordqvist R, 2005. Oskarshamn site investigation. Groundwater flow measurements and SWIW-tests in boreholes KLX02 and KSH02. SKB P-05-28, Svensk Kärnbränslehantering AB.

Gustafsson E, Nordqvist R, Thur P, 2005. Forsmark site investigation. Groundwater flow measurements and SWIW tests in boreholes KFM01A, KFM02A, KFM03A and KFM03B. SKB P-05-77, Svensk Kärnbränslehantering AB.

Gustafsson E, Nordqvist R, Thur P, 2006a. Oskarshamn site investigation. Groundwater flow measurements and SWIW-tests in borehole KLX03. SKB P-05-246, Svensk Kärnbränslehantering AB.

Gustafsson E, Nordqvist R, Thur P, 2006b. Forsmark site investigation. Groundwater flow measurements and SWIW tests in borehole KFM08A. SKB P-06-90, Svensk Kärnbränslehantering AB.

Halevy E, Moser H, Zellhofer O, Zuber A, 1967. Borehole dilution techniques – a critical review. In: Isotopes in Hydrology, Proceedings of a Symposium, Vienna 1967, IAEA, Vienna, pp 530–564.

Nordqvist R, Gustafsson E, 2004. Single-well injection-withdrawal tests (SWIW). Investigation of evaluation aspects under heterogeneous crystalline bedrock conditions. SKB R-04-57, Svensk Kärnbränslehantering AB.

Rhén I, Forsmark T, Gustafson G, 1991. Transformation of dilution rates in borehole sections to groundwater flow in the bedrock. Technical note 30. In: Liedholm M. (ed) 1991. SKB-Äspö Hard Rock Laboratory, Conceptual Modeling of Äspö, technical Notes 13–32. General Geological, Hydrogeological and Hydrochemical information. Äspö Hard Rock Laboratory Progress Report PR 25-90-16b.

SKB, 2001a. Program för platsundersökning vid Forsmark. SKB R-01-42 (in Swedish), Svensk Kärnbränslehantering AB.

SKB, 2001b. Site investigations – Investigation methods and general execution programme. SKB TR-01-29, Svensk Kärnbränslehantering AB.

Thur P, Nordqvist R, Gustafsson E, 2007. Oskarshamn site investigation. Groundwater flow measurements and SWIW test in borehole KLX18A. SKB Report (in prep.).

Voss C I, 1984. SUTRA – Saturated-Unsaturated Transport. A finite element simulation model for saturated-unsaturated fluid-density-dependent groundwater flow with energy transport or chemically-reactive single-species solute transport. U.S. Geological Survey Water-Resources Investigations Report 84-4369.

Väisäsvaara J, Leppänen H, Pekkanen J, 2006. Forsmark site investigation. Difference flow logging in borehole KFM01D. SKB P-06-161, Svensk Kärnbränslehantering AB.

Appendices

Appendix A

Borehole data KFM01D

SICADA – Information about KFM01D

Title	Value
	Information about cored borehole KFM01D (2006-06-27).

Borehole length (m): 1001.420
Reference level: Fläns casing

Drilling Period(s):

From Date	*To Date*	*Secup(m)*	*Seclow(m)*	*Drilling Type*
2003-05-20	2003-06-30	0.000	107.420	Percussion drilling
2003-08-25	2003-11-19	107.420	1001.420	Core drilling

Starting point coordinate:

Length(m)	*Northing(m)*	*Easting(m)*	*Elevation*	*Coord System*
0.000	6698921.744	1630978.964	8.771	RT90-RHB70

Angles:

Length(m)	*Bearing*	*Inclination (– = down)*	*Coord System*
0.000	45.244	–60.081	RT90-RHB70

Borehole diameter:

Secup(m)	*Seclow(m)*	*Hole Diam(m)*
0.000	12.030	0.350
12.030	107.330	0.247
107.330	107.420	0.161
107.420	108.690	0.086
108.690	1001.420	0.077

Core diameter:

Secup(m)	*Seclow(m)*	*Core Diam(m)*
107.420	108.690	0.072
108.690	1000.890	0.051
1000.890	1001.420	0.062

Casing diameter:

Secup(m)	*Seclow(m)*	*Case In(m)*	*Case Out(m)*	*Comment*
0.000	106.910	0.200	0.208	
0.000	12.030	0.265	0.273	
0.000	12.030	0.265	0.273	
0.000	106.910	0.200	0.208	
106.910	106.950	0.170	0.208	
106.910	106.950	0.170	0.208	

Grove milling:

Length(m)	*Trace detectable*
119.000	119
150.000	150
200.000	199
250.000	250
300.000	300
350.000	349
400.000	400
450.000	449
500.000	500
550.000	550
600.000	600
650.000	650
700.000	700
750.000	750
800.000	800
850.000	850
900.000	900
950.000	950

Installed sections:

Section no	*Start Date*	*Secup(m)*	*Seclow(m)*
1	2004-06-30	0.000	1001.420

Dilution measurement KFM01D 147.5–148.5 m

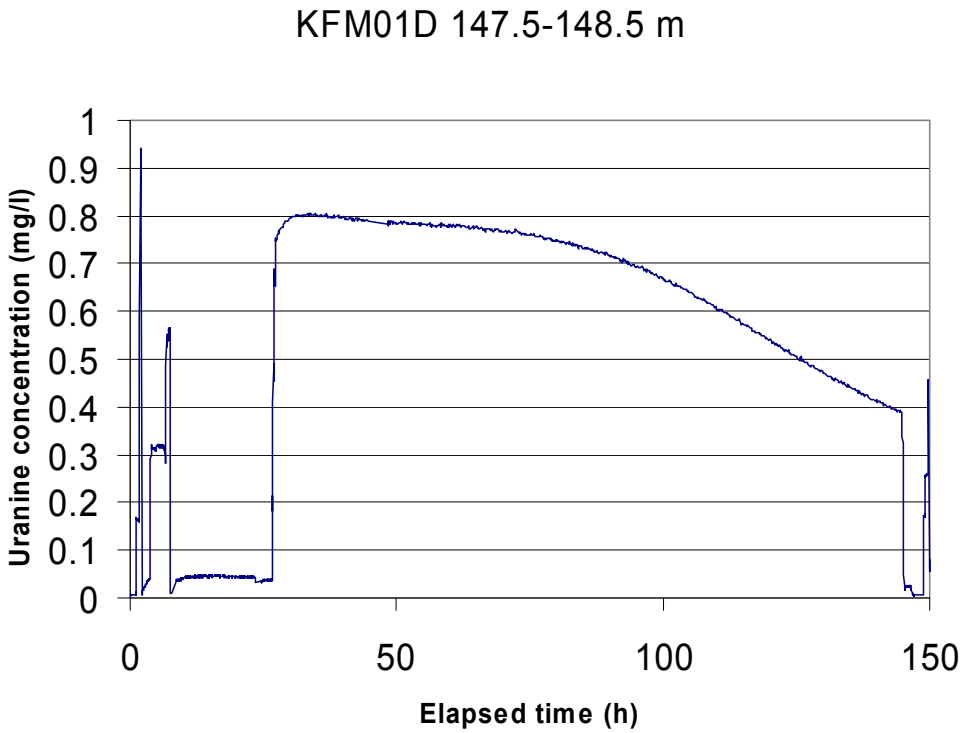

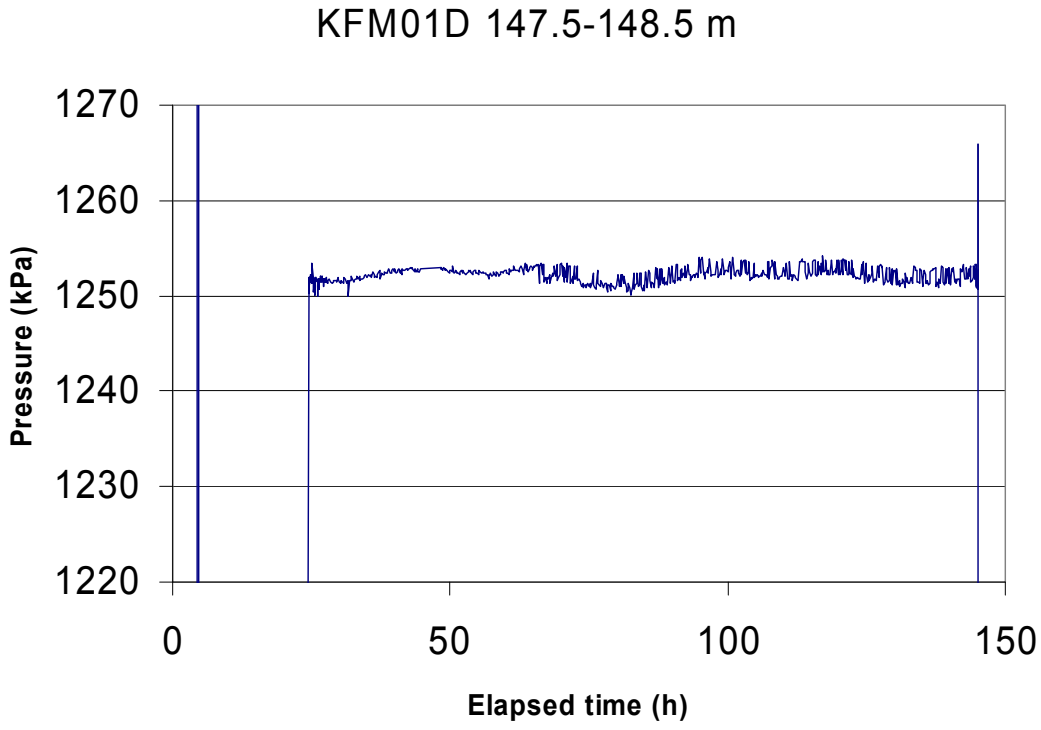

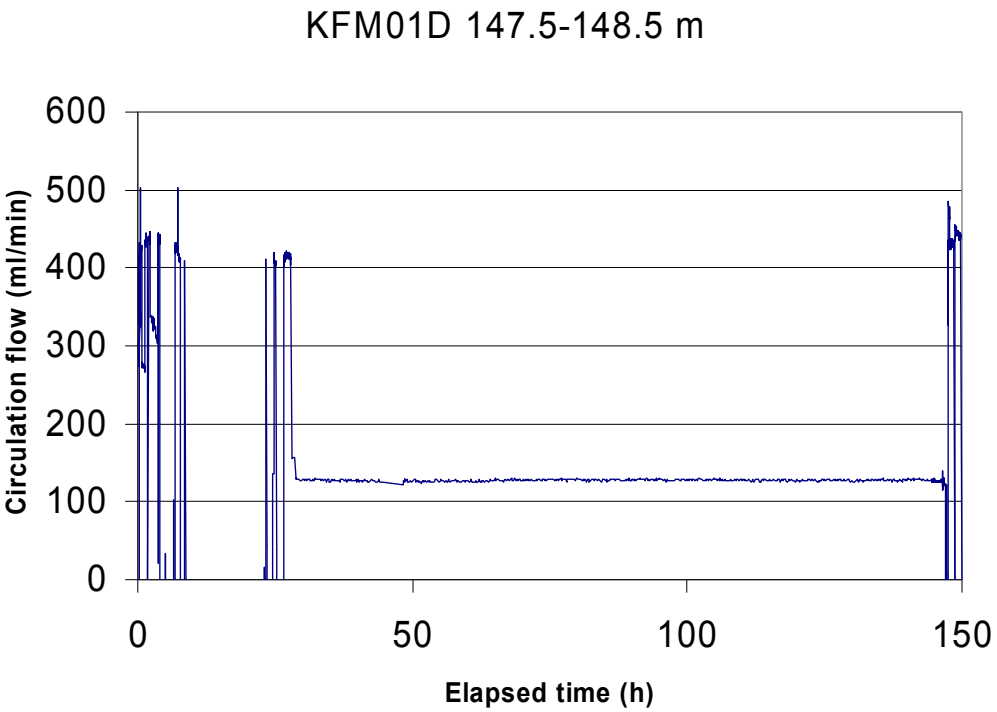
KFM01D 147.5-148.5 m
Circulation flow (ml/min)
600
500
400
300
200
100
0
0
50
100
150
Elapsed time (h)

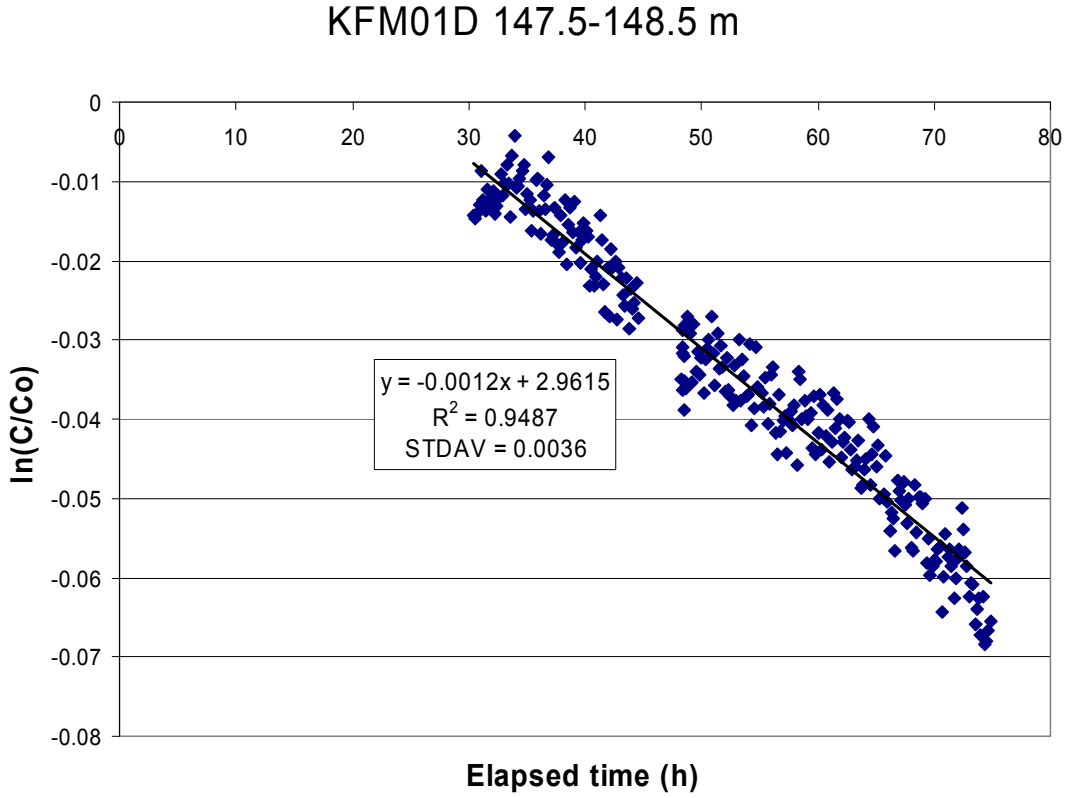

Part of dilution curve (h)	V (ml)	ln(C/Co)/t	Q (ml/h)	Q (ml/min)	Q (m3/s)	R2-value
30-75	1054	-0.0012	1.26	0.021	3.51E-10	0.9487

Part of dilution curve (h)	K (m/s)	Q (m3/s)	A (m2)	v(m/s)	I
30-75	5.32E-06	3.51E-10	0.1516	2.32E-09	0.0004

Dilution measurement KFM01D 316.4–317.4 m

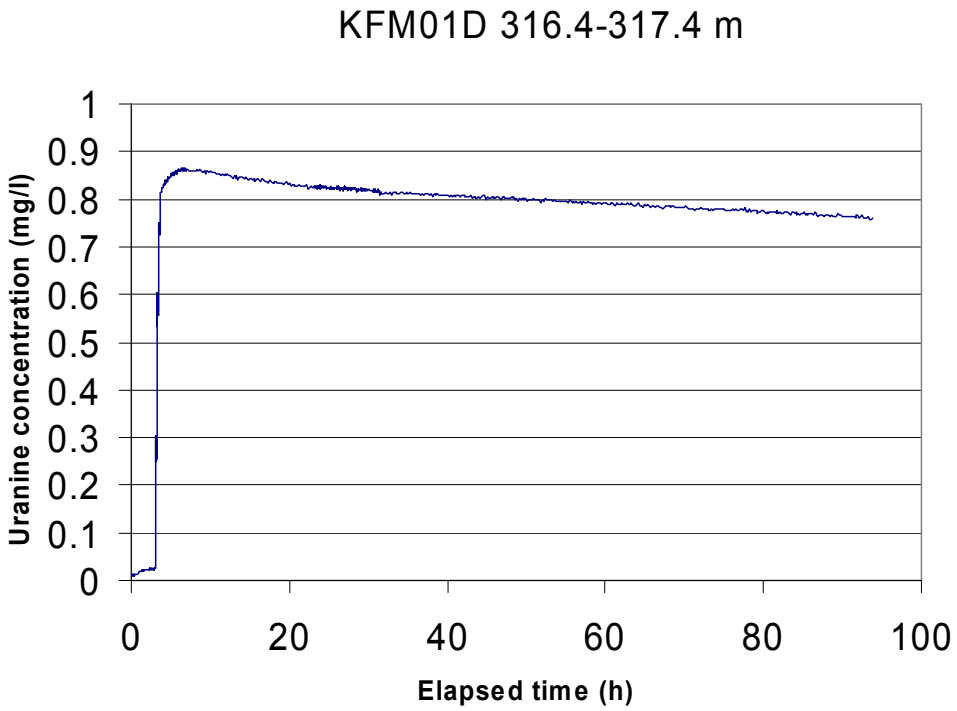

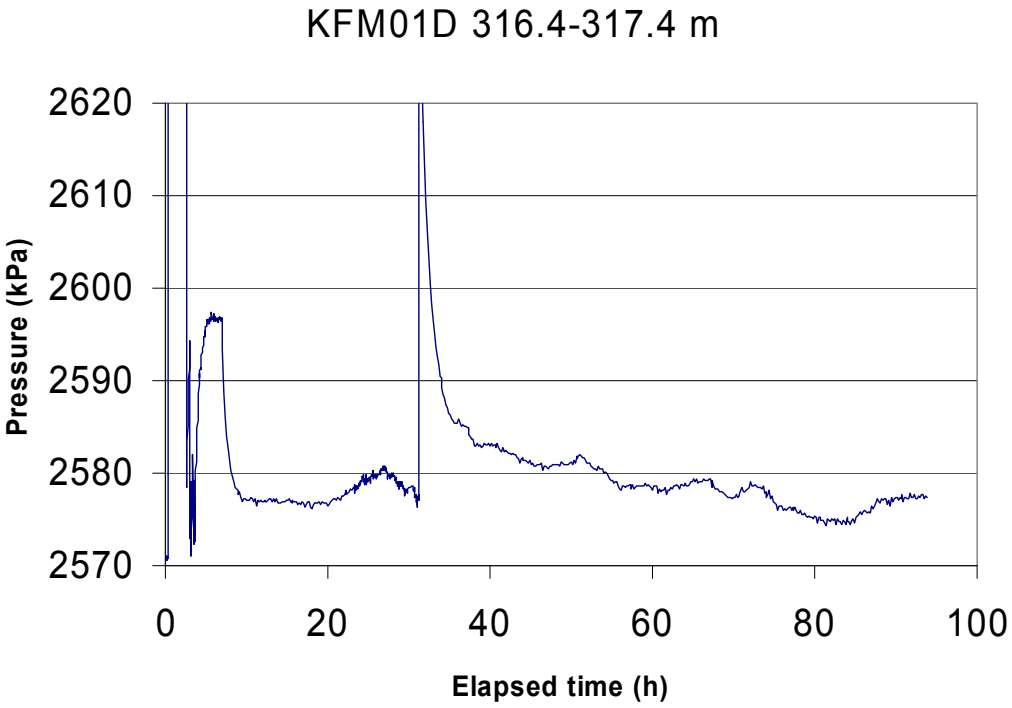

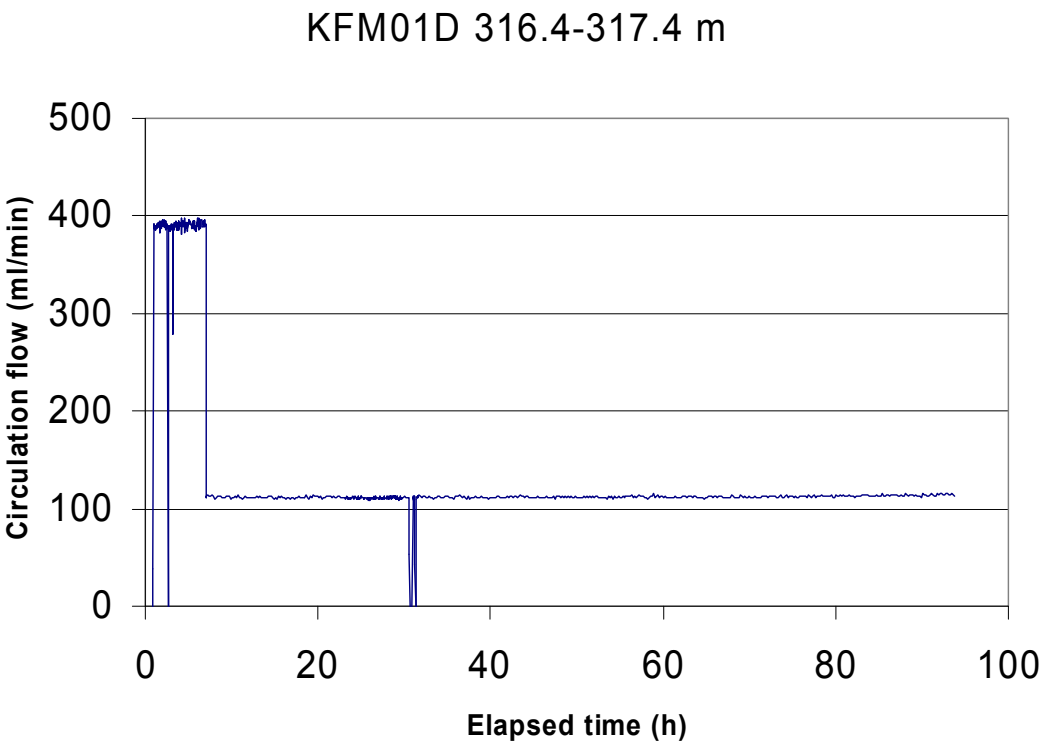
KFM01D 316.4-317.4 m
Circulation flow (ml/min)
500
400
300
200
100
0
0
20
40
60
80
100
Elapsed time (h)

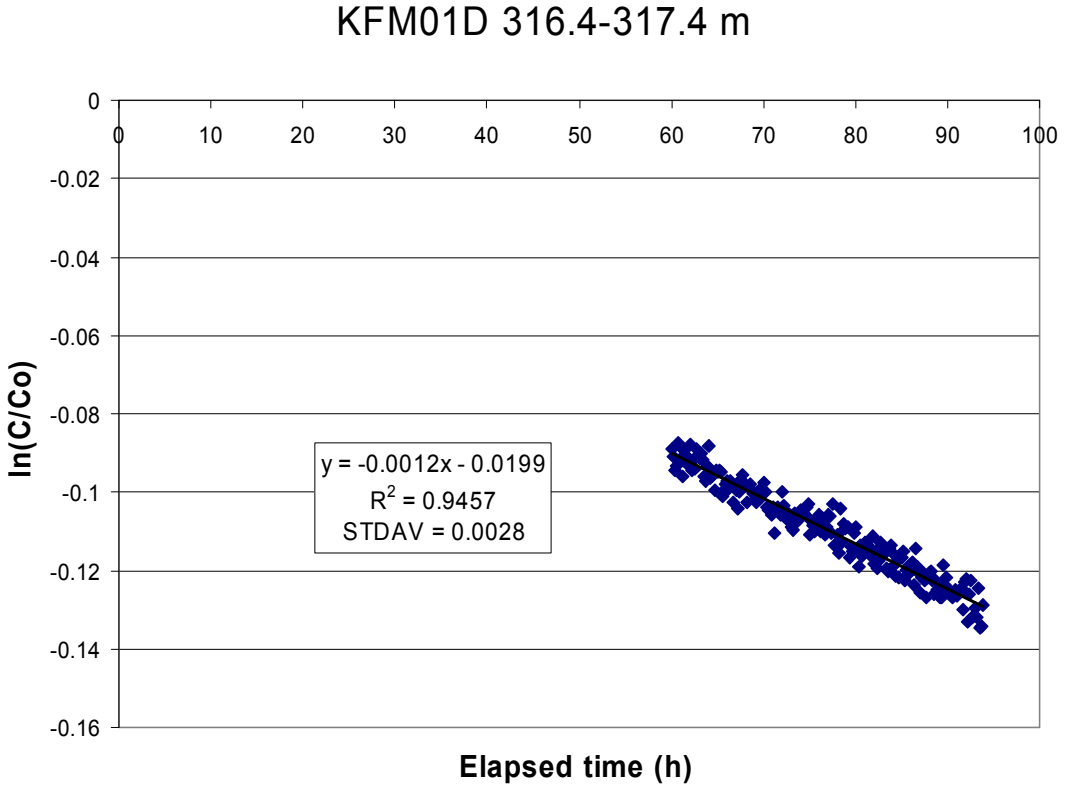

Part of dilution curve (h)	V (ml)	ln(C/Co)/t	Q (ml/h)	Q (ml/min)	Q (m3/s)	R2-value
60-94	1054	-0.0012	1.26	0.021	3.51E-10	0.9457

Part of dilution curve (h)	K (m/s)	Q (m3/s)	A (m2)	v(m/s)	I
60-94	1.65E-05	3.51E-10	0.1516	2.32E-09	0.0001

Dilution measurement KFM01D 377.4–378.4 m

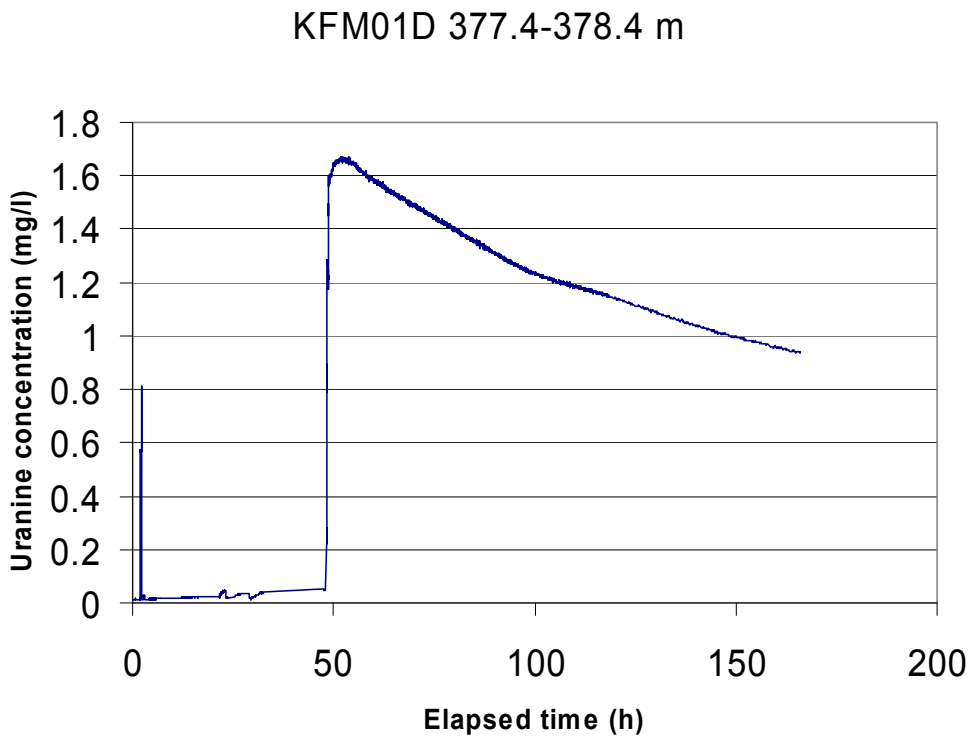

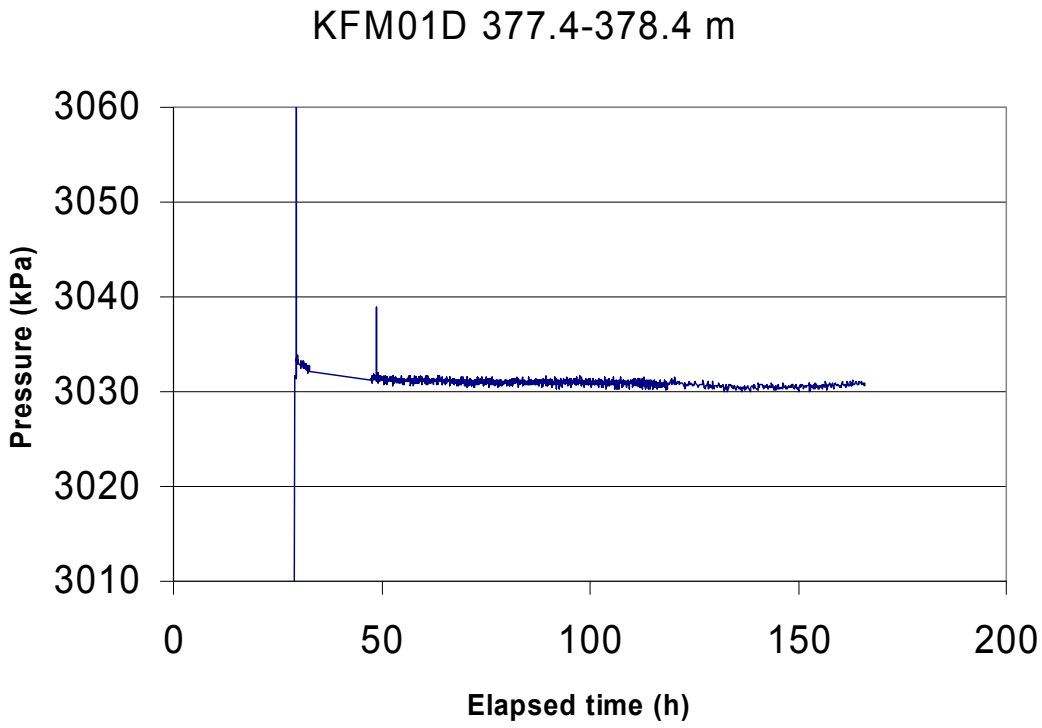

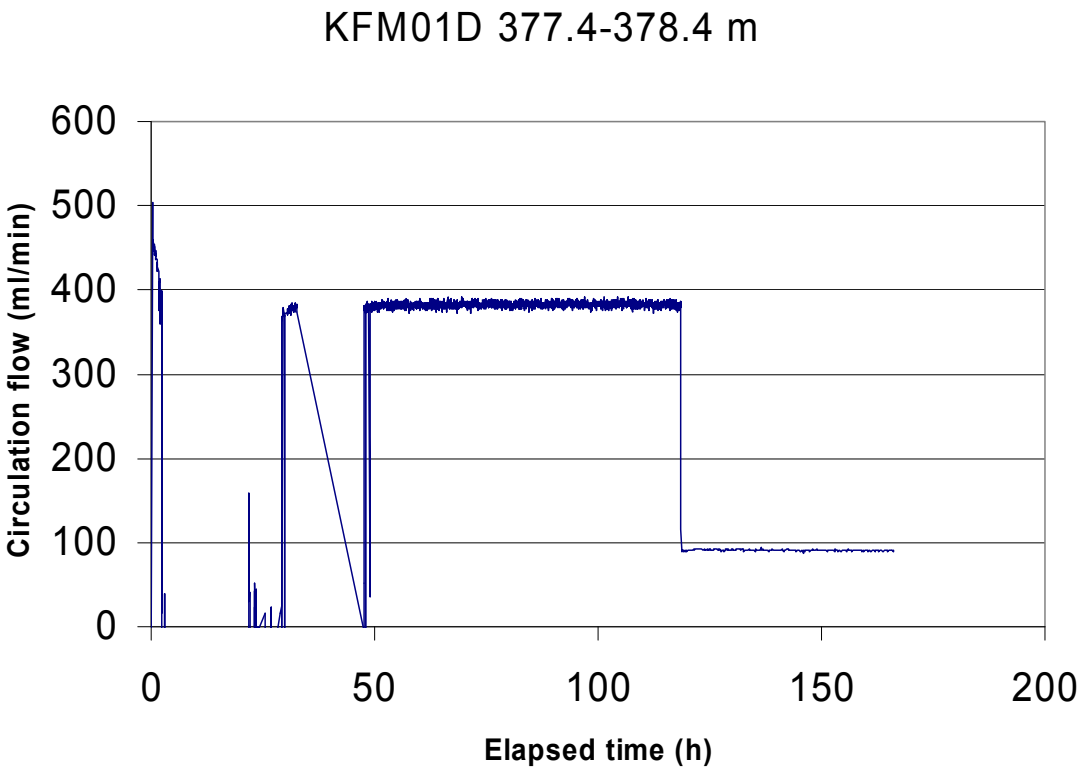
KFM01D 377.4-378.4 m
Circulation flow (ml/min)
600
500
400
300
200
100
0
0
50
100
150
200
Elapsed time (h)

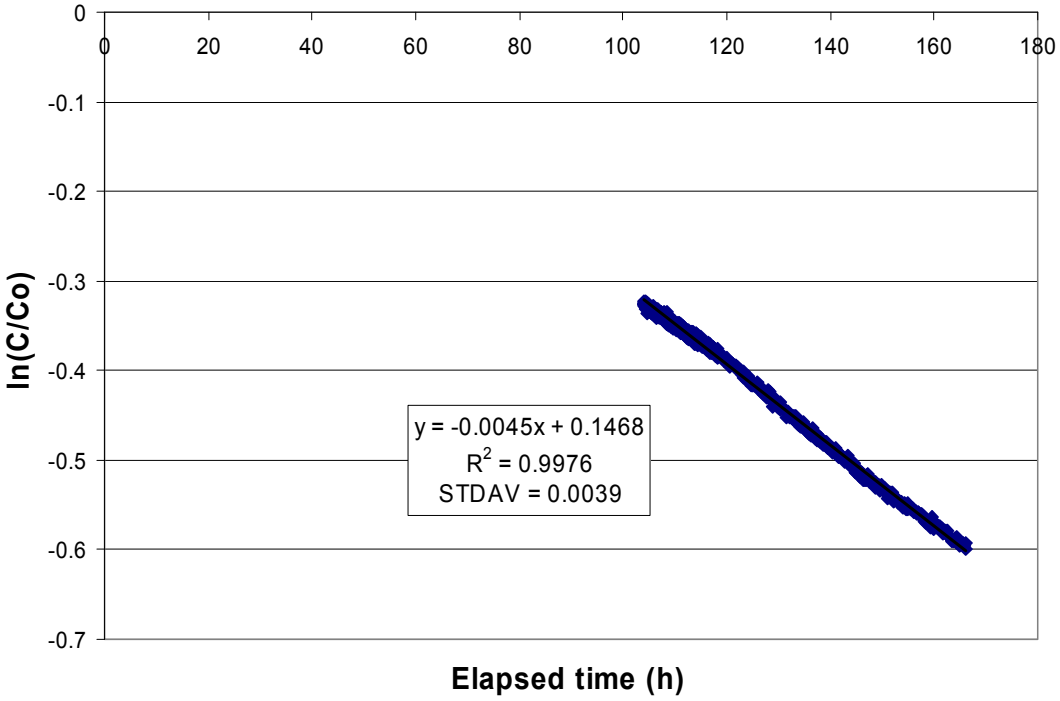

Part of dilution curve (h)	V (ml)	ln(C/Co)/t	Q (ml/h)	Q (ml/min)	Q (m3/s)	R2-value
104-166	1054	-0.0045	4.74	0.079	1.32E-09	0.9976

Part of dilution curve (h)	K (m/s)	Q (m3/s)	A (m2)	v(m/s)	I
104-166	3.15E-07	1.32E-09	1.516	8.69E-10	0.003

Dilution measurement KFM01D 431.0–432.0 m

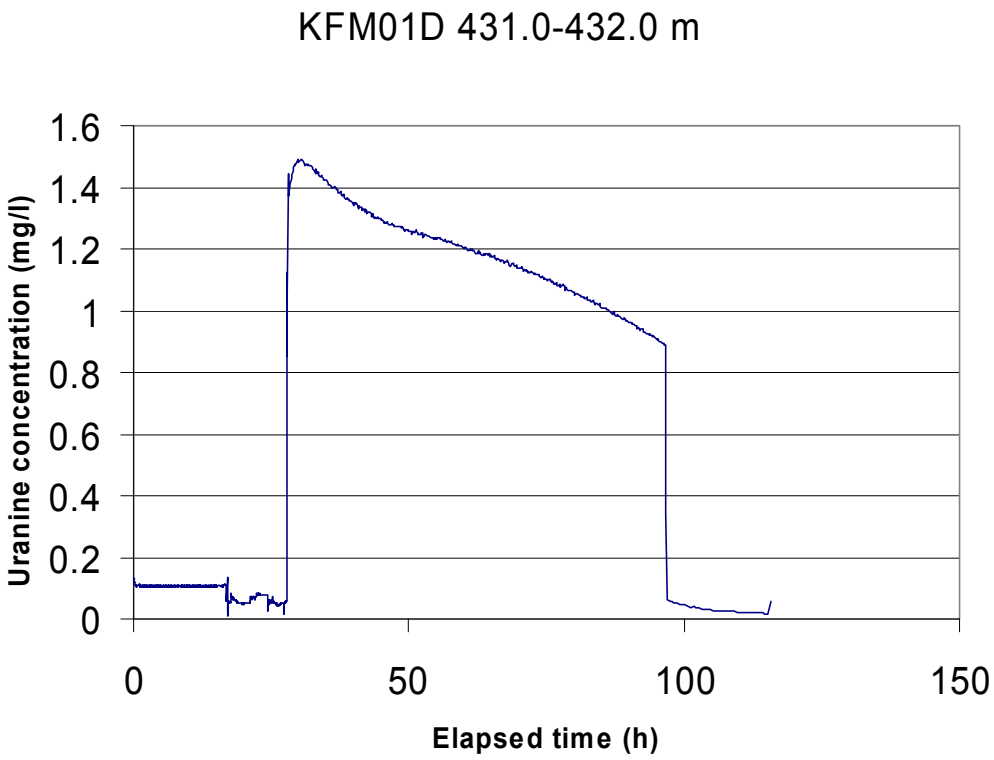

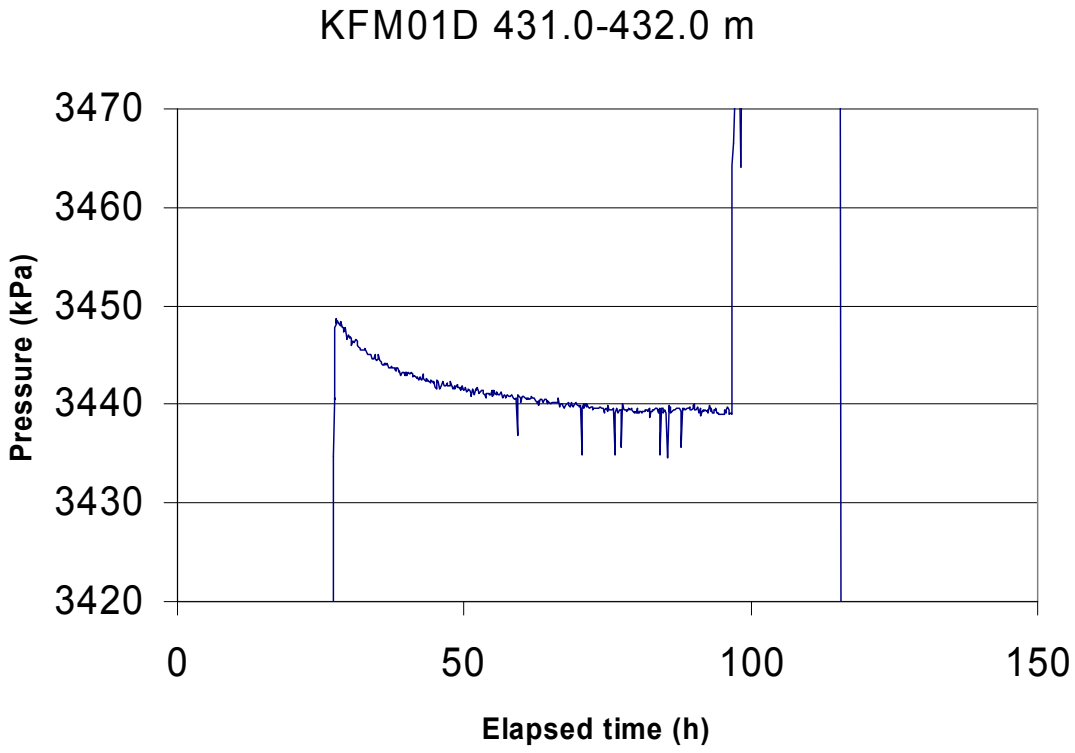

KFM01D 431.0-432.0 m

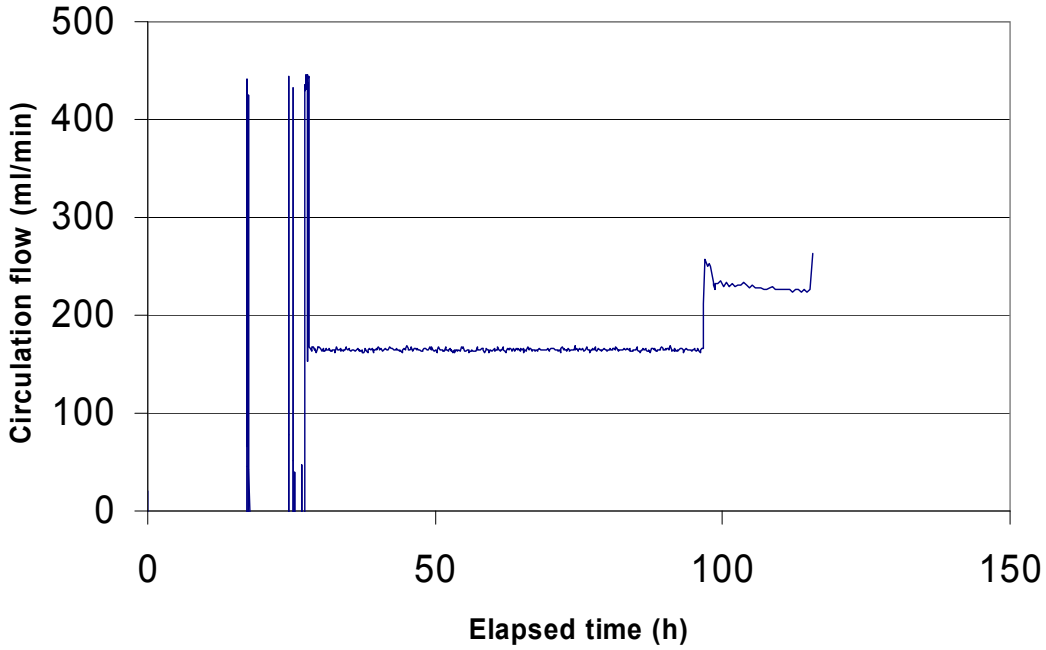

KFM01D 431.0-432.0 m

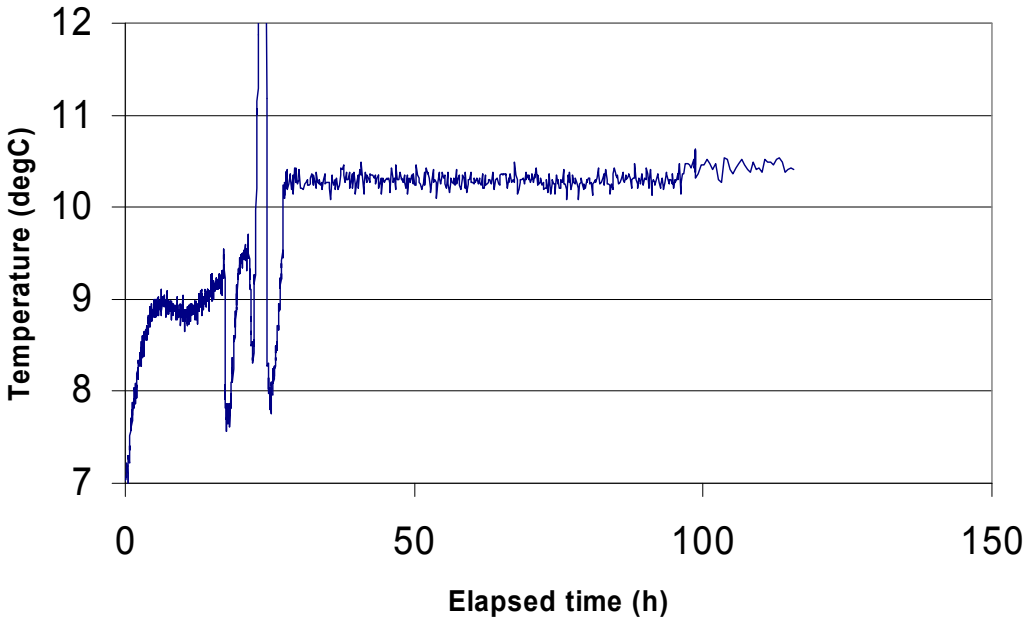

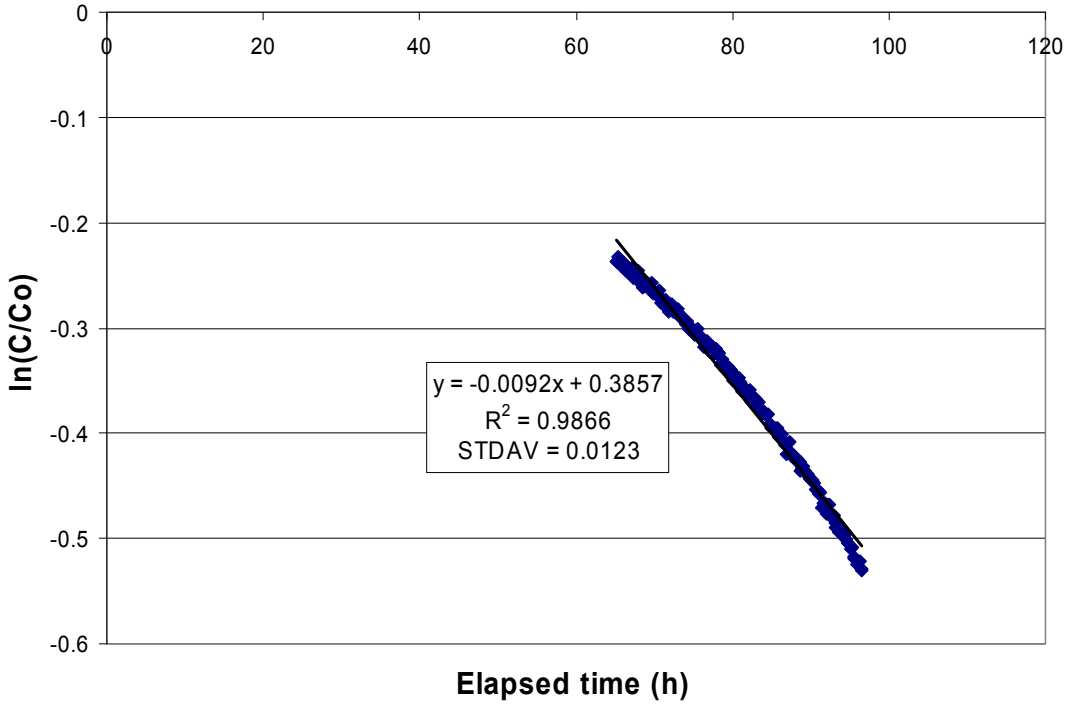

Part of dilution curve (h)	V (ml)	ln(C/Co)/t	Q (ml/h)	Q (ml/min)	Q (m3/s)	R2-value
65-96	1126	-0.0092	10.36	0.173	2.88E-09	0.9866

Part of dilution curve (h)	K (m/s)	Q (m3/s)	A (m2)	v(m/s)	I
65-96	9.95E-07	2.88E-09	0.1516	1.90E-08	0.019

Dilution measurement KFM01D 570.7–571.7 m

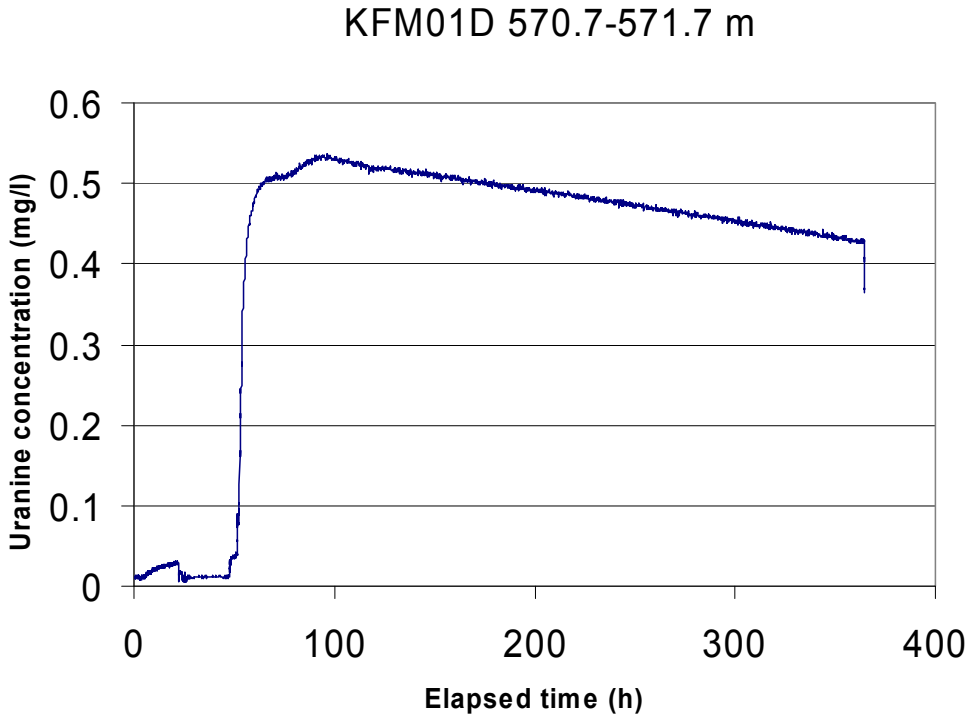

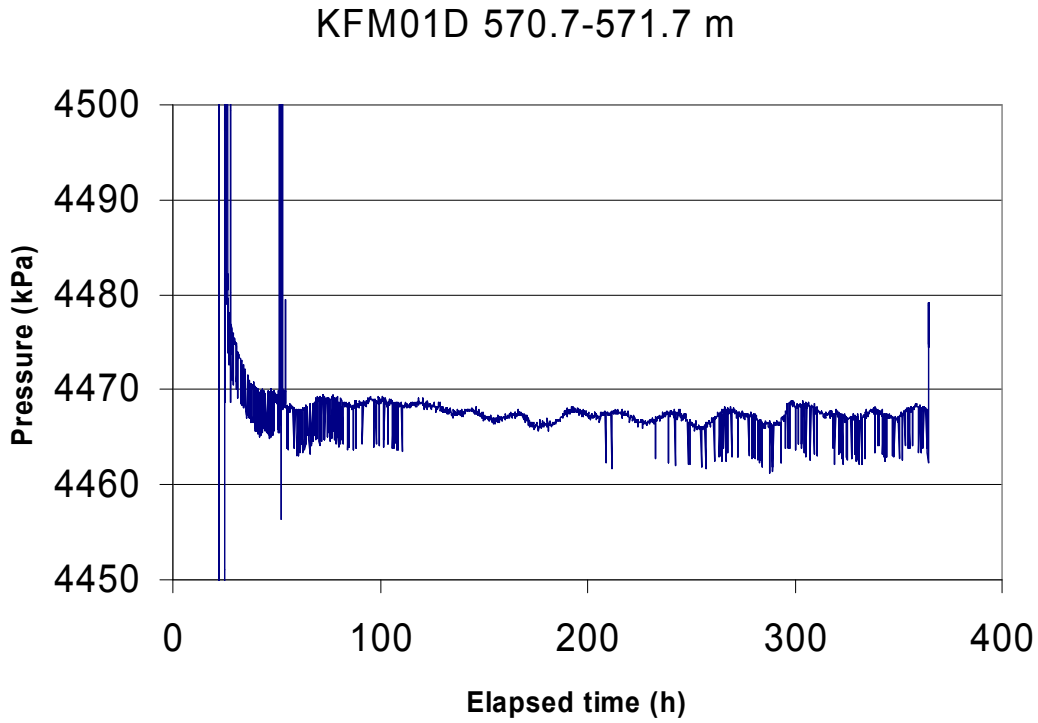

KFM01D 570.7-571.7 m

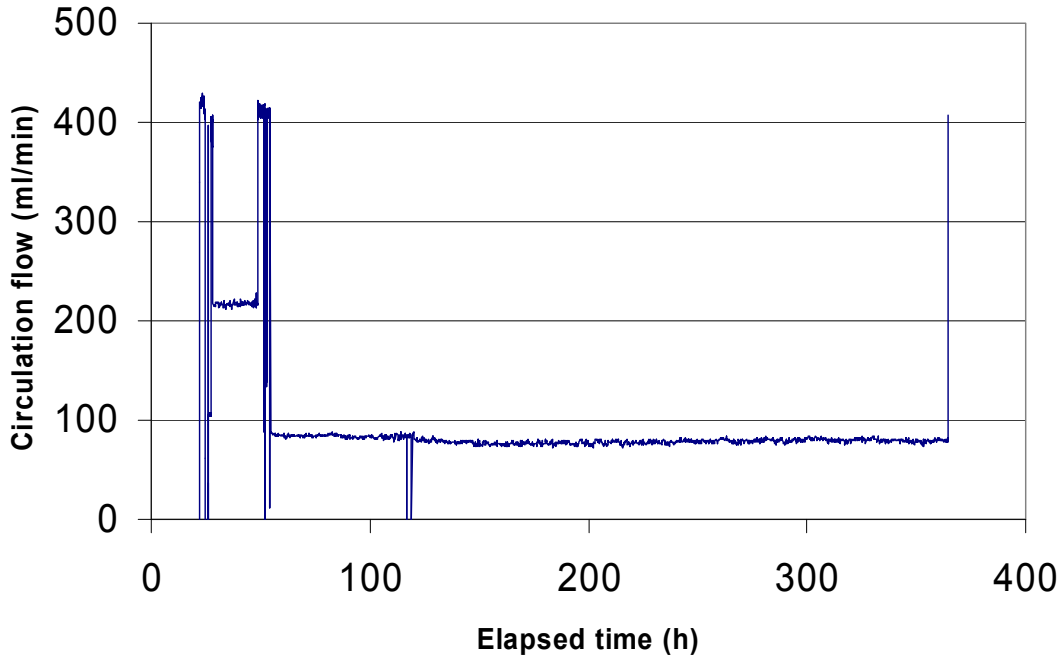

KFM01D 570.7-571.7 m

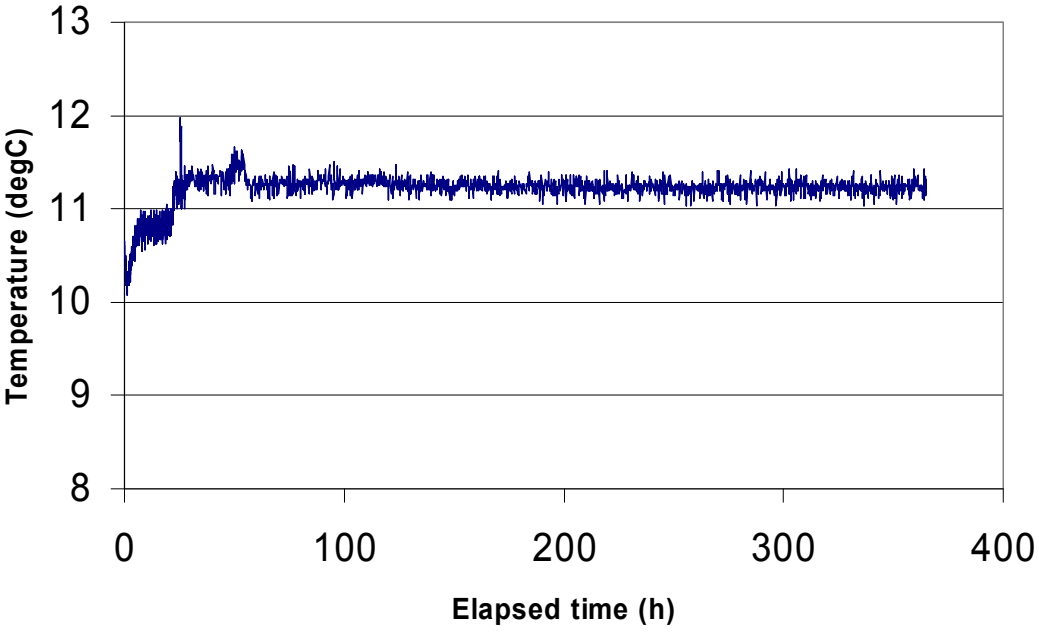

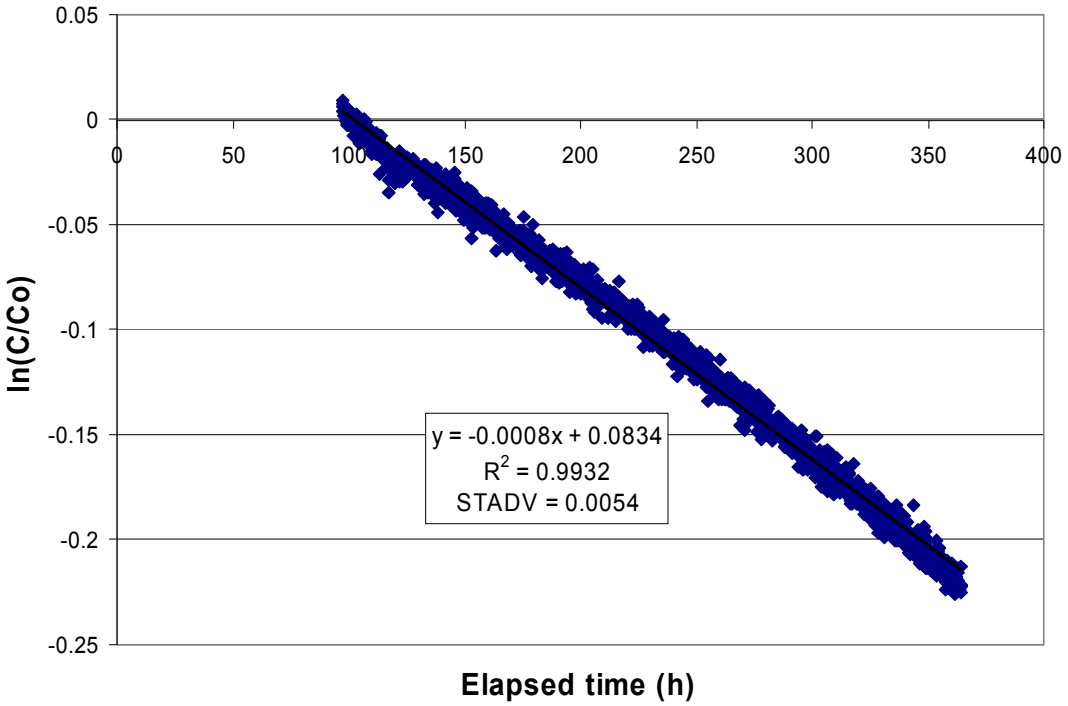

Part of dilution curve (h)	V (ml)	ln(C/Co)/t	Q (ml/h)	Q (ml/min)	Q (m3/s)	R2-value
97-364	1126	-0.0008	0.90	0.015	2.50E-10	0.9932

Part of dilution curve (h)	K (m/s)	Q (m3/s)	A (m2)	v(m/s)	I
97-364	1.27E-08	2.50E-10	0.1516	1.65E-09	0.130

Appendix C

BIPS logging KFM01D

Depth range: 375.000 – 380.000 m

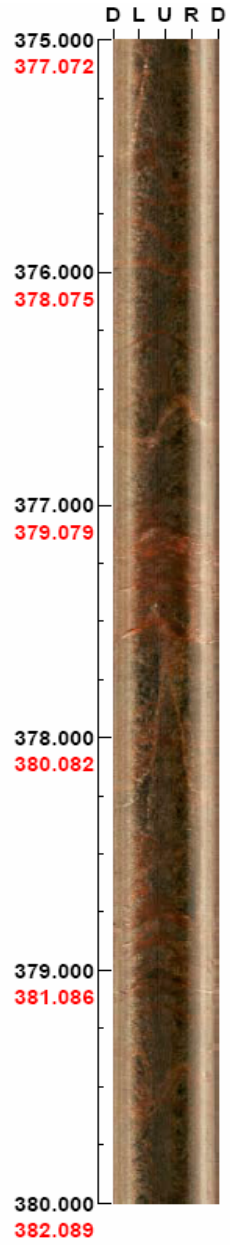

Black number = Recorded depth
Red number = Adjusted depth

Azimuth: 165
Scale: 1/25
Inclination: -50
Aspected ratio: 175%

Depth range: 430.000 – 435.000 m

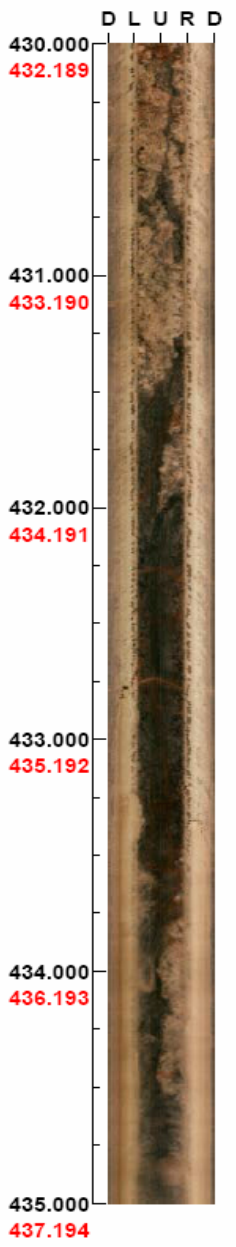

Black number = Recorded depth
Red number = Adjusted depth

Azimuth: 165
Scale: 1/25
Inclination: -50
Aspected ratio: 175%